THE UNIVERSITY OF MICHIGAN

7030-1-T

7030-1-T = RL-2146

ANALYTICAL AND NUMERICAL STUDIES OF THE BACK SCATTERING BEHAVIOR OF SPHERES

by

T.B.A. Senior

June 1965

Contract AF 04(694)-683

Prepared for

BALLISTIC SYSTEMS DIVISION
AIR FORCE SYSTEMS COMMAND
UNITED STATES AIR FORCE
NORTON AIR FORCE BASE, CALIFORNIA

MISSING PAGE

TABLE OF CONTENTS

I
INTRODUCTION

The scattering of a plane wave by a sphere has been one of the most widely studied of all problems in diffraction theory. A knowledge of the solution is important for many practical applications, but also relevant is the fact that the sphere is one of the very few shapes for which an exact solution can be obtained. With other and more general shapes it is necessary to resort to approximate techniques for the estimation of the scattering, and several of these have had their inspiration in a detailed and critical study of our small selection of exact results.

One of the most important features of the scattering from any smooth convex body is the effect of creeping waves which are launched in the vicinity of the shadow boundary and contribute to the back scattered field after having traversed the rear. Although usually regarded as a high frequency phenomenon appropriate only when the radii of curvature are all large in comparison with the wavelength ($ka \gg 1$), preliminary studies (Senior, 1965a) of data for the back scattering of a plane electromagnetic wave by a perfectly conducting sphere have suggested that the concept is still valid for ka as small as unity. What is more, a relatively simple expression for the creeping wave component is accurate for all $ka \geq 1$.

If the radii of curvature are not constant, the only method of calculating the creeping wave contribution available at the moment is that proposed by Keller (1958) which treats the waves as scalar disturbances following geodesics on the surface and, furthermore, assumes that the only relevant curvature is that in the direction of travel. This has proved adequate for most computational purposes when ka is large, but is somewhat less than satisfactory when ka is of order 10 or less. Is this evidence of a failure in the concept of creeping waves as ka gets smaller, or is it merely a reflection of the essentially high frequency character of the assumptions made in the generalization from a sphere to a body of varying curvature?

To throw some light on this question and, at the same time, to place the earlier results for a metallic sphere on a firmer footing, a detailed analytical and computational study of the back scattering of a plane acoustic wave by soft and hard spheres, and of a plane electromagnetic wave by a perfectly conducting sphere, was undertaken. The analytical procedures used are, of course, not new, and the treatment differs from those that can be found throughout the literature only in the uniformity of approach and (in some instances) the derivation of more complete expressions than have previously been available.

With each of the three problems the starting point is the standard Mie series representation. Application of a Watson transformation then leads naturally to a separation into creeping wave and optics components, the formulae for which are evaluated asymptotically under the assumption $ka \gg 1$. Sufficient terms are retained to ensure a high degree of accuracy for $ka \geq 5$, and the extent to which the resulting expressions are still applicable at lower frequencies is determined by comparison of computed values with those obtained by direct evaluation of the Mie series forms.

The analyses for the soft and hard spheres are given in Sections 2 and 3 respectively. Whereas, for the soft sphere, relatively simple expressions for the creeping wave and optics components are quite adequate for ka as small as unity, the increased magnitude of the higher order terms in the hard body solution demand somewhat more involved expressions which, even then, are significantly in error when ka has decreased to 2. With the electromagnetic problem, however, the effectiveness of the asymptotic developments is truly astounding. A simple form for the creeping wave component appears to retain its accuracy for ka at least as small as 0.3, and with a two-term expression for the optics component, the resulting far field amplitude is in error by only 12 percent in modulus and 3^{o} in phase when $ka = 0.7$.

There seems little doubt that the basic concept of a disturbance traveling around the back of the sphere and interfering with a specular return originating on the front face is valid for a much wider range of dimension-to-wavelength ratios than had been supposed. In the vector problem at least there is no evidence of any coupling between these components even when the frequency is such that the first Fresnel zone is limited by the shadow boundary, and the asymptotic expressions for these components continue to provide accurate information down through $ka = 1$. For bodies of non-constant curvature some possible implications of these results are discussed in Section 5.

II
AN ACOUSTICALLY SOFT SPHERE

The first problem to be considered is the scalar one in which a plane acoustic wave is incident on a soft sphere at whose surface a Dirichlet boundary condition is imposed.

2.1 Far Field Amplitude

In terms of spherical polar coordinates (R, θ, ϕ) whose origin is at the center of the sphere, the equation of the sphere is assumed to be $R = a$. Incident in the direction $\theta = \pi$ is the plane wave disturbance*

$$U^i = e^{-ikR\cos\theta}, \tag{1}$$

and since this can be written alternatively as

$$U^i = \sum_{n=0}^{\infty} (n+\frac{1}{2})\, e^{-in\frac{\pi}{2}}\, j_n(kR) P_n(\cos\theta) \tag{2}$$

(Stratton, 1941; p. 409), where $j_n(x)$ is the spherical Bessel function

$$j_n(x) = \sqrt{\frac{2\pi}{x}}\, J_{n+1/2}(x),$$

the total (incident plus scattered) field is clearly

$$U = \sum_{n=0}^{\infty} (n+\frac{1}{2})\, e^{-in\frac{\pi}{2}} \left\{ j_n(kR) - \frac{j_n(\rho)}{h_n^{(1)}(\rho)}\, h_n^{(1)}(kR) \right\} P_n(\cos\theta) \tag{3}$$

where $\rho = ka$. In particular, for the back scattering direction $\theta = 0$,

$$U = \sum_{n=0}^{\infty} (n+\frac{1}{2})\, e^{-in\frac{\pi}{2}} \left\{ j_n(kR) - \frac{j_n(\rho)}{h_n^{(1)}(\rho)}\, h_n^{(1)}(kR) \right\}. \tag{4}$$

* A time factor $e^{-i\omega t}$ is assumed and suppressed.

The expression for the scattered field alone can be obtained from (4) by subtracting the incident field series (2) with $\theta = 0$. In the far zone, the spherical Hankel function $h_n^{(1)}(kR)$ can then be replaced by the leading term of its asymptotic expansion for large kR to give

$$U^s \sim S \frac{e^{ikR}}{kR} ,$$

where

$$S = i \sum_{n=0}^{\infty} (-1)^n (2n+1) \frac{j_n(\rho)}{h_n^{(1)}(\rho)} \tag{5}$$

is the far field amplitude. This is the quantity of interest to us.

The above series representation of S is convergent for all (real) ρ, but the rapidity of convergence decreases with increasing ρ. If $\rho < 10$, say, the first 15 terms are sufficient to compute S to about three-digit accuracy, and for $\rho < 1$ we can expand the first few Bessel function ratios in ascending powers of ρ to give

$$S = -\rho \left\{ 1 - i\rho - \frac{5}{3}\rho^2 + \frac{1}{3} i\rho^3 + \frac{38}{45}\rho^4 + \frac{13}{45} i\rho^5 + O(\rho^6) \right\} \tag{6}$$

(Senior, 1960). This is the low frequency expansion, whose radius of convergence is determined by the zero of $h_n^{(1)}(\rho)$ closest to the origin of the complex ρ plane, and is $|\rho| = 1$.

The limited convergence of (6) is brought about by the expansion of the functions $\left\{ h_n^{(1)}(\rho) \right\}^{-1}$, and no such restriction exists with the original Mie series form (5). We can therefore use this expression to compute S for any ρ and though it would be a tedious process to do so by hand if $\rho > 10$, say, the advent of high speed digital computers has made it reasonable and economic to determine S from (5) even for values of ρ as large as 50.

Nevertheless, there is an alternative representation of S which is well suited to the larger ρ. This is certainly more convenient for hand computation if ρ

is large, and is desirable for its own sake because of the insight into the nature of the scattered field that it provides.

2.2 Resolution into Creeping Wave and Optics Components

The resolution is a natural consequence of the application of a Watson transformation, but in order that the resulting path of integration be deformable in the required manner, it is necessary to treat the total field U rather than the scattered field U^S (Franz, 1954).

Using the fact that

$$j_n(x) = \frac{1}{2}\left\{h_n^{(1)}(x) + h_n^{(2)}(x)\right\} , \tag{7}$$

equation (4) becomes

$$U = \frac{1}{2}\sum_{n=0}^{\infty}(n+\tfrac{1}{2})\, e^{-in\frac{\pi}{2}}\left\{h_n^{(2)}(kR) - \frac{h_n^{(2)}(\rho)}{h_n^{(1)}(\rho)}\, h_n^{(1)}(kR)\right\} ,$$

and this can be written as

$$U = -\frac{1}{4}\, e^{i\frac{\pi}{4}}\int_C \left\{h_{\nu-1/2}^{(2)}(kR) - \frac{h_{\nu-1/2}^{(2)}(\rho)}{h_{\nu-1/2}^{(1)}(\rho)}\, h_{\nu-1/2}^{(1)}(kR)\right\} e^{i\nu\frac{\pi}{2}} \sec\nu\pi\ \nu d\nu \tag{8}$$

where C is a path which encloses in a clockwise sense the poles of $\sec\nu\pi$ on the positive real axis. For the integral over the lower portion of C we make the substitution

$$e^{i\nu\frac{\pi}{2}} = e^{-3i\nu\frac{\pi}{2}} + e^{-i\nu\frac{\pi}{2}} \cdot 2i\sin\nu\pi . \tag{9}$$

Since

$$h_{-\nu-1/2}^{(1)}(x) = e^{i\nu\pi}\, h_{\nu-1/2}^{(1)}(x) ,$$

$$h_{-\nu-1/2}^{(2)}(x) = e^{-i\nu\pi}\, h_{\nu-1/2}^{(2)}(x)$$

(Watson, 1948; p. 74), the integrand corresponding to the first term on the right hand side of (9) is an odd function of ν, and by reflecting the path in the origin of the ν plane, we obtain

$$U = -\frac{1}{4} e^{i\frac{\pi}{4}} \int_{-\infty+i\epsilon}^{\infty+i\epsilon} \left\{ h^{(2)}_{\nu-1/2}(kR) - \frac{h^{(2)}_{\nu-1/2}(\rho)}{h^{(1)}_{\nu-1/2}(\rho)} h^{(1)}_{\nu-1/2}(kR) \right\} e^{i\nu\frac{\pi}{2}} \sec\nu\pi \; \nu d\nu$$

$$+\frac{1}{4} e^{-i\frac{\pi}{4}} \int_{\infty-i\epsilon}^{0} \left\{ h^{(2)}_{\nu-1/2}(kR) - \frac{h^{(2)}_{\nu-1/2}(\rho)}{h^{(1)}_{\nu-1/2}(\rho)} h^{(1)}_{\nu-1/2}(kR) \right\} e^{-i\nu\frac{\pi}{2}} \tan\nu\pi \; \nu d\nu \qquad (10)$$

where ϵ is some positive number.

The first integrand in (10) is an exponentially decreasing function of ν as $|\nu| \to \infty$ with Im. $\nu > 0$. We can therefore close the path in the upper half ν plane and express the integral as a sum of residues at the poles $\nu = \nu_n$, $n = 1, 2, 3, \ldots$, of $1/h^{(1)}_{\nu-1/2}(\rho)$. This constitutes the creeping wave portion of the field. The second integral in (10) can be evaluated by the steepest descents method, and contains the optics portion of the field, including the incident field itself. To separate out the scattered field and, in particular, to determine the far field amplitude, it is only necessary to replace the radial functions by the leading terms of their asymptotic expansions for large kR. The resulting expression for S is then

$$S = S^c + S^o \qquad (11)$$

where

$$S^c = i\pi \sum_n \left[\frac{H^{(2)}_\nu(\rho)}{\frac{\partial}{\partial\nu} H^{(1)}_\nu(\rho)} \nu \sec\nu\pi \right]_{\nu=\nu_n} \qquad (12)$$

and

$$S^o = i \int_{\infty-i\epsilon}^{0} \frac{H^{(2)}_\nu(\rho)}{H^{(1)}_\nu(\rho)} \tan\nu\pi \; e^{-i\nu\frac{\pi}{2}} \nu d\nu \, . \qquad (13)$$

The affices "c" and "o" denote the creeping wave and optics contributions respectively, and for brevity we have here replaced the spherical Hankel functions by their cylindrical equivalents.

2.3 Evaluation of the Creeping Wave Contribution

To find an asymptotic representation of the zeros ν_n of the cylindrical Hankel function $H_\nu^{(1)}(\rho)$, a convenient starting point is the contour integral expression

$$H_\nu^{(1)}(\rho) = -\frac{i}{\pi}\int e^{\rho \sinh w - \nu w}\, dw$$

(Watson, 1948; p. 178), where the path of integration is chosen as the series of straight line segments running from $-\infty - i\pi$ to $(3^{-1/2} - i)\pi$ to $(3^{-1/2} + i)\pi$ to $\infty + i\pi$. In terms of the large parameter ρ, let

$$x = \frac{1}{\tau}(\nu - \rho) \tag{14}$$

with $\tau = (\rho/2)^{1/3}$. Hence

$$\nu = \rho + \tau x ,$$

and if we now write $w = t/\tau$, the above integral becomes

$$-\frac{i}{\pi\tau}\int \exp\left(\frac{1}{3}t^3 - xt\right) \exp\left\{2\sum_{n=1}^{\infty} \tau^{-2n}\frac{t^{2n+3}}{(2n+3)!}\right\} dt \tag{15}$$

in which the path of integration is such that

$$\int \exp\left(\frac{1}{3}t^3 - xt\right) dt = 2\pi i \left\{Ai(x) - iBi(x)\right\}$$

where Ai(x) and Bi(x) are the Airy integrals defined by Miller (1946). Hence

$$\int t^n \exp(\tfrac{1}{3}t^3 - xt)dt = 2\pi i(-1)^n \frac{d^n}{dx^n}\left\{Ai(x) - iBi(x)\right\} ,$$

and since all derivatives of Ai(x) and Bi(x) above the first can be eliminated using the differential equation

$$f'' = xf \qquad (f = Ai \text{ or } Bi) ,$$

it follows from equation (15) that

$$J_\nu(\rho) = \frac{1}{\tau}\left[Ai(x) - \frac{1}{60\tau^2}\left\{4xAi(x) + x^2Ai'(x)\right\} + \right.$$

$$\left. + \frac{1}{2520\tau^4}\left\{\left(\frac{7}{20}x^5 + 26x^2\right)Ai(x) + (6x^3 + 18)Ai'(x)\right\} + O(\tau^{-6})\right] \tag{16}$$

with a similar formula for $Y_\nu(\rho)$ in which Ai(x) and Ai'(x) are replaced by -Bi(x) and -Bi'(x) respectively.

Equation (16) is equivalent to

$$J_\nu(\rho) = \frac{1}{\tau}\left\{1 - \frac{x}{15\tau^2} + \frac{13x^2}{1260\tau^4} + O(\tau^{-6})\right\} Ai\left\{x - \frac{x^2}{60\tau^2}\right.$$

$$\left. + \frac{8x^3 + 45}{6300\tau^4} + O(\tau^{-6})\right\}$$

as can be seen by expanding the Airy integral using Taylor's theorem, and if we now define

$$\omega^2 y = x - \frac{x^2}{60\tau^2} + \frac{8x^3 + 45}{6300\tau^4} + O(\tau^{-6}) \tag{17}$$

where $\omega = e^{2i\pi/3}$ is a cube root of unity, we have

$$H_\nu^{(1)}(\rho) = \frac{1}{-} \left\{1 - \frac{x}{15\tau^2} + \frac{13x^2}{1260\tau^4} + O(\tau^{-6})\right\} \left\{Ai(\omega^2 y) - iBi(\omega^2 y)\right\} . \qquad (18)$$

But

$$Ai(\omega^2 y) = -\frac{1}{2}\omega \left\{Ai(y) + iBi(y)\right\}$$

$$Bi(\omega^2 y) = -\frac{1}{2}\omega \left\{Bi(y) + 3iAi(y)\right\}$$

(Miller, 1946; p. B9), and hence

$$H_\nu^{(1)}(\rho) = -\frac{2\omega}{\tau} \left\{1 - \frac{x}{15\tau^2} + \frac{13x^2}{1260\tau^4} + O(\tau^{-6})\right\} Ai(y) . \qquad (19)$$

The zeros of the Hankel function $H_\nu^{(1)}(\rho)$ can therefore be expressed in terms of the zeros $y = a_n$ of the Airy integral Ai(y) using equations (14) and (17). If the second of these equations is inverted to give x as a function of y, the expansion for ν_n becomes

$$\nu_n = \rho + \omega^2 \tau a_n + \frac{\omega a_n^2}{60\tau} - \frac{a_n^3 + 10}{1400\tau^3} + O(\tau^{-5}) . \qquad (20)$$

The first 50 of the a_n have been tabulated by Miller (1946), and when arranged in ascending order of magnitude they are

$$a_1 = -2.33810\ 741\ldots$$

$$a_2 = -4.08794\ 944\ldots$$

$$a_3 = -5.52055\ 983\ldots$$

. . . . . .

All are real and negative, and in order to emphasize the negative real character of the creeping wave exponent, we shall follow the notation of Logan (1959) by writing

$$a_n = -\alpha_n .$$

The α_n are then positive and the corresponding formula for ν_n is

$$\nu_n = \rho + e^{i\frac{\pi}{3}}\tau\alpha_n - e^{-i\frac{\pi}{3}}\frac{\alpha_n^2}{60\tau} + \frac{\alpha_n^3 - 10}{1400\tau^3} + O(\tau^{-5}) . \qquad (21)$$

The coefficients of $\rho^{1/3} e^{i\frac{\pi}{3}}$ and $\rho^{-1/3} e^{-i\frac{\pi}{3}}$ in this expansion have been computed for n = 1 through 5 by Franz (1954).

We now have to find an expression for

$$\left[\frac{H_\nu^{(2)}(\rho)}{\frac{\partial}{\partial\nu} H_\nu^{(1)}(\rho)}\right]_{\nu=\nu_n} .$$

Since $H_{\nu_n}^{(1)}(\rho) = 0$, this factor is equal to

$$2\left[\frac{J_\nu(\rho)}{\frac{\partial}{\partial\nu} H_\nu^{(1)}(\rho)}\right]_{\nu=\nu_n}$$

$$= \frac{i}{2}\left[\frac{(1 - \frac{x}{15\tau^2} + \frac{13x^2}{1260\tau^4} + \ldots.)\,\mathrm{Bi}(y)}{\frac{\partial}{\partial\nu}\left\{(1 - \frac{x}{15\tau^2} + \frac{13x^2}{1260\tau^4} + \ldots.)\mathrm{Ai}(y)\right\}}\right]_{\nu=\nu_n}$$

$$= \frac{i\tau}{2}\left[\frac{\mathrm{Bi}(y)}{\frac{\partial y}{\partial x}\mathrm{Ai}'(y)}\right]_{\nu=\nu_n}$$

where we have used the fact that

$$\frac{\partial}{\partial \nu} = \frac{1}{\tau}\frac{\partial y}{\partial x}\frac{\partial}{\partial y} .$$

Moreover,

$$\frac{\partial y}{\partial x} = \omega\left\{1 - \frac{x}{30\tau^2} + \frac{2x^2}{525\tau^4} + O(\tau^{-6})\right\}$$

$$= \omega\left\{1 - \frac{\omega^2 y}{30\tau^2} + \frac{41\omega y^2}{12600\tau^4} + O(\tau^{-6})\right\}$$

and

$$\mathrm{Bi}(-\alpha_n) = -\frac{1}{\pi \mathrm{Ai}'(-\alpha_n)} .$$

Hence

$$\left[\frac{H_\nu^{(2)}(\rho)}{\frac{\partial}{\partial \nu} H_\nu^{(1)}(\rho)}\right]_{\nu=\nu_n} = -\frac{\tau}{2\pi} e^{-i\frac{\pi}{6}}\left\{1 + e^{i\frac{\pi}{3}}\frac{\alpha_n}{30\tau^2} + e^{-i\frac{\pi}{3}}\frac{3\alpha_n^2}{1400\tau^4} + O(\tau^{-6})\right\}\frac{1}{\left\{\mathrm{Ai}'(-\alpha_n)\right\}^2}$$

from which it follows that

$$\left[\frac{\nu H_\nu^{(2)}(\rho)}{\frac{\partial}{\partial \nu} H_\nu^{(1)}(\rho)}\right]_{\nu=\nu_n} = -\frac{\tau^4}{\pi} e^{-i\frac{\pi}{6}}\left\{1 + e^{i\frac{\pi}{3}}\frac{8\alpha_n}{15\tau^2} - e^{-i\frac{\pi}{3}}\frac{4\alpha_n^2}{175\tau^4} + O(\tau^{-6})\right\}\frac{1}{\left\{\mathrm{Ai}'(-\alpha_n)\right\}^2} \tag{22}$$

Each of the zeros ν_n corresponds to a single mode in the creeping wave development of S^c, and to complete the representation in terms of physically meaningful quantities, we expand $\sec \nu\pi$ as

$$\sec \nu\pi = 2\sum_{\ell=0}^{\infty}(-1)^\ell e^{i(2\ell+1)\nu\pi} , \tag{23}$$

which is convergent since $\mathrm{Im}.\nu_n > 0$. Substituting from equations (21), (22) and (23) into equation (12), we now have

$$S^c = -2\tau^4 e^{i\frac{\pi}{3}} \sum_n \left\{ 1 + e^{i\frac{\pi}{3}} \frac{8\alpha_n}{15\tau^2} - e^{-i\frac{\pi}{3}} \frac{4\alpha_n^2}{175\tau^4} + O(\tau^{-6}) \right\} \cdot \frac{1}{\left\{ Ai'(-\alpha_n) \right\}^2}$$

$$\cdot \sum_{\ell=0}^{\infty} (-1)^\ell \exp\left[i(2\ell+1)\pi \left\{ \rho + e^{i\frac{\pi}{3}} \tau\alpha_n - e^{-i\frac{\pi}{3}} \frac{\alpha_n^2}{60\tau} + \frac{\alpha_n^3 - 10}{1400\tau^3} + O(\tau^{-5}) \right\} \right] . \qquad (24)$$

The interpretation of the various factors in this expression is discussed in Section 2.5, where we also explore the extent to which equation (24) can be simplified without loss of numerical accuracy.

2.4 Evaluation of the Optics Contribution

The optics portion of the far field amplitude is given by equation (13), and if $\tan\nu\pi$ is replaced by its exponential form, the expression for S^o can be written as

$$S^o = \int_{-\infty + i\epsilon}^{\infty - i\epsilon} \frac{H_\nu^{(2)}(\rho)}{H_\nu^{(1)}(\rho)} \frac{e^{-i\nu\pi}}{1 + e^{2i\nu\pi}} \nu d\nu . \qquad (25)$$

To evaluate this integral we note that if the Hankel functions are approximated under the assumption that the order is less than the argument, with the latter large compared with unity, a steepest descents analysis is appropriate and the saddle point is $\nu = 0$. This is evident from the Debye formula

$$H_\nu^{(1)}(\rho) = \sqrt{\frac{2}{\pi\rho\sin\beta}}\, e^{i\rho(\sin\beta - \beta\cos\beta) - i\frac{\pi}{4}} \sum_{m=0}^{\infty} \frac{(m - \frac{1}{2})!}{(-\frac{1}{2})!} \left(\frac{-2i}{\rho\sin\beta} \right)^m A_m \qquad (26)$$

(Watson, 1948; p. 244) in which

$$\nu = \rho \cos\beta \, .$$

The A_m are functions of $\cot^2\beta$ only, and are real. In particular,

$$A_o = 1$$

$$A_1 = \frac{1}{8}\left(1 + \frac{5}{3}\cot^2\beta\right)$$

$$A_2 = \frac{1}{128}\left(3 + \frac{154}{9}\cot^2\beta + \frac{385}{27}\cot^4\beta\right)$$

and using the scheme which Watson (1948; p. 242) describes for the generation of the coefficients, it can be shown that

$$A_3 = \frac{1}{2^{10}}\left\{5 + \left(\frac{39}{5}\right)^2 \cot^2\beta + \frac{7\cdot 11\cdot 13\cdot 17}{3^5}\cot^4\beta\left(\frac{9}{5} + \cot^2\beta\right)\right\} .$$

In terms of these coefficients,

$$H_\nu^{(1)}(\rho) = \sqrt{\frac{2}{\pi\rho\sin\beta}}\, e^{i\rho(\sin\beta - \beta\cos\beta) - i\frac{\pi}{4}}\left\{1 - \frac{i}{\rho\sin\beta}A_1 - \frac{3}{(\rho\sin\beta)^2}A_2 + \frac{15i}{(\rho\sin\beta)^3}A_3 + O(\rho^{-4})\right\} \qquad (27)$$

from which it follows that

$$\frac{H_\nu^{(2)}(\rho)}{H_\nu^{(1)}(\rho)} = ie^{-2i\rho(\sin\beta - \beta\cos\beta)}\left\{1 + \frac{2i}{\rho\sin\beta}A_1 - \frac{2}{(\rho\sin\beta)^2}A_1^2 - \frac{2i}{(\rho\sin\beta)^3}(A_1^3 - 3A_1A_2 + 15A_3) + \frac{2}{(\rho\sin\beta)^4}A_1(A_1^3 - 6A_1A_2 + 30A_3) + O(\rho^{-5})\right\} \qquad (28)$$

A knowledge of the A_m through $m = 3$ therefore serves to determine the Hankel function ratio correct to ρ^{-4}.

In order to apply the method of steepest descents, it is necessary to expand the right hand side of (28) in a neighborhood of $\nu = 0$. Using the definition of β, the exponential factor can be written as

$$\exp\left\{i\nu\pi - 2i\rho\sqrt{1-(\nu/\rho)^2} - 2i\nu\sin^{-1}\nu/\rho\right\}$$
$$= \exp\left(i\nu\pi - 2i\rho - i\frac{\nu^2}{\rho}\right)\left\{1+.....\right\} \qquad (29)$$

where the terms represented by the dots are produced by the higher order terms in the expansions of the square root and inverse sine. To achieve an expression for S^o correct to the first five orders in ρ, we have to include all terms of the form $\nu^{2m}\rho^{-n}$ for $m \geqslant n-4$, and the terms that then appear on the right hand side of (29) are

$$1 - \frac{i}{12}\frac{\nu^4}{\rho^3} - \frac{\nu^6}{\rho^5}\left(\frac{i}{40} + \frac{1}{288}\frac{\nu^2}{\rho}\right)$$
$$- \frac{\nu^8}{\rho^7}\left(\frac{5i}{2^6\cdot 7} + \frac{1}{480}\frac{\nu^2}{\rho} - \frac{i}{2^7\cdot 3^4}\frac{\nu^4}{\rho^2}\right)$$
$$- \frac{\nu^{10}}{\rho^9}\left(\frac{7i}{2^7\cdot 3^2} + \frac{167}{2^8\cdot 3\cdot 5^2}\frac{\nu^2}{\rho} + \frac{i}{2^8\cdot 3^2\cdot 5}\frac{\nu^4}{\rho^2} - \frac{1}{2^{11}\cdot 3^5}\frac{\nu^6}{\rho^3}\right)$$

where we have grouped them according to the powers of ρ produced. Similarly, by expanding $\sin\beta$ and the A_m to the required order, the bracketed terms on the right hand side of (28) become

$$1 + \frac{i}{4\rho}\left\{1 + \frac{13}{6}\left(\frac{\nu}{\rho}\right)^2 + \frac{69}{24}\left(\frac{\nu}{\rho}\right)^4 + \frac{55}{16}\left(\frac{\nu}{\rho}\right)^6\right\} - \frac{1}{32\rho^2}\left\{1 + \frac{13}{3}\left(\frac{\nu}{\rho}\right)^2 + \frac{94}{9}\left(\frac{\nu}{\rho}\right)^4\right\}$$
$$- \frac{i}{2^7\rho^3}\left\{17 + \frac{7187}{30}\left(\frac{\nu}{\rho}\right)^2\right\} + \frac{67}{2^{11}\rho^4} ,$$

and if the resulting expansion for the Hankel function ratio is now inserted into (25), we have, after some simplification,

$$S^o = -\frac{\rho}{2} e^{-2i\rho} \left[\left\{ 1 + \frac{i}{4\rho} - \frac{1}{32\rho^2} - \frac{17i}{2^7 \rho^3} + \frac{67}{2^{11} \rho^4} \right\} I_o \right.$$

$$+ \frac{13i}{24\rho^3} \left\{ 1 + \frac{i}{4\rho} - \frac{7187}{2^5 \cdot 5 \cdot 13 \rho^2} \right\} I_1$$

$$- \frac{i}{12\rho^3} \left\{ 1 + \frac{i}{4\rho} - \frac{277}{2^5 \rho^2} - \frac{1555i}{2^7 \cdot 3 \rho^3} \right\} I_2$$

$$- \frac{i}{40\rho^5} \left\{ 1 + \frac{37i}{18\rho} - \frac{10039}{2^5 \cdot 3^2 \rho^2} \right\} I_3$$

$$- \frac{1}{288\rho^6} \left\{ 1 + \frac{97i}{28\rho} - \frac{24623}{2^5 \cdot 5 \cdot 7 \rho^2} \right\} I_4$$

$$- \frac{1}{480\rho^8} \left\{ 1 + \frac{293i}{72\rho} \right\} I_5 + \frac{i}{2^7 \cdot 3^4 \rho^9} \left\{ 1 + \frac{9193i}{700\rho} \right\} I_6$$

$$\left. + \frac{i}{2^8 \cdot 45 \rho^{11}} I_7 + \frac{1}{2^{11} 3^5} I_8 + O(\rho^{-5}) \right] \qquad (30)$$

where

$$I_n = -\frac{2i}{\rho} \int_{-\infty + i\epsilon}^{\infty - i\epsilon} e^{-i\nu^2/\rho} \frac{\nu^{2n+1}}{1 + e^{2i\nu\pi}} d\nu \, . \qquad (31)$$

Scott (1949), in an appendix to his report, has considered the integral

$$\phi_n(\epsilon) = \int_{-\infty e^{i\beta}}^{\infty e^{i\beta}} e^{-\epsilon u^2} \frac{u^{2n+1}}{1 + e^{-u}} du \, , \qquad (32)$$

in which $|\beta| < \pi/2$ and $-\pi/2 - \arg\varepsilon < 2\beta < \pi/2 - \arg\varepsilon$, and has shown that*

$$\phi_n(\varepsilon) = \frac{n!}{2\varepsilon^{n+1}} - \sum_{j=0} \frac{(2^{2j+2n+1} - 1)\pi^{2j+2n+2}}{j!(j+n+1)} (-\varepsilon)^j B_{j+n+1} \tag{33}$$

where the B_m are Bernoulli numbers, i.e.

$$B_1 = \frac{1}{6}, \quad B_2 = \frac{1}{30}, \quad B_3 = \frac{1}{42}, \quad B_4 = \frac{1}{30}, \ldots\ldots$$

Equation (32), however, can also be written as

$$\phi_n(\varepsilon) = (2i\pi)^{2n+2} \int_{-\infty e^{i(\frac{\pi}{2}+\beta)}}^{\infty e^{i(\frac{\pi}{2}+\beta)}} e^{4\pi^2 \varepsilon \nu^2} \frac{\nu^{2n+1}}{1+e^{2i\nu\pi}} \, d\nu$$

and hence, by comparison with (31),

$$I_n = \frac{1}{\pi\rho(2i\pi)^{2n+1}} \phi_n\left(\frac{1}{4i\pi^2\rho}\right) . \tag{34}$$

It now follows that

$$I_n = (-i\rho)^n n! \left\{1 + (-1)^n \sum_{j=0} \frac{(1 - 2^{-2j-2n-1})}{j!\,n!\,(j+n+1)} \frac{B_{j+n+1}}{(-i\rho)^{j+n+1}}\right\} \tag{35}$$

and for the first few values of n we have

$$I_o = 1 + \frac{i}{12\rho} - \frac{7}{480\rho^2} - \frac{31}{2^7 3^2 7} \frac{i}{\rho^3} + \frac{127}{2^{11} 3^2 5} \frac{1}{\rho^4} + O(\rho^{-5})$$

$$I_1 = -i\rho \left\{1 + \frac{7}{480\rho^2} + O(\rho^{-3})\right\}$$

---

* Note the $(-1)^j$ error in Scott's formula.

$$I_2 = -2\rho^2 \left\{1 - \frac{31i}{2^7 3^2 7\rho^3} + O(\rho^{-4})\right\}$$

where the terms displayed are those required for use in equation (30). For $n > 2$ the leading term in (35) is sufficient.

When the above formulae are inserted into equation (30), the expression for the optics contribution S^o reduces to

$$S^o = -\frac{\rho}{2} e^{-2i\rho} \left\{1 + \frac{i}{2\rho} + \frac{1}{2\rho^2} - \frac{5i}{4\rho^3} - \frac{5}{\rho^4} + O(\rho^{-5})\right\} . \qquad (36)$$

In view of the large numbers appearing throughout the analysis, the simplicity of the final result is gratifying, but even so there is no obvious relation between the coefficients of successive powers of ρ. The first three terms in (36) were previously obtained by Keller et al (1956) using the Kline-Luneberg expansion technique.

2.5 Numerical Considerations

Although the expressions we have derived for S^c and S^o are only asymptotic for large ρ, they (and the pseudo-physical theories which they inspire) are generally our only means for predicting the scattering behavior of bodies whose radii of curvature are comparable with the wavelength. It is therefore important to have some feeling for the accuracy with which they reproduce the far field amplitude not only for $\rho \gg 1$, but also for values as small as 3 or even 1.

Bearing in mind the phase origin of the incident field at the center of the sphere, the phase of the optics component S^o identifies it as a return from the front face, and it is natural to regard the whole expression as a representation of the "specular" contribution. The leading term in S^o is that provided by geometrical optics. The rise in the coefficients of the successive powers of ρ should be noted, and whereas the second real term, $1/2\rho^2$, produces a correction to the first (unity) term exceeding 10 percent if $\rho < 2.23$, the third real term corrects the second one by more than 10 percent if $\rho < 5$.

The other component S^c is made up of creeping wave returns, and to judge from the phase of a typical term, the corresponding wave contributes to the back scattered field after having traveled around the rear of the sphere. It is presumed that the waves are launched in the vicinity of the shadow boundary and henceforth travel independently, radiating energy in the tangential direction as they proceed. As a consequence of the radiation, the amplitude of a wave decreases, and this decay is evidenced by the negative real part of the exponent. When the wave reaches the region of the shadow boundary diametrically opposite to that in which it was launched, the radiated energy is in the back scattering direction and contributes to S^c. The wave, however, continues to travel around the surface, passing through the lit region and into the shadow once again, but it is not until it has traveled a further 2π radians that it can once more radiate in the back scattering direction. Such repeated contributions, produced by waves which have traveled more than the minimum distance around the surface, are represented by the summation over ℓ.

Each individual creeping wave is generated by a zero $\nu=\nu_n$ of the Hankel function $H_\nu^{(1)}(\rho)$. The rate of attenuation and, hence, the magnitude of the contribution to S^c, are determined by $\text{Im.}\nu_n$, and due to the manner in which the zeros have been ordered, the dominant wave is that corresponding to $n=1$, the sub-dominant one to $n=2$, and so on.

Because of the asymptotic nature of the analysis in Section 2.3, the expression for S^c is "complete" only to the extent that the asymptotic formula for ν_n is. Nevertheless, it is seldom necessary to retain the full complexity of equation (24), and for most numerical work a far simpler version is sufficient. In the first place, the attenuation of all waves including the dominant one is large enough for us to omit the contributions resulting from waves which have completed one or more circuits of the sphere. Only the leading term ($\ell=0$) in the second summation then remains. We can also neglect all waves except the dominant one, and to illustrate the error thereby incurred, the contribution of the sub-dominant wave is less than 1 percent of that for the dominant wave if $\rho > 1.81$.

Both of the infinite sums in equation (24) have now been removed, leaving an expression for S^c based on a single wave alone, but even this can be simplified without significant loss of accuracy. In the exponent, the term involving $(\alpha_1^3 - 10)$ does not contribute to the amplitude, and for $\rho = 10$ its effect on the phase is only 0.07^o. Since the phase contribution is still less than 1^o for $\rho = 1$, the term can certainly be neglected. The preceding term in the exponent is, however, more important. When $\rho = 10$ it produces a 13 percent variation in the amplitude of the creeping wave component, and a 4.8^o change in phase. Both figures increase rapidly with decreasing ρ and the term will therefore be retained, but we can omit the third term in the factor multiplying the exponential. For $\rho = 10$ this contributes 0.3 percent in amplitude and 0.6^o in phase, and the expression for S^c resulting from all these simplifications is

$$S^c = -2\tau^4 e^{i\frac{\pi}{3}} \left\{ 1 + e^{i\frac{\pi}{3}} \frac{8\alpha_1}{15\tau^2} + O(\tau^{-4}) \right\} \cdot \frac{1}{\left\{ Ai'(-\alpha_1) \right\}^2}$$

$$\cdot \exp\left\{ i\pi\rho - e^{-i\frac{\pi}{6}} \tau\pi\alpha_1 - e^{i\frac{\pi}{6}} \frac{\pi\alpha_1^2}{60\tau} + O(\tau^{-3}) \right\} \qquad (37)$$

where

$$\alpha_1 = 2.33810\ 741....$$

$$Ai'(-\alpha_1) = 0.70121\ 082....$$

This is an accurate approximation to (24) (if not to the "exact" expression for S^o shown in equation 12) for ρ greater than (about) unity, and is the formula that we shall employ henceforth.

In terms of the far field amplitude S, the back scattering cross section σ is given by

$$\sigma = \frac{\lambda^2}{\pi} |S|^2 . \qquad (38)$$

As $\rho \to \infty$, $|S| \to \rho/2$ (see equation 36), and for numerical purposes it is convenient to normalize the cross section with respect to its high frequency limit πa^2. We therefore introduce a normalized far field amplitude G which is related to S by the equation

$$G = \frac{2}{\rho} S, \tag{39}$$

from which we have

$$\frac{\sigma}{\pi a^2} = |G|^2 . \tag{40}$$

$|G|$ is, in effect, a voltage gain factor.

The creeping wave and optics components of G are, from equations (37) and (36) respectively,

$$G^c = -2\tau e^{i\frac{\pi}{3}} \left\{ 1 + e^{i\frac{\pi}{3}} \frac{8\alpha_1}{15\tau^2} + O(\tau^{-4}) \right\} \frac{1}{\left\{ Ai'(-\alpha_1) \right\}^2}$$

$$\cdot \exp\left\{ i\pi\rho - e^{-i\frac{\pi}{6}} \tau\pi\alpha_1 - e^{i\frac{\pi}{6}} \frac{\pi\alpha_1^2}{60\tau} + O(\tau^{-3}) \right\} \tag{41}$$

and

$$G^o = -e^{-2i\rho} \left\{ 1 + \frac{i}{2\rho} + \frac{1}{2\rho^2} - \frac{5i}{4\rho^3} - \frac{5}{\rho^4} + O(\rho^{-5}) \right\} \tag{42}$$

whilst the Mie series representation of G is (see equation 5)

$$G = \frac{2i}{\rho} \sum_{n=0}^{\infty} (-1)^n (2n+1) \frac{j_n(\rho)}{h_n^{(1)}(\rho)} . \tag{43}$$

To provide data with which to asses the numerical effectiveness of the high frequency approximations (41) and (42), the expression for G shown in equation (43)

was programmed for evaluation on the IBM 7090 computer of The University of Michigan. Computations were carried out for $\rho = 0.1(0.1)10.0$ using a maximum of 21 terms in the series, and in Table 1 the real and imaginary parts of G are listed, along with the values of $|G|$ and $|G|^2$. The normalized cross section $|G|^2$ is also plotted as a function of ρ in Fig. 1. We observe that it exceeds unity throughout the entire range, increasing slowly as ρ decreases to about unity, and thereafter more rapidly. As $\rho \to 0$, $|G|^2 \to 4$ (see equations 6 and 39). For $\rho > 3$ there is only the barest trace of any oscillation, and since the presence of a significant creeping wave contribution must inevitably produce an oscillation whose period (in ρ) is approximately 1.2, it would appear that for most of the range G is dominated by its optics component G^o.

Although the concept of creeping waves is generally regarded as a high frequency one, and certainly the expressions for G^c and G^o shown in equations (41) and (42) cannot be presumed valid for ρ comparable with unity, it is nevertheless of interest to examine the numerical effectiveness of these formulae when ρ is not large.

In Table 2 the amplitude and phase of G^c computed from equation (41) are listed for selected values of ρ in the range $0.5 \leqslant \rho \leqslant 10.0$. The amplitude increases by over two orders of magnitude as ρ decreases from 10 to 1 and though it is still small compared with $|G|$, it is sufficient to account for the oscillations in Fig. 1. This can be seen by subtracting G^c from G. For ease of comparison with the optics component a factor $e^{2i\rho}$ is also removed, and in Table 3 the real and imaginary parts of $(G - G^c)e^{2i\rho}$, computed from the data in Tables 1 and 2, are presented. These are plotted as functions of ρ in Fig. 2, and the feature to note is that the curves are quite smooth.

By definition,

$$(G - G^c)\, e^{2i\rho} = G^o e^{2i\rho} , \qquad (44)$$

Table 1: Exact Far Field Amplitude

ρ	Re. G	Im. G	$\|G\|$	$\|G\|^2$
.1	-1.966834	0.199328	1.976909	3.908169
.2	-1.869310	0.394491	1.910483	3.649945
.3	-1.713041	0.580755	1.808808	3.271786
.4	-1.506497	0.752535	1.683996	2.835843
.5	-1.260030	0.903553	1.550511	2.404084
.6	-0.984965	1.027322	1.423217	2.025547
.7	-0.692902	1.117785	1.315126	1.729556
.8	-0.395224	1.169920	1.234874	1.524914
.9	-0.102749	1.180216	1.184680	1.403467
1.0	0.174531	1.146995	1.160198	1.346059
1.1	0.427669	1.070575	1.152837	1.329033
1.2	0.648955	0.953295	1.153219	1.329914
1.3	0.832062	0.799426	1.153867	1.331409
1.4	0.972175	0.614970	1.150353	1.323312
1.5	1.066070	0.407377	1.141255	1.302463
1.6	1.112159	0.185185	1.127471	1.271191
1.7	1.110493	-0.042385	1.111302	1.234992
1.8	1.062736	-0.265868	1.095487	1.200092
1.9	0.972076	-0.475985	1.082356	1.171495
2.0	0.843120	-0.664069	1.073238	1.151840
2.1	0.681726	-0.822446	1.068254	1.141167
2.2	0.494805	-0.944759	1.066491	1.137403
2.3	0.290092	-1.026235	1.066448	1.137311
2.4	0.075870	-1.063867	1.066569	1.137569
2.5	-0.139309	-1.056515	1.065659	1.135629
2.6	-0.346939	-1.004929	1.063132	1.130250
2.7	-0.538860	-0.911690	1.059032	1.121549
2.8	-0.707566	-0.781067	1.053905	1.110716
2.9	-0.846486	-0.618819	1.048559	1.099476
3.0	-0.950237	-0.431935	1.043800	1.089518
3.1	-1.014836	-0.228327	1.040204	1.082024
3.2	-1.037854	-0.016499	1.037985	1.077413
3.3	-1.018524	0.194805	1.036986	1.075340
3.4	-0.957768	0.396959	1.036772	1.074896

Table 1: (continued)

ρ	Re. G	Im. G	$\|G\|$	$\|G\|^2$
3.5	-0.858167	0.581791	1.036789	1.074931
3.6	-0.723862	0.741907	1.036533	1.074401
3.7	-0.560383	0.870974	1.035676	1.072625
3.8	-0.374436	0.963959	1.034127	1.069419
3.9	-0.173621	1.017313	1.032022	1.065069
4.0	0.033868	1.029100	1.029657	1.060194
4.1	0.239584	0.999057	1.027382	1.055514
4.2	0.435165	0.928593	1.025501	1.051652
4.3	0.612682	0.820722	1.024190	1.048965
4.4	0.764958	0.679938	1.023462	1.047474
4.5	0.885857	0.512023	1.023186	1.046910
4.6	0.970538	0.323820	1.023134	1.046803
4.7	1.015640	0.122959	1.023056	1.046644
4.8	1.019423	-0.082458	1.022752	1.046022
4.9	0.981827	-0.284148	1.022118	1.044725
5.0	0.904470	-0.474027	1.021160	1.042768
5.1	0.790578	-0.644482	1.019985	1.040369
5.2	0.644844	-0.788695	1.018756	1.037864
5.3	0.473238	-0.900913	1.017644	1.035599
5.4	0.282756	-0.976667	1.016775	1.033831
5.5	0.081136	-1.012963	1.016207	1.032677
5.6	-0.123458	-1.008386	1.015916	1.032085
5.7	-0.322764	-0.963169	1.015810	1.031870
5.8	-0.508758	-0.879171	1.015764	1.031777
5.9	-0.673971	-0.759812	1.015653	1.031551
6.0	-0.811790	-0.609928	1.015389	1.031015
6.1	-0.916718	-0.435580	1.014939	1.030101
6.2	-0.984592	-0.243806	1.014328	1.028861
6.3	-1.012745	-0.042342	1.013630	1.027446
6.4	-1.000109	0.160694	1.012936	1.026039
6.5	-0.947252	0.357126	1.012336	1.024824
6.6	-0.856354	0.539052	1.011889	1.023919
6.7	-0.731114	0.699160	1.011609	1.023353

Table 1: (continued)

ρ	Re. G	Im. G	$\|G\|$	$\|G\|^2$
6.8	-0.576602	0.831025	1.011470	1.023072
6.9	-0.399053	0.929361	1.011412	1.022954
7.0	-0.205612	0.990239	1.011361	1.022851
7.1	-0.004057	1.011243	1.011251	1.022629
7.2	0.197523	0.991558	1.011041	1.022204
7.3	0.391041	0.932012	1.010722	1.021559
7.4	0.568746	0.835031	1.010321	1.020749
7.5	0.723521	0.704545	1.009884	1.019866
7.6	0.849176	0.545826	1.009468	1.019026
7.7	0.940692	0.365273	1.009121	1.018325
7.8	0.994418	0.170154	1.008870	1.017819
7.9	1.008220	-0.031682	1.008717	1.017510
8.0	0.981566	-0.232130	1.008640	1.017355
8.1	0.915542	-0.423146	1.008598	1.017270
8.2	0.812814	-0.597076	1.008547	1.017167
8.3	0.677517	-0.746954	1.008449	1.016969
8.4	0.515089	-0.866790	1.008286	1.016641
8.5	0.332054	-0.951800	1.008059	1.016183
8.6	0.135758	-0.998601	1.007787	1.015635
8.7	-0.065922	-1.005342	1.007501	1.015058
8.8	-0.264899	-0.971781	1.007238	1.014528
8.9	-0.453195	-0.899285	1.007024	1.014097
9.0	-0.623265	-0.790781	1.006873	1.013793
9.1	-0.768299	-0.650633	1.006780	1.013606
9.2	-0.882491	-0.484473	1.006729	1.013503
9.3	-0.961277	-0.298965	1.006694	1.013433
9.4	-1.001511	-0.101546	1.006645	1.013334
9.5	-1.001595	0.099876	1.006562	1.013167
9.6	-0.961542	0.297236	1.006436	1.012913
9.7	-0.882974	0.482636	1.006270	1.012579
9.8	-0.769051	0.648658	1.006080	1.012197
9.9	-0.624352	0.788665	1.005886	1.011807
10.0	-0.454685	0.897059	1.005711	1.011455

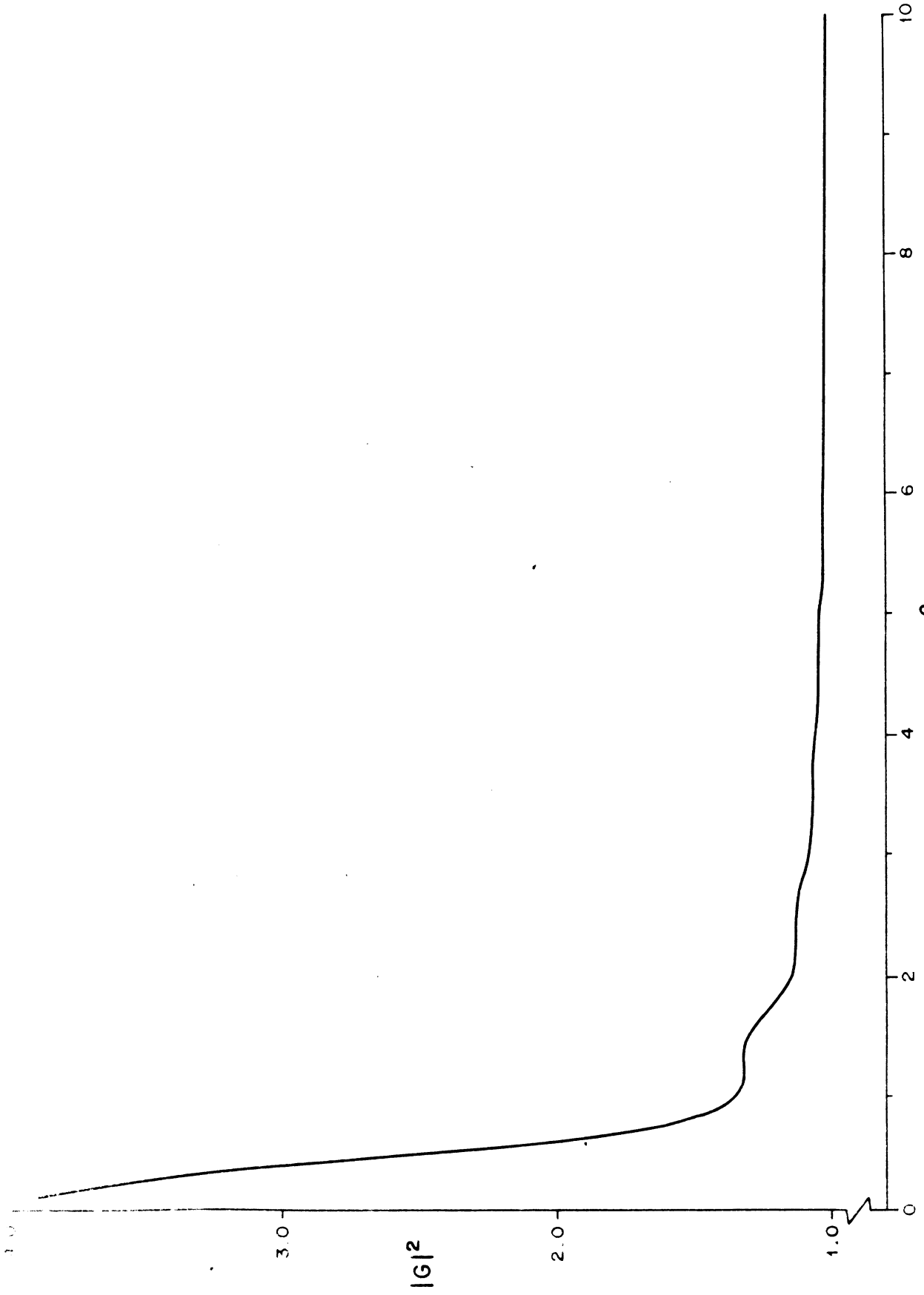

FIG. 1: NORMALIZED BACK SCATTERING CROSS SECTION OF A SOFT SPHERE

Table 2: Theoretical Creeping Wave Component

ρ	$\lvert G\rvert^c$	$\arg G^c$ (degrees)
0.5	$1.17675 \cdot 10^{-1}$	136.170
0.6	$9.02871 \cdot 10^{-2}$	161.840
0.7	$7.13842 \cdot 10^{-2}$	186.613
0.8	$5.77547 \cdot 10^{-2}$	210.713
0.9	$4.75916 \cdot 10^{-2}$	234.285
1.0	$3.98081 \cdot 10^{-2}$	257.433
1.1	$3.37156 \cdot 10^{-2}$	280.231
1.3	$2.49285 \cdot 10^{-2}$	324.985
1.5	$1.90295 \cdot 10^{-2}$	368.360
2.0	$1.06908 \cdot 10^{-2}$	475.861
2.5	$6.61027 \cdot 10^{-3}$	580.256
3.0	$4.36000 \cdot 10^{-3}$	682.899
3.5	$3.01265 \cdot 10^{-3}$	784.265
4.0	$2.15688 \cdot 10^{-3}$	884.650
4.5	$1.58813 \cdot 10^{-3}$	984.252
5.0	$1.19521 \cdot 10^{-3}$	1083.221
5.5	$9.18489 \cdot 10^{-4}$	1181.626
6.0	$7.16587 \cdot 10^{-4}$	1279.580
6.5	$5.60845 \cdot 10^{-4}$	1377.134
7.0	$4.53818 \cdot 10^{-4}$	1474.334
7.5	$3.67190 \cdot 10^{-4}$	1571.223
8.0	$2.99901 \cdot 10^{-4}$	1667.831
8.5	$2.47008 \cdot 10^{-4}$	1764.188
9.0	$2.04990 \cdot 10^{-4}$	1860.317
9.5	$1.71278 \cdot 10^{-4}$	1956.236
10.0	$1.44105 \cdot 10^{-4}$	2051.992

Table 3: Comparison of Optics Components

	$(G-G^c)e^{2i\rho}$		5-term optics		3-term optics	
ρ	Real	Imag.	Real	Imag.	Real	Imag.
0.5	-1.32667	-0.54468	77.00000	9.00000	-3.00000	-1.00000
0.6	-1.25710	-0.47601	36.19154	4.95370	-2.38888	-0.83333
0.7	-1.21534	-0.42156	18.80425	2.93003	-2.02041	-0.71429
0.8	-1.18882	-0.38045	10.42578	1.81641	-1.78125	-0.62500
0.9	-1.16995	-0.34993	6.00351	1.15912	-1.61728	-0.55556
1.0	-1.15452	-0.32691	3.50000	0.75000	-1.50000	-0.50000
1.1	-1.14054	-0.30863	2.00184	0.48460	-1.41322	-0.45455
1.3	-1.11497	-0.27887	0.45478	0.18434	-1.29586	-0.38462
1.5	-1.09386	-0.25261	-0.23457	0.03704	-1.22222	-0.33333
2.0	-1.06400	-0.20125	-0.81250	-0.09375	-1.12500	-0.25000
2.5	-1.04711	-0.16973	-0.95200	-0.12000	-1.08000	-0.20000
3.0	-1.03568	-0.14572	-0.99383	-0.12037	-1.05555	-0.16667
3.5	-1.02841	-0.12810	-1.00750	-0.11370	-1.04082	-0.14286
4.0	-1.02281	-0.11409	-1.01172	-0.10547	-1.03125	-0.12500
4.5	-1.01894	-0.10282	-1.01250	-0.09739	-1.02469	-0.11111
5.0	-1.01583	-0.09360	-1.01200	-0.09000	-1.02000	-0.10000
5.5	-1.01349	-0.08581	-1.01106	-0.08340	-1.01653	-0.09091
6.0	-1.01160	-0.07927	-1.01003	-0.07755	-1.01389	-0.08333
6.5	-1.01008	-0.07358	-1.00903	-0.07237	-1.01183	-0.07692
7.0	-1.00885	-0.06868	-1.00812	-0.06778	-1.01020	-0.07143
7.5	-1.00781	-0.06437	-1.00731	-0.06370	-1.00889	-0.06667
8.0	-1.00687	-0.06057	-1.00659	-0.06006	-1.00781	-0.06250
8.5	-1.00623	-0.05718	-1.00596	-0.05679	-1.00692	-0.05882
9.0	-1.00562	-0.05414	-1.00541	-0.05384	-1.00617	-0.05556
9.5	-1.00509	-0.05141	-1.00493	-0.05117	-1.00554	-0.05263
10.0	-1.00462	-0.04893	-1.00450	-0.04875	-1.00500	-0.05000

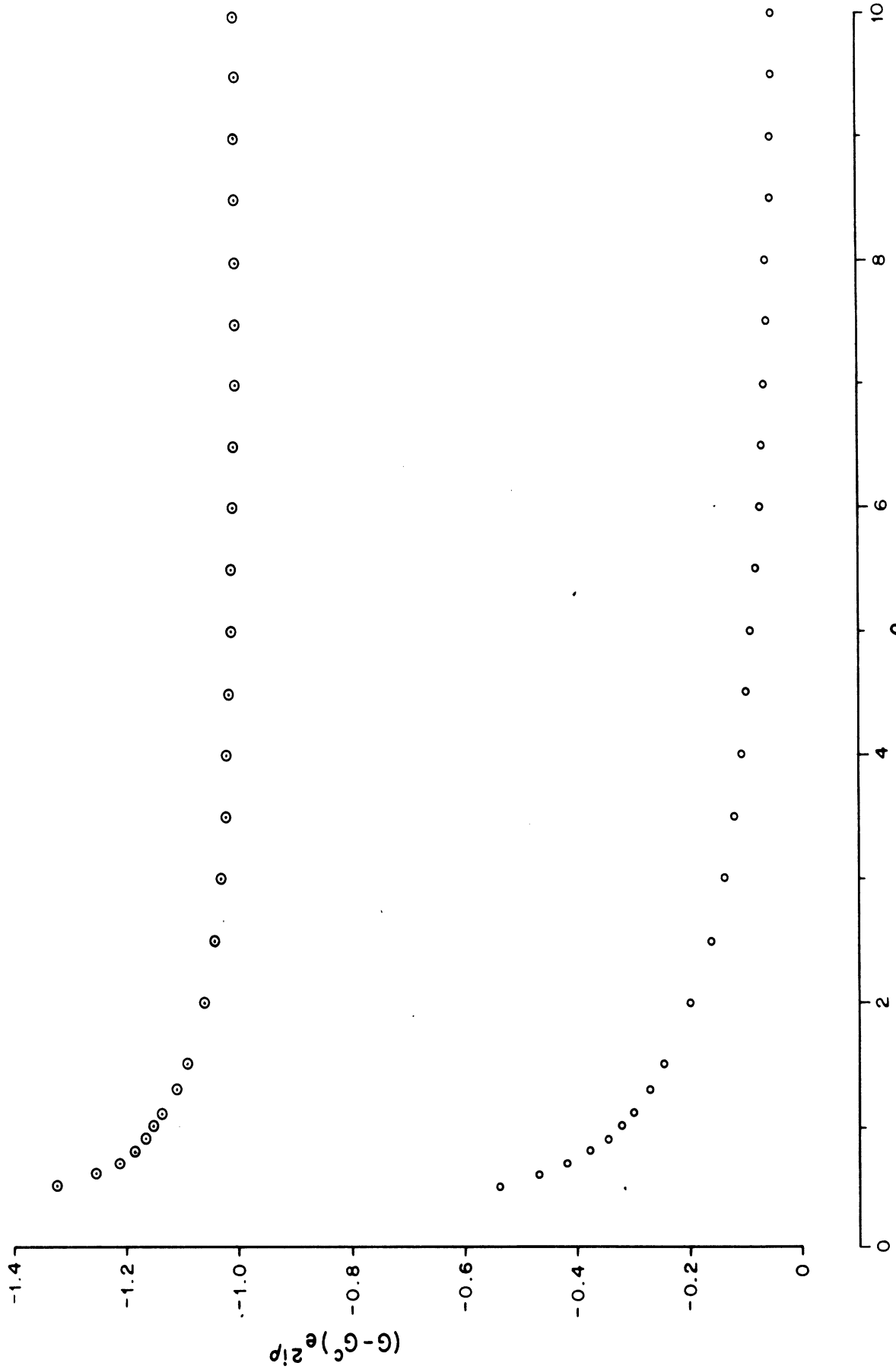

FIG. 2: REAL (⊙⊙⊙) AND IMAGINARY (∘∘∘) PARTS OF THE "ACTUAL" OPTICS CONTRIBUTION

and from the absence of any oscillations in Fig. 2, even for ρ as small as unity (or less), it seems reasonable to conclude that these curves provide a valid estimate of the "actual" optics contribution for most (if not all) of the range considered. From equation (42), however,

$$G^o e^{2i\rho} = -\left\{1 + \frac{i}{2\rho} + \frac{1}{2\rho^2} - \frac{5i}{4\rho^3} - \frac{5}{\rho^4} + O(\rho^{-5})\right\} \qquad (45)$$

and the real and imaginary parts of this expression are also included in Table 3 under the heading "5-term optics". Since (45) is derived from the exact asymptotic expansion of the optics component, it is not surprising that computations based on it are accurate when ρ is large. For $\rho = 10$ the agreement between corresponding columns in Table 3 are extremely good, and the real and imaginary parts of (45) are in error by only 0.01 and 0.02 percent respectively. As ρ decreases, the errors increase, with those for the imaginary part being greater. For $\rho = 5$ the errors are 0.38 and 3.9 percent, rising to 9.1 and 29.3 percent when $\rho = 2.5$. The expression for the optics component given in (45) is now underestimating the real and imaginary parts of the "actual" component by significant amounts, and if ρ is decreased still further, the 5-term optics expression ceases to have any relevance. Indeed, the imaginary part of (45) changes sign when $\rho = 1.581$; the real part suffers a similar change when $\rho = 1.414$, and thereafter both increase without limit.

The main reason for the "failure" of (45) when ρ is less than (about) 3 is the relatively large magnitude of the coefficients of the higher powers of ρ. These terms provide little contribution for $\rho \sim 10$, but are disastrous for $\rho \sim 1$. Can we therefore do better by ignoring them completely? To answer this question, the real and imaginary parts of $G^o e^{2i\rho}$ were computed using only the first three terms on the right hand side of (45), and the results are shown in Table 3 under the heading "3-term optics". For the largest values of ρ, the agreement with the "actual" component is somewhat poorer (errors of 0.04 and 2.2 percent in the real and imaginary

parts respectively when $\rho = 10$), but as ρ decreases below (about) 6 the 3-term expression becomes progressively more superior. Even when $\rho = 1$ the real and imaginary parts are in error by only 29.9 and 52.9 percent, and for many purposes the errors when $\rho = 0.7$ (66.2 and 69.4 percent) are not intolerable.

For the entire range of ρ, the 3-term expression overestimates the real part of the optics component, and this suggests that the agreement could be improved still further by using a 2-term expression instead. The values in the next to the last column in Table 3 would then be replaced by -1 throughout. The error in the real part for $\rho = 10$ is thereby increased to 0.05 percent (a negligible change), and from 0.41 to 1.6 percent at $\rho = 5$. For $\rho < 2$, however, the error is decreased and is now only 13.4 percent at $\rho = 1$, rising to 17.7 percent at $\rho = 0.7$. Overall, it would therefore seem that the 2-term expression for the optics component is superior.

2.6 Remarks

Based on the fact that the real and imaginary parts of the quantity $(G - G^c)\, e^{2i\rho}$ do not show any detectable oscillation as functions of ρ, it is concluded that the expression for G^c given in equation (41) is an accurate approximation to the creeping wave component of the normalized far field amplitude for values of ρ down to unity and, perhaps, smaller. The omission of any of the terms in (41) decreases the accuracy, and the retention of the term in τ^{-1} in the exponent is particularly important when ρ is not large.

The 5-term expression for G^o shown in equation (42) is extremely good for large ρ, but its accuracy falls off rapidly with decreasing ρ. For ρ less than (about) 2 it is entirely inappropriate. The 3-term expression obtained by omitting the terms in ρ^{-3} and ρ^{-4} from (42) is not much inferior for large ρ, and is markedly superior for $\rho < 2$. Best of all, however, is the 2-term expression

$$G^o = -e^{-2i\rho}\left\{1 + \frac{i}{2\rho} + O(\rho^{-2})\right\}, \qquad (46)$$

and until such time as a closed-form determination of G^o is achieved, this probably provides the greatest overall accuracy obtainable from a single representation. As an illustration of the accuracy with which the normalized cross section can be estimated, equations (41) and (46) give $|G|^2 = 1.22314$ for $\rho = 1$ and 1.62503 for $\rho = 0.7$, whereas from Table 1, the exact values are 1.34606 and 1.72956. The errors are 6.0 and 9.1 percent respectively.

III
AN ACOUSTICALLY HARD SPHERE

The second scalar problem to be examined is the scattering of a plane acoustic wave by a hard (or rigid) sphere at whose surface a Neumann boundary condition is imposed. The general analysis, leading to a Mie series representation of the far field amplitude and thence to a decomposition into creeping wave and optics components, is similar in all respects to that for the soft sphere, and the details will be omitted.

3.1 The Analysis

If the plane wave (1) is incident on a hard sphere of radius a at whose surface the boundary condition is

$$\frac{\partial U}{\partial R} = 0 \ ,$$

the total field in the back scattering direction $\theta = 0$ is

$$U = \sum_{n=0}^{\infty} (n+\tfrac{1}{2}) e^{-in\frac{\pi}{2}} \left\{ j_n(kR) - \frac{j_n'(\rho)}{h_n^{(1)'}(\rho)} h_n^{(1)}(kR) \right\} \tag{47}$$

where the prime denotes differentiation with respect to ρ. The far field amplitude is therefore

$$S = i \sum_{n=0}^{\infty} (-1)^n (2n+1) \frac{j_n'(\rho)}{h_n^{(1)'}(\rho)} \tag{48}$$

(cf equation 5).

For sufficiently small ρ, S has the power series expansion

$$S = -\frac{5}{6}\rho^3 \left\{ 1 - \frac{229}{450}\rho^2 - \frac{i}{30}\rho^3 + O(\rho^4) \right\} \tag{49}$$

(Senior, 1960), convergent for $\rho < 1$. As regards the powers of ρ that occur, this is similar to the low frequency expansion for the scattering of an electromagnetic wave by a perfectly conducting sphere, and is quite distinct from the development for a soft sphere (see equation 6).

Because of its limited convergence, the series in (49) is inappropriate to the larger ρ, but there is an alternative representation of S which is well suited to values of $\rho \gg 1$. This can be obtained by application of a Watson transformation to (47), and leads naturally to a separation into creeping wave and optics components. The procedure differs from that given in Section 2.2 only in having the spherical Hankel function ratio replaced by a ratio of the first derivatives, and the resulting expression for S is

$$S = S^c + S^o$$

where

$$S^c = i\pi \sum_n \left[\frac{\frac{\partial}{\partial\rho}\left\{\rho^{-1/2} H_\nu^{(2)}(\rho)\right\}}{\frac{\partial}{\partial\nu}\frac{\partial}{\partial\rho}\left\{\rho^{-1/2} H_\nu^{(1)}(\rho)\right\}} \nu \sec\nu\pi \right]_{\nu=\nu_n}, \tag{50}$$

$$S^o = i \int_{\infty - i\epsilon}^{0} \frac{\frac{\partial}{\partial\rho}\left\{\rho^{-1/2} H_\nu^{(2)}(\rho)\right\}}{\frac{\partial}{\partial\rho}\left\{\rho^{-1/2} H_\nu^{(1)}(\rho)\right\}} \tan\nu\pi \; e^{-i\nu\frac{\pi}{2}} \nu d\nu . \tag{51}$$

The symbol ν_n now denotes the zeros of $\partial/\partial\rho \left\{\rho^{-1/2} H_\nu^{(1)}(\rho)\right\}$, and to maintain the analogy with the soft body formulae (12) and (13), the cylindrical equivalents of the spherical Hankel functions have been employed.

3.2 Evaluation of the Creeping Wave Contribution

To find an asymptotic representation of the zeros ν_n, we again start with an expansion for the cylindrical functions in terms of Airy integrals. Since

$$\frac{\partial\tau}{\partial\rho} = \frac{1}{6\tau^2}$$

and

$$\frac{\partial x}{\partial \rho} = -\frac{1}{\tau}\left(1+\frac{x}{6\tau^2}\right) ,$$

where x is as defined in equation (14), it follows from (16) that

$$\frac{\partial}{\partial \rho} J_\nu(\rho) = -\frac{1}{\tau^2}\left[Ai'(x) - \frac{1}{60\tau^2}\left\{(x^3-6)Ai(x) - 4xAi'(x)\right\} + \right.$$

$$\left. + \frac{1}{2520\tau^2}\left\{(\frac{3}{4}x^4 - 42x)Ai(x) + (\frac{7}{20}x^5 - 19x^2)Ai'(x)\right\} + O(\tau^{-6})\right] . \qquad (52)$$

But

$$\frac{\partial}{\partial \rho}\left\{\rho^{-1/2} J_\nu(\rho)\right\} = \rho^{-1/2}\left\{\frac{\partial}{\partial \rho} J_\nu(\rho) - \frac{1}{2\rho} J_\nu(\rho)\right\}$$

and hence

$$\frac{\partial}{\partial \rho}\left\{\rho^{-1/2} J_\nu(\rho)\right\} = -\frac{\rho^{-1/2}}{\tau^2}\left[Ai'(x) - \frac{1}{60\tau^2}\left\{(x^3-21)Ai(x) - 4xAi'(x)\right\}\right.$$

$$\left. + \frac{1}{2520\tau^4}\left\{(\frac{3}{4}x^4 - 84x)Ai(x) + (\frac{7}{20}x^5 - \frac{59}{2}x^2)Ai'(x)\right\} + O(\tau^{-6})\right] . \qquad (53)$$

with a similar formula for $\partial/\partial\rho\left\{\rho^{-1/2} Y_\nu(\rho)\right\}$ in which Ai(x) and Ai'(x) are replaced by -Bi(x) and -Bi'(x) respectively.

Equation (53) is equivalent to

$$\frac{\partial}{\partial \rho}\left\{\rho^{-1/2} J_\nu(\rho)\right\} = -\frac{\rho^{-1/2}}{\tau^2}\left\{1 + \frac{x}{15\tau^2} - \frac{1}{\tau^4 x}\left(\frac{37}{6300}x^3 + \frac{49}{800}\right) + O(\tau^{-6})\right\}$$

$$\cdot Ai'\left\{x - \frac{1}{60\tau^2 x}(x^3-21) + \frac{1}{\tau^4 x^3}\left(\frac{2}{1575}x^6 - \frac{61}{1200}x^3 - \frac{49}{800}\right) + O(\tau^{-6})\right\} ,$$

and if we now define

$$\omega^2 y = x - \frac{1}{60\tau^2 x}(x^3 - 21) + \frac{1}{\tau^4 x^3}\left(\frac{2}{1575}x^6 - \frac{61}{1200}x^3 - \frac{49}{800}\right) + O(\tau^{-6}) , \tag{54}$$

we have

$$\frac{\partial}{\partial\rho}\left\{\rho^{-1/2} H_\nu^{(1)}(\rho)\right\} = -\frac{\rho^{-1/2}}{\tau^2}\left\{1 + \frac{x}{15\tau^2} - \frac{1}{\tau^4 x}\left(\frac{37}{6300}x^3 + \frac{49}{800}\right) + O(\tau^{-6})\right\} \cdot \left\{Ai'(\omega^2 y) - iBi'(\omega^2 y)\right\} ,$$

which reduces to

$$\frac{\partial}{\partial\rho}\left\{\rho^{-1/2} H_\nu^{(1)}(\rho)\right\} = 2\omega^2 \frac{\rho^{-1/2}}{\tau^2}\left\{1 + \frac{x}{15\tau^2} - \frac{1}{\tau^4 x}\left(\frac{37}{6300}x^3 + \frac{49}{800}\right) + O(\tau^{-6})\right\} Ai'(y) \tag{55}$$

by using the rotational relations for the Airy integral. The zeros ν_n can therefore be expressed in terms of the zeros $y = b_n$ of the Airy integral derivative $Ai'(y)$, and if equation (54) is inverted to give x as a function of y, the formula for ν_n becomes

$$\nu_n = \rho + \omega^2 \tau b_n + \frac{\omega}{60\tau b_n}(b_n^3 - 21) - \frac{1}{\tau^3 b_n^3}\left(\frac{b_n^6}{1400} - \frac{9}{200}b_n^3 + \frac{49}{800}\right) + O(\tau^{-5}) . \tag{56}$$

The first 50 of the b_n have been tabulated by Miller (1946) and when arranged in ascending order of magnitude they are

$$b_1 = -1.01879\ 297$$

$$b_2 = -3.24819\ 758$$

$$b_3 = -4.82009\ 921$$

. . . . . .

All are real and negative, but for convenience we shall again follow Logan (1959) by writing

$$b_n = -\beta_n \ .$$

The β_n are therefore positive and the corresponding expression for ν_n is

$$\nu_n = \rho + e^{i\frac{\pi}{3}}\tau\beta_n - \frac{e^{-i\frac{\pi}{3}}}{60\tau\beta_n}(\beta_n^3+21) + \frac{1}{1400\tau^3\beta_n^3}(\beta_n^6+63\beta_n^3+\frac{343}{4}) + O(\tau^{-5}) \ . \tag{57}$$

The coefficients of $\rho^{1/3}e^{i\frac{\pi}{3}}$ and $\rho^{-1/3}e^{-i\frac{\pi}{3}}$ have been computed for $n=1$ through 5 by Franz (1954), and are listed* in his Tables 1 and 5.

The next task is to find an expression for

$$\left[\frac{\frac{\partial}{\partial\rho}\left\{\rho^{-1/2}H_\nu^{(2)}(\rho)\right\}}{\frac{\partial}{\partial\nu}\frac{\partial}{\partial\rho}\left\{\rho^{-1/2}H_\nu^{(1)}(\rho)\right\}}\right]_{\nu=\nu_n} .$$

Since $\frac{\partial}{\partial\rho}\left\{\rho^{-1/2}H_{\nu_n}^{(1)}(\rho)\right\} = 0$, this factor can be written as

$$2\left[\frac{\frac{\partial}{\partial\rho}\left\{\rho^{-1/2}J_\nu(\rho)\right\}}{\frac{\partial}{\partial\nu}\frac{\partial}{\partial\rho}\left\{\rho^{-1/2}H_\nu^{(1)}(\rho)\right\}}\right]_{\nu=\nu_n} = \frac{i\tau}{2}\left[\frac{\mathrm{Bi}'(y)}{\frac{\partial y}{\partial x}\mathrm{Ai}''(y)}\right]$$

where we have used the fact that

$$\frac{\partial}{\partial\nu} = \frac{1}{\tau}\frac{\partial y}{\partial x}\frac{\partial}{\partial y} \ .$$

But

$$\mathrm{Bi}'(y) = \frac{1}{\pi\,\mathrm{Ai}(y)} \ ,$$

* Note that the headings of the two columns in Franz's Table 5 are interchanged.

$$Ai''(y) = yAi(y)$$

and, from equation (54),

$$\omega^2 \frac{\partial y}{\partial x} = 1 - \frac{1}{60\tau^2 x^2}(2x^3+21) + \frac{1}{\tau^4 x^4}\left(\frac{2}{525}x^6 + \frac{147}{800}\right) + O(\tau^{-6})$$

$$= 1 - \frac{\omega^2}{60\tau^2 y^2}(2y^3+21) + \frac{\omega}{\tau^4 y^4}\left(\frac{41}{12600}y^6 + \frac{7}{300}y^3 - \frac{49}{800}\right) + O(\tau^{-6})$$

giving

$$\frac{1}{\partial y/\partial x} = \omega^2\left\{1 + \frac{\omega^2}{60\tau^2 y^2}(2y^3+21) - \frac{3\omega}{1400\tau^4 y^4}\left(y^6 - \frac{343}{4}\right) + O(\tau^{-6})\right\} .$$

We now have

$$\left[\frac{\frac{\partial}{\partial\rho}\left\{\rho^{-1/2}H_\nu^{(2)}(\rho)\right\}}{\frac{\partial}{\partial\nu}\frac{\partial}{\partial\rho}\left\{\rho^{-1/2}H_\nu^{(1)}(\rho)\right\}}\right]_{\nu=\nu_n} = -\frac{\tau}{2\pi}e^{-i\frac{\pi}{6}}\left\{1 + \frac{e^{i\frac{\pi}{3}}}{60\tau^2\beta_n^2}(2\beta_n^3 - 21)\right.$$

$$\left. + e^{-i\frac{\pi}{3}}\frac{3}{1400\tau^4\beta_n^4}\left(\beta_n^6 - \frac{343}{4}\right) + O(\tau^{-6})\right\}\frac{1}{\beta_n\left\{Ai(-\beta_n)\right\}^2}$$

from which it follows that

$$\left[\frac{\nu\frac{\partial}{\partial\rho}\left\{\rho^{-1/2}H_\nu^{(2)}(\rho)\right\}}{\frac{\partial}{\partial\nu}\frac{\partial}{\partial\rho}\left\{\rho^{-1/2}H_\nu^{(1)}(\rho)\right\}}\right]_{\nu=\nu_n} = -\frac{\tau^4}{\pi}e^{-i\frac{\pi}{6}}\left\{1 + \frac{e^{i\frac{\pi}{3}}}{60\tau^2\beta_n^2}(2\beta_n^3 + 9)\right.$$

$$\left. - \frac{e^{-i\frac{\pi}{3}}}{\tau^4\beta_n^4}\left(\frac{4}{175}\beta_n^6 + \frac{147}{800}\right) + O(\tau^{-6})\right\}\frac{1}{\beta_n\left\{Ai(-\beta_n)\right\}^2} . \qquad (58)$$

Each of the zeros ν_n corresponds to a creeping wave mode, and if we also expand $\sec \nu\pi$ in a series of exponentials, convergent for $\mathrm{Im}.\nu > 0$, substitution from equations (23), (57) and (58) into (50) leads to a representation of the creeping wave component S^c in the form

$$S^c = -2\tau^4 e^{i\frac{\pi}{3}} \sum_n \left\{ 1 + \frac{e^{i\frac{\pi}{3}}}{60\tau^2\beta_n^2}(2\beta_n^3+9) - \frac{e^{-i\frac{\pi}{3}}}{\tau^4\beta_n^4}\left(\frac{4}{175}\beta_n^6 + \frac{147}{800}\right) \right.$$

$$\left. + O(\tau^{-6}) \right\} \cdot \frac{1}{\beta_n \left\{ Ai(-\beta_n) \right\}^2} \sum_{\ell=0}^{\infty} (-1)^\ell \exp \left[i(2\ell+1)\pi \left\{ \rho + e^{i\frac{\pi}{3}} \tau\beta_n \right. \right.$$

$$\left. \left. - \frac{e^{-i\frac{\pi}{3}}}{60\tau\beta_n}(\beta_n^3+21) + \frac{1}{1400\tau^3\beta_n^3}(\beta_n^6+63\beta_n^3+\frac{343}{4}) + O(\tau^{-5}) \right\} \right] . \qquad (59)$$

The extent to which this can be simplified without substantial loss of accuracy is explored in Section 3.4.

3.3 Evaluation of the Optics Contribution

The optics contribution to the far field amplitude is given in equation (51), and when $\tan \nu\pi$ is replaced by its exponential equivalent, S^o becomes

$$S^o = \int_{-\infty - i\epsilon}^{\infty - i\epsilon} \frac{\frac{\partial}{\partial\rho}\left\{\rho^{-1/2} H_\nu^{(2)}(\rho)\right\}}{\frac{\partial}{\partial\rho}\left\{\rho^{-1/2} H_\nu^{(1)}(\rho)\right\}} \frac{e^{-i\nu\pi}}{1+e^{2i\nu\pi}} \nu d\nu \quad . \qquad (60)$$

From the Debye formula (26) for the Hankel function,

$$\rho^{-1/2} H_\nu^{(1)}(\rho) = \frac{1}{\rho}\sqrt{\frac{2}{\pi \sin\beta}}\, e^{i\rho(\sin\beta - \beta\cos\beta) - i\frac{\pi}{4}} \sum_{m=0}^{\infty} \frac{(m-\frac{1}{2})!}{(-\frac{1}{2})!} \left(\frac{-2i}{\rho\sin\beta}\right)^m A_m$$

where $\nu = \rho\cos\beta$ and the A_m are real functions of $\cot^2\beta$ only. Differentiating with respect to ρ and observing that

$$\frac{\partial\beta}{\partial\rho} = \frac{1}{\rho}\cot\beta \ ,$$

we have

$$\frac{\partial}{\partial\rho}\left\{\rho^{-1/2}H_\nu^{(1)}(\rho)\right\} = \frac{1}{\rho}\sqrt{\frac{2\sin\beta}{\pi}}\ e^{i\rho(\sin\beta-\beta\cos\beta)+i\frac{\pi}{4}} \cdot \sum_{m=0}^{\infty}\frac{(m-\frac{1}{2})!}{(-\frac{1}{2})!}\left(\frac{-2i}{\rho\sin\beta}\right)^m B_m \ . \quad (61)$$

The first few coefficients B_m are given in terms of the A_m by the equations

$$B_o = A_o$$

$$B_1 = A_1 - 1 - \frac{1}{2}\cot^2\beta$$

$$B_2 = A_2 - \frac{2}{3}A_1 - \frac{1}{2}A_1\cot^2\beta + \frac{1}{3}\cot\beta\frac{\partial A_1}{\partial\beta}$$

$$B_3 = A_3 - \frac{3}{5}A_2 - \frac{1}{2}A_2\cot^2\beta + \frac{1}{5}\cot\beta\frac{\partial A_2}{\partial\beta} \ .$$

Hence, by analogy with (28)

$$\frac{\frac{\partial}{\partial\rho}\left\{\rho^{-1/2}H_\nu^{(2)}(\rho)\right\}}{\frac{\partial}{\partial\rho}\left\{\rho^{-1/2}H_\nu^{(1)}(\rho)\right\}} = -ie^{-2i\rho(\sin\beta-\beta\cos\beta)}\left\{1+\frac{2i}{\rho\sin\beta}B_1 - \frac{2}{(\rho\sin\beta)^2}B_1^2 - \frac{2i}{(\rho\sin\beta)^3}(B_1^3-3B_1B_2+15B_3) + \frac{2}{(\rho\sin\beta)^4}B_1(B_1^3-6B_1B_2+30B_3)+O(\rho^{-5})\right\} \quad (62)$$

so that a knowledge of the A_m (and therefore B_m) through $m=3$ again serves to determine the Hankel function ratio correct to ρ^{-4}.

In order to apply the method of steepest descents, it is necessary to expand the right hand side of (62) in a neighborhood of $\nu = 0$. Using the expressions for the A_m given in Section 2.4,

$$B_1 = -\frac{7}{8}\left(1+\frac{1}{3}\cot^2\beta\right)$$

$$B_2 = -\frac{1}{2^7\cdot 3}\left\{23+\frac{238}{3}\cot^2\beta+O(\cot^4\beta)\right\}$$

$$B_3 = -\frac{1}{2^{10}\cdot 5}\left\{47+\frac{19811}{45}\cot^2\beta+O(\cot^4\beta)\right\}$$

and if we also expand $\sin\beta$ and $\cot^2\beta$ near $\nu = 0$, the bracketed terms on the right hand side of (62) become

$$1-\frac{7i}{4\rho}\left\{1+\frac{5}{6}\left(\frac{\nu}{\rho}\right)^2+\frac{7}{8}\left(\frac{\nu}{\rho}\right)^4+\frac{15}{16}\left(\frac{\nu}{\rho}\right)^6\right\}-\frac{49}{32\rho^2}\left\{1+\frac{5}{3}\left(\frac{\nu}{\rho}\right)^2+\frac{22}{9}\left(\frac{\nu}{\rho}\right)^4\right\}$$

$$+\frac{i}{2^7\rho^3}\left\{247+\frac{30733}{30}\left(\frac{\nu}{\rho}\right)^2\right\}+\frac{35\cdot 129}{2^{11}\rho^4}$$

where we have retained only those terms required to give S^0 correct to the first five orders in ρ. The expansion for the exponential factor in (62) was derived in Section 2.4, and when this is multiplied by the above, we obtain, after some simplification,

$$S^o = \frac{\rho}{2} e^{-2i\rho} \left[\left\{ 1 - \frac{7i}{4\rho} - \frac{49}{32\rho^2} + \frac{247i}{2^7 \rho^3} + \frac{35 \cdot 129}{2^{11} \rho^4} \right\} I_o \right.$$

$$- \frac{35i}{24\rho^3} \left\{ 1 - \frac{7i}{4\rho} - \frac{30733}{2^5 5^2 7\rho^2} \right\} I_1$$

$$- \frac{i}{12\rho^3} \left\{ 1 - \frac{7i}{4\rho} + \frac{539}{32\rho^2} - \frac{16507i}{2^7 \cdot 3\rho^3} \right\} I_2$$

$$- \frac{i}{40\rho^5} \left\{ 1 - \frac{238i}{36\rho} + \frac{16009}{2^5 \cdot 3^2 \cdot 5\rho^2} \right\} I_3$$

$$- \frac{1}{288\rho^6} \left\{ 1 + \frac{41i}{28\rho} + \frac{1643}{32\rho^2} \right\} I_4$$

$$- \frac{1}{480\rho^8} \left\{ 1 - \frac{91i}{72\rho} \right\} I_5 + \frac{i}{2^7 \cdot 3^4 \rho^9} \left\{ 1 + \frac{7793i}{700\rho} \right\} I_6$$

$$\left. + \frac{i}{2^8 \cdot 3^2 \cdot 5\rho^{11}} I_7 + \frac{1}{2^{11} \cdot 3^5 \rho^{12}} I_8 + O(\rho^{-5}) \right] \qquad (63)$$

where I_n is as defined in equation (31).

If we now insert the asymptotic development for I_n shown in equation (35), the expression for the optics component S^o finally reduces to

$$S^o = \frac{\rho}{2} e^{-2i\rho} \left\{ 1 - \frac{3i}{2\rho} - \frac{5}{2\rho^2} + \frac{25i}{4\rho^3} + \frac{22}{\rho^4} + O(\rho^{-5}) \right\} . \qquad (64)$$

Once again the simplicity of the result we have obtained is gratifying, but it has not proved possible to discover any systematic relationship between the coefficients of successive powers of ρ. The first three terms in (64) were previously derived by Keller et al (1956) using the Kline-Luneburg expansion technique.

3.4 Numerical Considerations

As in the case of the soft sphere, the expression for S^c and S^o are only asymptotic for large ρ and it is therefore presumptuous of us to seek to employ them when ρ is as small as 3 or even unity. Nevertheless, they form the basis for most predictions of the scattering behavior of bodies whose radii of curvature are comparable to or greater than the wavelength, and the creeping wave component for the hard body in particular is one of the cornerstones of the geometrical theory of diffraction. It is therefore important to have some feel for the accuracy of (59) and (64) not only when ρ is large compared with unity, but when it is near to unity as well.

The phase of the optics component S^o identifies it as a return from the front face of the sphere, and the whole expression can be regarded as a representation of the specular contribution. The leading term is that produced by geometrical optics, but somewhat surprisingly the obvious analogue to the physical optics method in electromagnetic scattering fails to predict the correct second term. The coefficients of successive powers of ρ in the expansion for S^o increase even more rapidly than those for the soft sphere, and if we write equation (64) in the form

$$S^o = \frac{\rho}{2} e^{-2i\rho}\left\{1+\sum_{n=1}\left(\frac{-ia_n}{\rho}\right)^n\right\}, \tag{65}$$

we have

$$a_1 = 1.500, \qquad a_2 = 1.581, \qquad a_3 = 1.842, \qquad a_4 = 2.166.$$

In effect, each a_n is a "convergence coefficient" (Senior, 1961) indicating the value of ρ at which the corresponding term has a magnitude of unity. For the soft body, on the other hand, the representation equivalent to (65) is

$$S^o = \frac{\rho}{2} e^{-2i\rho}\left\{-1+\sum_{n=1}\left(\frac{-ia_n}{\rho}\right)^n\right\}, \tag{66}$$

and

$$a_1 = 0.500, \qquad a_2 = 0.707, \qquad a_3 = 1.077, \qquad a_4 = 1.495,$$

which illustrates quite dramatically the increased importance of the higher order terms in equation (65) compared with those in (36). In fact, for the hard sphere the second real term produces a correction to the first (unity) term exceeding 10 percent if $\rho < 5$, and the third real term corrects the second by more than 10 percent if $\rho < 9.38$. For the two imaginary terms shown, the appropriate value of ρ is 6.46, and such bahavior is certainly indicative of the asymptotic character of the expansion.

The other component S^c is produced by the creeping waves and the phenomenological description of these is the same as for the soft sphere. Each wave, however, produces a much larger contribution than does the corresponding wave in (24). Taking, for example, the dominant wave ($n = 1$), its contribution after having traveled the minimum distance ($\ell = 0$) around the sphere is, when $\rho = 10$, 2.97×10^{-1} for the hard sphere, but only 7.21×10^{-4} for the soft sphere. The ratio is over 400, and every higher order hard body contribution exceeds the soft body one by a similar amount.

As in the case of equation (24), it is seldom (if ever) necessary to retain the full complexity of (59). For most numerical work a far simpler form is sufficient. The attenuation of all the waves, including the dominant one, is large enough for us to ignore the contributions from waves which have completed one or more circuits of the sphere, and we can therefore replace the second summation (over ℓ) by its first term ($\ell = 0$). We can also omit all waves except the dominant one, and to judge from the leading term in the decay exponent, even the sub-dominant wave ($n = 2$) provides a contribution whose magnitude does not reach 1 percent of that produced by the dominant wave until ρ has decreased to below 0.88. The effect of waves for $n > 2$ is, of course, still less.

Both of the infinite sums have now been removed, leaving an expression for S^c based on a single wave alone, but this can be further simplified without significant loss of accuracy. In the amplitude factor associated with the dominant creeping wave the term $O(\tau^{-4})$ produces amplitude and phase corrections amounting to only 0.13 percent and 0.15^o for $\rho = 10$, rising to 0.85 percent and 1.2^o for $\rho = 2$. We can therefore neglect the term in comparison with the preceding two. The term $O(\tau^{-2})$ is, however, of sufficient importance to warrant retention, and this is true also of the term $O(\tau^{-3})$ in the exponent. We have already noted that the successive terms in the expansion of S^o for the hard sphere are larger than the corresponding ones in the soft body expansion, and whereas the term $O(\tau^{-3})$ in the exponent of equation (24) contributes only an amount 0.07^o to the phase for $\rho = 10$, the analogous term in (59) provides a phase correction 3.6^o for $\rho = 10$, increasing to 18.7^o for $\rho = 2$. This is too large for us to ignore, but with the other simplifications to equation (59) described above, the expression for S^c becomes

$$S^c = -2\tau^4 e^{i\frac{\pi}{3}} \left\{ 1 + \frac{e^{i\frac{\pi}{3}}}{30\tau^2\beta_1^2}\left(\beta_1^3 + \frac{9}{2}\right) + O(\tau^{-4}) \right\} \cdot \frac{1}{\beta_1 \left\{ \mathrm{Ai}(-\beta_1) \right\}^2}$$

$$\cdot e \left\{ i\pi\rho - e^{-i\frac{\pi}{6}} \tau\pi\beta_1 - e^{i\frac{\pi}{6}} \frac{\pi}{60\tau\beta_1}\left(\beta_1^3 + 21\right) + \frac{i\pi}{1400\tau^3\beta_1^3}\left(\beta_1^6 \right.\right.$$

$$\left.\left. + 63\beta_1^3 + \frac{343}{4}\right) + O(\tau^{-5}) \right\} \qquad (67)$$

where

$$\beta_1 = 1.01879\ 297....$$

$$\mathrm{Ai}(-\beta_1) = 0.53565\ 666....$$

It is presumed that (67) is an accurate approximation to (59) (if not to the exact expression for S^c shown in equation 50) for ρ greater than (about) unity, and is the formula we shall henceforth employ.

The back scattering cross section σ is given in terms of the far field amplitude S by equation (38). For numerical purposes, however, it is convenient to normalize the cross section with respect to its high frequency limit, and since $|S| \to \rho/2$ as $\rho \to \infty$, we shall again define a function G by equation (39).

The creeping wave and optics components of G are, from equations (67) and (66) respectively,

$$G^c = -2\tau e^{i\frac{\pi}{3}} \left\{1 + \frac{e^{i\frac{\pi}{3}}}{30\tau^2\beta_1^2}(\beta_1^3 + \frac{9}{2}) + O(\tau^{-4})\right\} \cdot \frac{1}{\beta_1\{Ai(-\beta_1)\}^2}$$

$$\cdot \exp\left\{i\pi\rho - e^{-i\frac{\pi}{6}}\tau\pi\beta_1 - e^{i\frac{\pi}{6}}\frac{\pi}{60\tau\beta_1}(\beta_1^3 + 21)\right.$$

$$\left. + \frac{i\pi}{1400\tau^3\beta_1^3}(\beta_1^6 + 63\beta_1^3 + \frac{343}{4}) + O(\tau^{-5})\right\} \qquad (68)$$

and

$$G^o = e^{-2i\rho}\left\{1 - \frac{3i}{2\rho} - \frac{5}{2\rho^2} + \frac{25i}{4\rho^3} + \frac{22}{\rho^4} + O(\rho^{-5})\right\} , \qquad (69)$$

whilst the Mie series representation of G is, from equation (48) ,

$$G = \frac{2i}{\rho}\sum_{n=0}^{\infty}(-1)^n(2n+1)\frac{j_n'(\rho)}{h_n^{(1)'}(\rho)} . \qquad (70)$$

In the course of a recent study (Senior, 1965b) of the effect of surface loading on the acoustic scattering properties of a rigid sphere, the series

$$\sum_{n=0}^{\infty} (-1)^n (2n+1) \frac{j_n'(\rho)}{h_n^{(1)'}(\rho)}$$

was programmed for evaluation on the IBM 7090 computer of The University of Michigan. Reference to equation (48) shows that this is, in fact, -iS, and using a maximum of 21 terms in the series, the real and imaginary parts and modulus were determined for $\rho = 0.3(0.1)10.0$. For consistency with the soft sphere data given in Table 1, the above values of -iS were converted to values of G by multiplying by $2i/\rho$, and in Table 4 the real and imaginary parts of G are listed, along with the values of $|G|$ and $|G|^2$. The results for $\rho = 0.1$ and 0.2 were obtained by hand computation.

The normalized cross section $|G|^2$ is plotted as a function of ρ in Fig. 3. For small ρ,

$$|G|^2 \sim \frac{25}{9} \rho^4$$

(see equations 39 and 49), leading to an initially rapid increase in cross section, giving way to an oscillation of decreasing magnitude. The mean level increases uniformly with ρ and is less than unity throughout. The levels of the maxima increase through the fourth peak and thereafter decrease, whereas the levels of all minima increase with ρ. As a consequence the depth of oscillation decreases, but even when ρ is as large as 10 the depth is still around ± 10 percent, indicating that the two contributors to the cross section are not too different in magnitude. In this respect, the behavior is more akin to that for the scattering of an electromagnetic wave by a perfectly conducting sphere than for the scattering of an acoustic wave by a soft sphere (see Fig. 1).

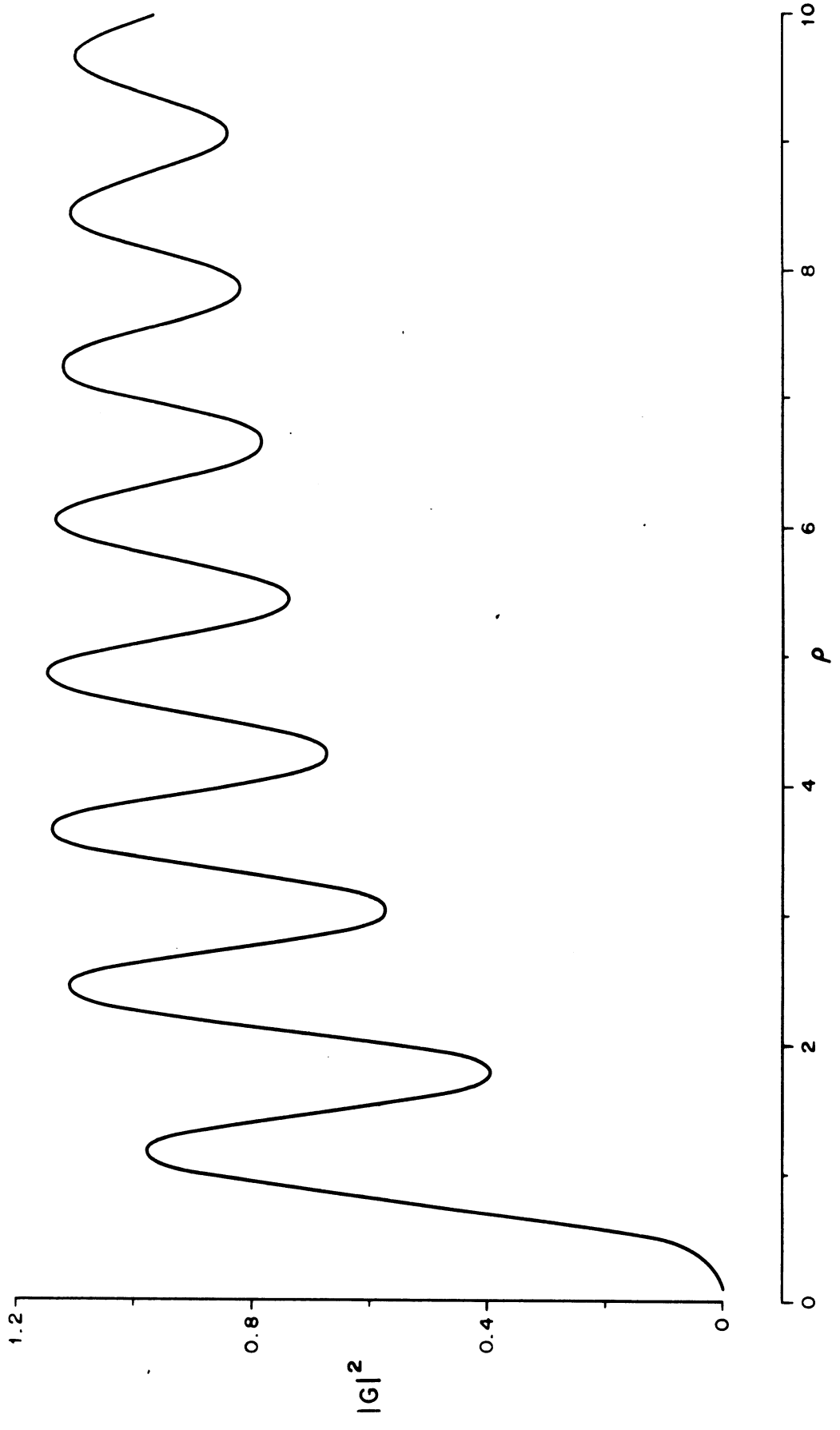

FIG. 3: NORMALIZED BACK SCATTERING CROSS SECTION OF A HARD SPHERE

One of the most striking features of Fig. 3 is the regularity of the oscillations and the comparative uniformity of the spacing between successive maxima and minima. The locations of the turning points in Fig. 3 can be obtained by graphical interpolation of the data in Table 4, and these are listed in Table 5. Apart from the first two or three, the separations between adjacent maxima and minima are almost constant, reinforcing our belief that there are only two significant contributors to the cross section. The maximum and minimum values of $|G|^2$ are also given, and by taking the adjacent turning points in pairs, the values G_1 and G_2 of the two components can be determined on the assumption that they are constant over the appropriate interval in ρ. As shown in Table 4, G_1 increases fairly uniformly from 0.81 when $\rho \sim 1.8$ to 0.99 when $\rho = 9.6$, and from equation (69) it is obvious that G_1 must correspond to the optics component G^o. G_2, on the other hand, decreases from 0.18 to 0.065 over the same range, and though it is not quite so uniform in behavior, it is (presumably) the creeping wave component G^c. In Fig. 4 these values of G_1 and G_2 are denoted by the circled points placed at the midpoints of the ρ-intervals for which they are appropriate.

Using equation (68) the amplitude and phase of the theoretical creeping wave component G^c have been computed for selected values of ρ in the range $0.5 \leqslant \rho \leqslant 10.0$. The results are given in Table 6 and the amplitude is shown as a solid line in Fig. 4. The agreement with the points representing G_2 is remarkably good even down to $\rho = 1.47$ (the smallest ρ for which G_2 can be found). This suggests that at least the amplitude of the "actual" creeping wave component is closely approximated by the expression in (68) for all $\rho \geqslant 1.47$, but it does not, of course, give any check for smaller ρ, nor does it confirm the phase. As ρ decreases still further, $|G^c|$ increases to a local maximum of 0.207 at $\rho = 0.7$ and thereafter decreases.

For the optics component it is convenient to remove the factor $e^{-2i\rho}$ as we did with the soft sphere, and to treat $G^o e^{2i\rho}$. From equation (69)

Table 4: Exact Far Field Amplitude

ka	Re. G	Im. G	$\|G\|$	$\|G\|^2$
0.1	$-1.65821 \cdot 10^{-2}$	$5.39179 \cdot 10^{-7}$	$1.65821 \cdot 10^{-2}$	$2.74966 \cdot 10^{-4}$
0.2	$-6.32062 \cdot 10^{-2}$	$1.57988 \cdot 10^{-5}$	$6.32062 \cdot 10^{-2}$	$3.99502 \cdot 10^{-3}$
0.3	$-1.43271 \cdot 10^{-1}$	$1.03841 \cdot 10^{-4}$	$1.43271 \cdot 10^{-1}$	$2.05267 \cdot 10^{-2}$
0.4	$-2.45694 \cdot 10^{-1}$	$3.61912 \cdot 10^{-4}$	$2.45695 \cdot 10^{-1}$	$6.03660 \cdot 10^{-2}$
0.5	$-3.66262 \cdot 10^{-1}$	$8.89196 \cdot 10^{-4}$	$3.66264 \cdot 10^{-1}$	$1.34149 \cdot 10^{-1}$
0.6	$-4.97223 \cdot 10^{-1}$	$1.79840 \cdot 10^{-3}$	$4.97227 \cdot 10^{-1}$	$2.47234 \cdot 10^{-1}$
0.7	$-6.29623 \cdot 10^{-1}$	$3.36497 \cdot 10^{-3}$	$6.29631 \cdot 10^{-1}$	$3.96436 \cdot 10^{-1}$
0.8	$-7.53680 \cdot 10^{-1}$	$6.32778 \cdot 10^{-3}$	$7.53708 \cdot 10^{-1}$	$5.68075 \cdot 10^{-1}$
0.9	$-8.59464 \cdot 10^{-1}$	$1.22271 \cdot 10^{-2}$	$8.59551 \cdot 10^{-1}$	$7.38828 \cdot 10^{-1}$
1.0	$-9.37826 \cdot 10^{-1}$	$2.35658 \cdot 10^{-2}$	$9.38122 \cdot 10^{-1}$	$8.80073 \cdot 10^{-1}$
1.1	$-9.81453 \cdot 10^{-1}$	$4.35998 \cdot 10^{-2}$	$9.82420 \cdot 10^{-1}$	$9.65149 \cdot 10^{-1}$
1.2	$-9.85707 \cdot 10^{-1}$	$7.57330 \cdot 10^{-2}$	$9.88612 \cdot 10^{-1}$	$9.77353 \cdot 10^{-1}$
1.3	$-9.49025 \cdot 10^{-1}$	$1.22714 \cdot 10^{-1}$	$9.56926 \cdot 10^{-1}$	$9.15708 \cdot 10^{-1}$
1.4	$-8.72830 \cdot 10^{-1}$	$1.85927 \cdot 10^{-1}$	$8.92413 \cdot 10^{-1}$	$7.96401 \cdot 10^{-1}$
1.5	$-7.61115 \cdot 10^{-1}$	$2.64971 \cdot 10^{-1}$	$8.05920 \cdot 10^{-1}$	$6.49507 \cdot 10^{-1}$
1.6	$-6.19930 \cdot 10^{-1}$	$3.57545 \cdot 10^{-1}$	$7.15648 \cdot 10^{-1}$	$5.12151 \cdot 10^{-1}$
1.7	$-4.56840 \cdot 10^{-1}$	$4.59527 \cdot 10^{-1}$	$6.47972 \cdot 10^{-1}$	$4.19867 \cdot 10^{-1}$
1.8	$-2.80372 \cdot 10^{-1}$	$5.65149 \cdot 10^{-1}$	$6.30874 \cdot 10^{-1}$	$3.98003 \cdot 10^{-1}$
1.9	$-9.93879 \cdot 10^{-2}$	$6.67266 \cdot 10^{-1}$	$6.74627 \cdot 10^{-1}$	$4.55122 \cdot 10^{-1}$
2.0	$7.76204 \cdot 10^{-2}$	$7.57781 \cdot 10^{-1}$	$7.61746 \cdot 10^{-1}$	$5.80257 \cdot 10^{-1}$
2.1	$2.43200 \cdot 10^{-1}$	$8.28279 \cdot 10^{-1}$	$8.63245 \cdot 10^{-1}$	$7.45192 \cdot 10^{-1}$
2.2	$3.91435 \cdot 10^{-1}$	$8.70827 \cdot 10^{-1}$	$9.54755 \cdot 10^{-1}$	$9.11556 \cdot 10^{-1}$
2.3	$5.18176 \cdot 10^{-1}$	$8.78809 \cdot 10^{-1}$	1.02020	1.04081
2.4	$6.21001 \cdot 10^{-1}$	$8.47642 \cdot 10^{-1}$	1.05078	1.10413
2.5	$6.99018 \cdot 10^{-1}$	$7.75235 \cdot 10^{-1}$	1.04385	1.08962
2.6	$7.52564 \cdot 10^{-1}$	$6.62278 \cdot 10^{-1}$	1.00248	1.00496
2.7	$7.82881 \cdot 10^{-1}$	$5.12248 \cdot 10^{-1}$	$9.35578 \cdot 10^{-1}$	$8.75306 \cdot 10^{-1}$
2.8	$7.91786 \cdot 10^{-1}$	$3.31280 \cdot 10^{-1}$	$8.58293 \cdot 10^{-1}$	$7.36667 \cdot 10^{-1}$
2.9	$7.81255 \cdot 10^{-1}$	$1.27832 \cdot 10^{-1}$	$7.91641 \cdot 10^{-1}$	$6.26696 \cdot 10^{-1}$
3.0	$7.53133 \cdot 10^{-1}$	$-8.78513 \cdot 10^{-2}$	$7.58240 \cdot 10^{-1}$	$5.74928 \cdot 10^{-1}$
3.1	$7.08832 \cdot 10^{-1}$	$-3.04452 \cdot 10^{-1}$	$7.71445 \cdot 10^{-1}$	$5.95128 \cdot 10^{-1}$
3.2	$6.49219 \cdot 10^{-1}$	$-5.10416 \cdot 10^{-1}$	$8.25838 \cdot 10^{-1}$	$6.82008 \cdot 10^{-1}$
3.3	$5.74713 \cdot 10^{-1}$	$-6.94788 \cdot 10^{-1}$	$9.01679 \cdot 10^{-1}$	$8.13025 \cdot 10^{-1}$
3.4	$4.85442 \cdot 10^{-1}$	$-8.47947 \cdot 10^{-1}$	$9.77071 \cdot 10^{-1}$	$9.54667 \cdot 10^{-1}$
3.5	$3.81554 \cdot 10^{-1}$	$-9.62229 \cdot 10^{-1}$	1.03512	1.07147

Table 4: (continued)

ka	Re. G	Im. G	$\|G\|$	$\|G\|^2$
3.6	$2.63517 \cdot 10^{-1}$	-1.03233	1.06544	1.13516
3.7	$1.32413 \cdot 10^{-1}$	-1.05558	1.06385	1.13179
3.8	$-9.79653 \cdot 10^{-3}$	-1.03198	1.03202	1.06507
3.9	$-1.60064 \cdot 10^{-1}$	$-9.64103 \cdot 10^{-1}$	$9.77297 \cdot 10^{-1}$	$9.55110 \cdot 10^{-1}$
4.0	$-3.14148 \cdot 10^{-1}$	$-8.56785 \cdot 10^{-1}$	$9.12565 \cdot 10^{-1}$	$8.32775 \cdot 10^{-1}$
4.1	$-4.66647 \cdot 10^{-1}$	$-7.16663 \cdot 10^{-1}$	$8.55200 \cdot 10^{-1}$	$7.31367 \cdot 10^{-1}$
4.2	$-6.11190 \cdot 10^{-1}$	$-5.51586 \cdot 10^{-1}$	$8.23286 \cdot 10^{-1}$	$6.77799 \cdot 10^{-1}$
4.3	$-7.40791 \cdot 10^{-1}$	$-3.70044 \cdot 10^{-1}$	$8.28070 \cdot 10^{-1}$	$6.85700 \cdot 10^{-1}$
4.4	$-8.48295 \cdot 10^{-1}$	$-1.80616 \cdot 10^{-1}$	$8.67314 \cdot 10^{-1}$	$7.52233 \cdot 10^{-1}$
4.5	$-9.26929 \cdot 10^{-1}$	$8.52498 \cdot 10^{-3}$	$9.26969 \cdot 10^{-1}$	$8.59271 \cdot 10^{-1}$
4.6	$-9.70796 \cdot 10^{-1}$	$1.90000 \cdot 10^{-1}$	$9.89217 \cdot 10^{-1}$	$9.78551 \cdot 10^{-1}$
4.7	$-9.75421 \cdot 10^{-1}$	$3.57501 \cdot 10^{-1}$	1.03887	1.07926
4.8	$-9.38162 \cdot 10^{-1}$	$5.05971 \cdot 10^{-1}$	1.06591	1.13616
4.9	$-8.58563 \cdot 10^{-1}$	$6.31637 \cdot 10^{-1}$	1.06588	1.13610
5.0	$-7.38540 \cdot 10^{-1}$	$7.31960 \cdot 10^{-1}$	1.03981	1.08121
5.1	$-5.82396 \cdot 10^{-1}$	$8.05451 \cdot 10^{-1}$	$9.93949 \cdot 10^{-1}$	$9.87935 \cdot 10^{-1}$
5.2	$-3.96638 \cdot 10^{-1}$	$8.51500 \cdot 10^{-1}$	$9.39350 \cdot 10^{-1}$	$8.82378 \cdot 10^{-1}$
5.3	$-1.89657 \cdot 10^{-1}$	$8.70151 \cdot 10^{-1}$	$8.90577 \cdot 10^{-1}$	$7.93128 \cdot 10^{-1}$
5.4	$2.87974 \cdot 10^{-2}$	$8.61919 \cdot 10^{-1}$	$8.62400 \cdot 10^{-1}$	$7.43734 \cdot 10^{-1}$
5.5	$2.48172 \cdot 10^{-1}$	$8.27676 \cdot 10^{-1}$	$8.64084 \cdot 10^{-1}$	$7.46641 \cdot 10^{-1}$
5.6	$4.57761 \cdot 10^{-1}$	$7.68575 \cdot 10^{-1}$	$8.94568 \cdot 10^{-1}$	$8.00252 \cdot 10^{-1}$
5.7	$6.47337 \cdot 10^{-1}$	$6.86025 \cdot 10^{-1}$	$9.43225 \cdot 10^{-1}$	$8.89673 \cdot 10^{-1}$
5.8	$8.07786 \cdot 10^{-1}$	$5.81724 \cdot 10^{-1}$	$9.95452 \cdot 10^{-1}$	$9.90924 \cdot 10^{-1}$
5.9	$9.31620 \cdot 10^{-1}$	$4.57786 \cdot 10^{-1}$	1.03802	1.07748
6.0	1.01339	$3.16830 \cdot 10^{-1}$	1.06176	1.12733
6.1	1.04995	$1.62124 \cdot 10^{-1}$	1.06239	1.12867
6.2	1.04055	$-2.31787 \cdot 10^{-3}$	1.04055	1.08275
6.3	$9.86771 \cdot 10^{-1}$	$-1.71698 \cdot 10^{-1}$	1.00160	1.00320
6.4	$8.92303 \cdot 10^{-1}$	$-3.40481 \cdot 10^{-1}$	$9.55053 \cdot 10^{-1}$	$9.12126 \cdot 10^{-1}$
6.5	$7.62625 \cdot 10^{-1}$	$-5.02517 \cdot 10^{-1}$	$9.13302 \cdot 10^{-1}$	$8.34120 \cdot 10^{-1}$
6.6	$6.04612 \cdot 10^{-1}$	$-6.51273 \cdot 10^{-1}$	$8.88658 \cdot 10^{-1}$	$7.89712 \cdot 10^{-1}$
6.7	$4.26057 \cdot 10^{-1}$	$-7.80107 \cdot 10^{-1}$	$8.88869 \cdot 10^{-1}$	$7.90087 \cdot 10^{-1}$
6.8	$2.35206 \cdot 10^{-1}$	$-8.82638 \cdot 10^{-1}$	$9.13441 \cdot 10^{-1}$	$8.34375 \cdot 10^{-1}$
6.9	$4.03090 \cdot 10^{-2}$	$-9.53151 \cdot 10^{-1}$	$9.54003 \cdot 10^{-1}$	$9.10122 \cdot 10^{-1}$
7.0	$-1.50790 \cdot 10^{-1}$	$-9.86991 \cdot 10^{-1}$	$9.98443 \cdot 10^{-1}$	$9.96888 \cdot 10^{-1}$

Table 4: (continued)

ka	Re. G	Im. G	$\|G\|$	$\|G\|^2$
7.1	$-3.30963 \cdot 10^{-1}$	$-9.80958 \cdot 10^{-1}$	1.03528	1.07181
7.2	$-4.94033 \cdot 10^{-1}$	$-9.33614 \cdot 10^{-1}$	1.05627	1.11571
7.3	$-6.34910 \cdot 10^{-1}$	$-8.45510 \cdot 10^{-1}$	1.05735	1.11800
7.4	$-7.49646 \cdot 10^{-1}$	$-7.19268 \cdot 10^{-1}$	1.03890	1.07931
7.5	$-8.35427 \cdot 10^{-1}$	$-5.59549 \cdot 10^{-1}$	1.00550	1.01103
7.6	$-8.90508 \cdot 10^{-1}$	$-3.72889 \cdot 10^{-1}$	$9.65429 \cdot 10^{-1}$	$9.32053 \cdot 10^{-1}$
7.7	$-9.14122 \cdot 10^{-1}$	$-1.67382 \cdot 10^{-1}$	$9.29322 \cdot 10^{-1}$	$8.63640 \cdot 10^{-1}$
7.8	$-9.06369 \cdot 10^{-1}$	$4.77256 \cdot 10^{-2}$	$9.07623 \cdot 10^{-1}$	$8.23780 \cdot 10^{-1}$
7.9	$-8.68104 \cdot 10^{-1}$	$2.62532 \cdot 10^{-1}$	$9.06932 \cdot 10^{-1}$	$8.22525 \cdot 10^{-1}$
8.0	$-8.00863 \cdot 10^{-1}$	$4.67028 \cdot 10^{-1}$	$9.27090 \cdot 10^{-1}$	$8.59496 \cdot 10^{-1}$
8.1	$-7.06810 \cdot 10^{-1}$	$6.51669 \cdot 10^{-1}$	$9.61383 \cdot 10^{-1}$	$9.24257 \cdot 10^{-1}$
8.2	$-5.88712 \cdot 10^{-1}$	$8.07905 \cdot 10^{-1}$	$9.99644 \cdot 10^{-1}$	$9.99288 \cdot 10^{-1}$
8.3	$-4.49923 \cdot 10^{-1}$	$9.28627 \cdot 10^{-1}$	1.03188	1.06478
8.4	$-2.94410 \cdot 10^{-1}$	1.00855	1.05065	1.10386
8.5	$-1.26725 \cdot 10^{-1}$	1.04448	1.05214	1.10700
8.6	$4.79953 \cdot 10^{-2}$	1.03539	1.03650	1.07434
8.7	$2.24103 \cdot 10^{-1}$	$9.82446 \cdot 10^{-1}$	1.00768	1.01542
8.8	$3.95539 \cdot 10^{-1}$	$8.88852 \cdot 10^{-1}$	$9.72889 \cdot 10^{-1}$	$9.46512 \cdot 10^{-1}$
8.9	$5.55987 \cdot 10^{-1}$	$7.59604 \cdot 10^{-1}$	$9.41342 \cdot 10^{-1}$	$8.86124 \cdot 10^{-1}$
9.0	$6.99098 \cdot 10^{-1}$	$6.01147 \cdot 10^{-1}$	$9.22016 \cdot 10^{-1}$	$8.50113 \cdot 10^{-1}$
9.1	$8.18749 \cdot 10^{-1}$	$4.20971 \cdot 10^{-1}$	$9.20633 \cdot 10^{-1}$	$8.47565 \cdot 10^{-1}$
9.2	$9.09354 \cdot 10^{-1}$	$2.27204 \cdot 10^{-1}$	$9.37307 \cdot 10^{-1}$	$8.78544 \cdot 10^{-1}$
9.3	$9.66174 \cdot 10^{-1}$	$2.81710 \cdot 10^{-2}$	$9.66585 \cdot 10^{-1}$	$9.34286 \cdot 10^{-1}$
9.4	$9.85638 \cdot 10^{-1}$	$-1.67984 \cdot 10^{-1}$	$9.99851 \cdot 10^{-1}$	$9.99702 \cdot 10^{-1}$
9.5	$9.65615 \cdot 10^{-1}$	$-3.53648 \cdot 10^{-1}$	1.02834	1.05748
9.6	$9.05638 \cdot 10^{-1}$	$-5.22025 \cdot 10^{-1}$	1.04532	1.09269
9.7	$8.07041 \cdot 10^{-1}$	$-6.67334 \cdot 10^{-1}$	1.04721	1.09665
9.8	$6.73020 \cdot 10^{-1}$	$-7.84949 \cdot 10^{-1}$	1.03397	1.06910
9.9	$5.08545 \cdot 10^{-1}$	$-8.71465 \cdot 10^{-1}$	1.00899	1.01807
10.0	$3.20206 \cdot 10^{-1}$	$-9.24698 \cdot 10^{-1}$	$9.78570 \cdot 10^{-1}$	$9.57599 \cdot 10^{-1}$

Table 5: Deductions from Table 4

Max/min	ρ	Separation in ρ	$\lvert G^2 \rvert$	G_1	G_2
M	1.16		0.982		
m	1.78	0.62	0.394	0.810	0.182
M	2.44	0.66	1.112	0.841	0.213
m	3.02	0.58	0.572	0.905	0.149
M	3.64	0.62	1.149	0.914	0.158
m	4.24	0.60	0.671	0.946	0.126
M	4.85	0.61	1.148	0.946	0.126
m	5.45	0.60	0.736	0.965	0.107
M	6.05	0.60	1.138	0.962	0.104
m	6.65	0.60	0.782	0.975	0.109
M	7.25	0.60	1.127	0.973	0.089
m	7.85	0.60	0.816	0.983	0.079
M	8.45	0.60	1.113	0.979	0.076
m	9.05	0.60	0.844	0.987	0.068
M	9.65	0.60	1.102	0.985	0.065

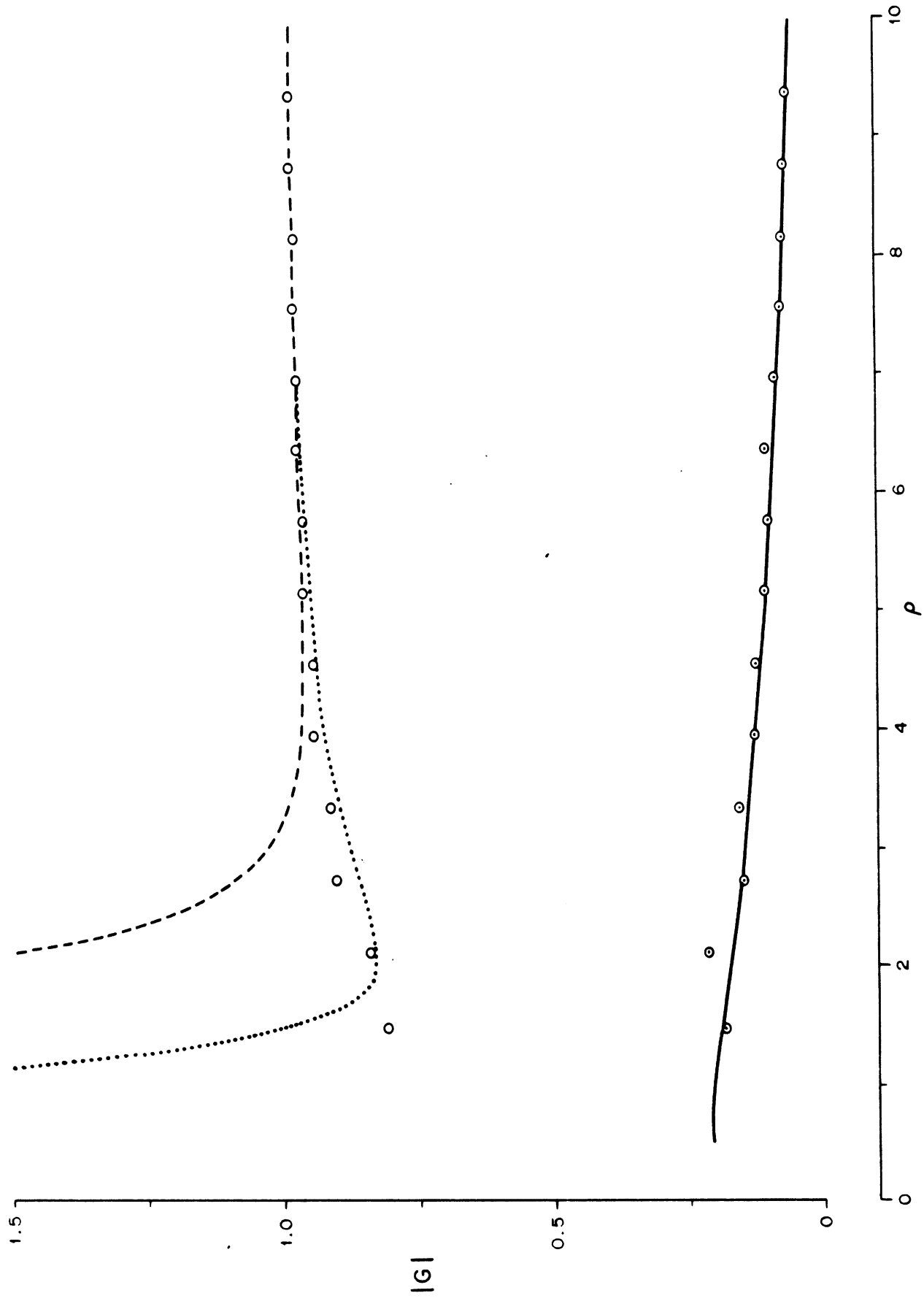

FIG. 4: COMPARISON OF DEDUCED VALUES OF G_2 (o o o) AND G_1 (o o o) WITH THEORETICAL EXPRESSIONS FOR $|G^c|$ (——) AND $|G^o|$ USING 5 TERMS (– – –) AND 3 TERMS (· · · ·) IN EQUATION (71).

Table 6: Theoretical Creeping Wave Component

ρ	$\left\|G^c\right\|$	arg G^c (degrees)
0.5	$2.03393 \cdot 10^{-1}$	407.169
0.6	$2.06178 \cdot 10^{-1}$	439.122
0.7	$2.07118 \cdot 10^{-1}$	452.634
0.8	$2.06825 \cdot 10^{-1}$	467.877
0.9	$2.05685 \cdot 10^{-1}$	484.226
1.0	$2.03955 \cdot 10^{-1}$	501.311
1.1	$2.01810 \cdot 10^{-1}$	518.906
1.3	$1.96733 \cdot 10^{-1}$	555.078
1.5	$1.91086 \cdot 10^{-1}$	592.036
2.0	$1.76388 \cdot 10^{-1}$	685.954
2.5	$1.62332 \cdot 10^{-1}$	780.604
3.0	$1.49505 \cdot 10^{-1}$	875.333
3.5	$1.37974 \cdot 10^{-1}$	969.935
4.0	$1.27650 \cdot 10^{-1}$	1064.346
4.5	$1.18404 \cdot 10^{-1}$	1158.551
5.0	$1.10106 \cdot 10^{-1}$	1252.556
5.5	$1.02634 \cdot 10^{-1}$	1346.375
6.0	$9.58887 \cdot 10^{-2}$	1440.020
6.5	$8.97752 \cdot 10^{-2}$	1533.507
7.0	$8.42178 \cdot 10^{-2}$	1626.850
7.5	$7.91500 \cdot 10^{-2}$	1720.060
8.0	$7.45155 \cdot 10^{-2}$	1813.148
8.5	$7.02655 \cdot 10^{-2}$	1906.124
9.0	$6.63578 \cdot 10^{-2}$	1998.998
9.5	$6.27564 \cdot 10^{-2}$	2091.776
10.0	$5.94294 \cdot 10^{-2}$	2184.466

$$G^o e^{2i\rho} = 1 - \frac{3i}{2\rho} + \frac{5}{2\rho^2} + \frac{25i}{4\rho^3} + \frac{22}{\rho^4} + O(\rho^{-5}) \ . \qquad (71)$$

The real and imaginary parts and modulus of this expression have been computed for the same selected values of ρ, and the results are listed in Table 7 under the heading "5-term optics". In Fig. 4 the modulus is plotted as a broken line, and for the large ρ ($\rho \geqslant 5$, say) the agreement with the open circles representing G_1 is very good. G_1, however, decreases more or less uniformly with ρ and does so at a greater rate as ρ gets smaller. The modulus of the optics component does not show this behavior. It decreases relatively little, reaches a shallow minimum of 0.9353 at $\rho = 4.57$, and then increases without limit, becoming more than twice G_1 for $\rho \leqslant 2$.

The main reason for this "failure" on the part of equation (71) is the large magnitude of the coefficients of the higher powers of ρ. These contribute little when ρ is large (of order 10, say), but dominate the expression when ρ is small. Can we therefore do better by omitting them? Since G_1 is less than unity, it is obviously necessary to retain the terms through ρ^{-2} on the right hand side of (71) if we are to have any hope of matching G_1, but if the terms in ρ^{-3} and ρ^{-4} are ignored, the values of the real and imaginary parts and modulus of $G^o e^{2i\rho}$ are as shown in Table 7 under the heading "3-term optics". In Fig. 4 the modulus appears as a dotted line and, as expected, is almost indistinguishable from the 5-term result for the large ρ ($\rho \geqslant 7$, say). As ρ decreases, however, the 3-term answer falls progressively below the 5-term one, and remains in good agreement with G_1 down to $\rho = 2$. Ultimately, this also fails. The modulus of the 3-term expression has a minimum value 0.8351 at $\rho = 2.13$, and increases rapidly for $\rho < 2$. Its values then bear no resemblance to those of G_1.

Because of the assumptions inherent in the derivation of G_1 and G_2 and the resulting uncertainties associated with their values, the above comparisons are

Table 7: Theoretical Optics Components

ρ	5-term optics			3-term optics		
	Real	Imag.	Modulus	Real	Imag.	Modulus
0.5	343.00000	47.00000	346.20514	-9.00000	-3.00000	9.48683
0.6	163.80865	26.43519	165.92798	-5.94444	-2.50000	6.44875
0.7	87.52645	16.07872	88.99103	-4.10204	-2.14286	4.62802
0.8	50.80469	10.33203	51.84465	-2.90625	-1.87500	3.45860
0.9	31.44505	6.90672	32.19463	-2.08642	-1.66667	2.67038
1.0	20.50000	4.75000	20.60498	-1.50000	-1.50000	2.12132
1.1	13.96018	3.33208	14.35233	-1.06612	-1.36364	1.73093
1.3	7.22352	1.69094	7.41880	-0.47929	-1.15385	1.24943
1.5	4.23457	0.85185	4.31940	-0.11111	-1.00000	1.00615
2.0	1.75000	0.03125	1.75028	0.37500	-0.75000	0.83853
2.5	1.16320	-0.20000	1.18027	0.60000	-0.60000	0.84853
3.0	0.99383	-0.26852	1.02946	0.72222	-0.50000	0.87841
3.5	0.94252	-0.28280	0.98404	0.79592	-0.42857	0.90397
4.0	0.92969	-0.27734	0.97017	0.84375	-0.37500	0.92333
4.5	0.93019	-0.26474	0.96714	0.87654	-0.33333	0.93778
5.0	0.93520	-0.25000	0.96804	0.90000	-0.30000	0.94868
5.5	0.94140	-0.23516	0.97032	0.91736	-0.27273	0.95704
6.0	0.94753	-0.22106	0.97298	0.93056	-0.25000	0.96355
6.5	0.95315	-0.20801	0.97559	0.94083	-0.23077	0.96872
7.0	0.95814	-0.19606	0.97800	0.94898	-0.21429	0.97287
7.5	0.96251	-0.18519	0.98016	0.95556	-0.20000	0.97626
8.0	0.96631	-0.17529	0.98208	0.96094	-0.18750	0.97906
8.5	0.96961	-0.16629	0.98377	0.96540	-0.17647	0.98139
9.0	0.97249	-0.15809	0.98526	0.96914	-0.16667	0.98336
9.5	0.97500	-0.15061	0.98656	0.97230	-0.15789	0.98504
10.0	0.97720	-0.14375	0.98772	0.97500	-0.15000	0.98647

little more than suggestive of the probable accuracy of the expressions for G^c and G^o. Though it appears indisputable that the 3-term optics expression is, on the whole, numerically superior to the 5-term one, Fig. 4 provides no confirmation of the phase. The real test comes when G^c and G^o are combined with due account of phase or, alternatively, when either G^c or G^o is subtracted from G, where this is computed from the exact formula (70). Of these procedures, the most critical is that used for the soft sphere. If the real and imaginary parts of $(G-G^c)\, e^{2i\rho}$ are examined, the presence (or absence) of any oscillations of the same period as those in Fig. 3 is an immediate check on the numerical effectiveness of the formula for G^c, and a comparison with the real and imaginary parts of $G^o e^{2i\rho}$ also serves as a check on the optics expression.

Using the values for G obtained from the exact Mie series (70) and listed in Table 4, and the data for G^c computed from the expression (68) and given in Table 6, the real and imaginary parts of $(G-G^c)\, e^{2i\rho}$ have been determined for selected values of ρ. These are shown in Table 8, and are plotted as functions of ρ in Figs. 5 and 6. We observe that for large ρ there is only the slightest trace of an oscillation, amounting to less than 1/2 percent in the real part and perhaps 3 percent in the imaginary. As ρ decreases, the oscillation begins to assert itself and is quite obvious for $\rho < 5$, but when expressed as a percentage of the mean level the amplitude is hardly significant. The largest values are about 3 and 6 percent for the real and imaginary parts respectively, and occur near $\rho = 2$. Overall, the real part decreases with ρ and does so at an increasing rate as ρ gets smaller. It is negative for $\rho \leqslant 0.62$. In contrast, the imaginary part increases at an increasing rate, reaching a maximum of 0.69 when $\rho = 0.85$, but falling off rapidly for ρ less than this.

Bearing in mind the relatively large magnitude of the creeping wave contribution to the far field amplitude, the suppression of the oscillations achieved by the asymptotic representation (68) of G^c is almost as effective as that previously found

Table 8: $(G-G^c)e^{2i\rho}$

ρ	Real	Imag.	Modulus
0.5	-0.14784	-0.50466	0.52587
0.6	-0.02232	-0.56666	0.56710
0.7	0.09518	-0.64682	0.65379
0.8	0.21058	-0.68433	0.71600
0.9	0.32270	-0.68846	0.76034
1.0	0.41852	-0.66476	0.78553
1.1	0.49025	-0.62419	0.79370
1.3	0.56079	-0.54030	0.77873
1.5	0.57847	-0.50228	0.76611
2.0	0.69302	-0.50800	0.85927
2.5	0.78345	-0.41412	0.88617
3.0	0.81161	-0.39266	0.90160
3.5	0.87037	-0.34595	0.93660
4.0	0.87718	-0.31276	0.93127
4.5	0.91028	-0.29372	0.95649
5.0	0.91852	-0.25981	0.95456
5.5	0.93122	-0.25054	0.96434
6.0	0.94422	-0.22497	0.97065
6.5	0.94582	-0.21458	0.96985
7.0	0.95859	-0.20013	0.97925
7.5	0.95836	-0.18638	0.97631
8.0	0.96602	-0.17956	0.98257
8.5	0.96877	-0.16563	0.98282
9.0	0.97073	-0.16092	0.98398
9.5	0.97596	-0.15080	0.98754
10.0	0.97527	-0.14445	0.98590

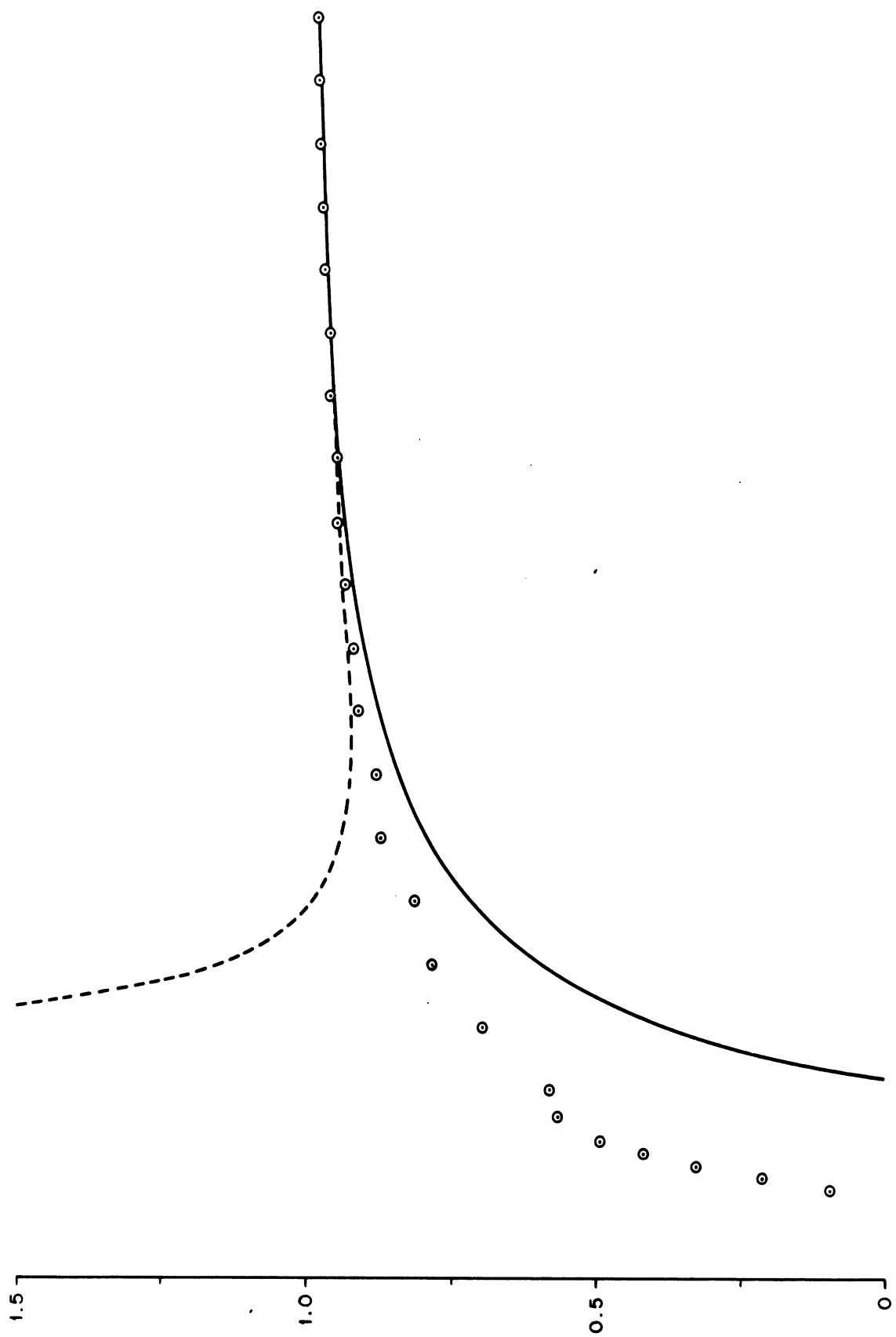

FIG. 5: COMPARISON OF THE REAL PART OF THE "ACTUAL" OPTICS CONTRIBUTION (⊙⊙⊙) AND THE REAL PARTS OF THE 3-TERM (——) AND 5-TERM (---) OPTICS EXPRESSIONS:

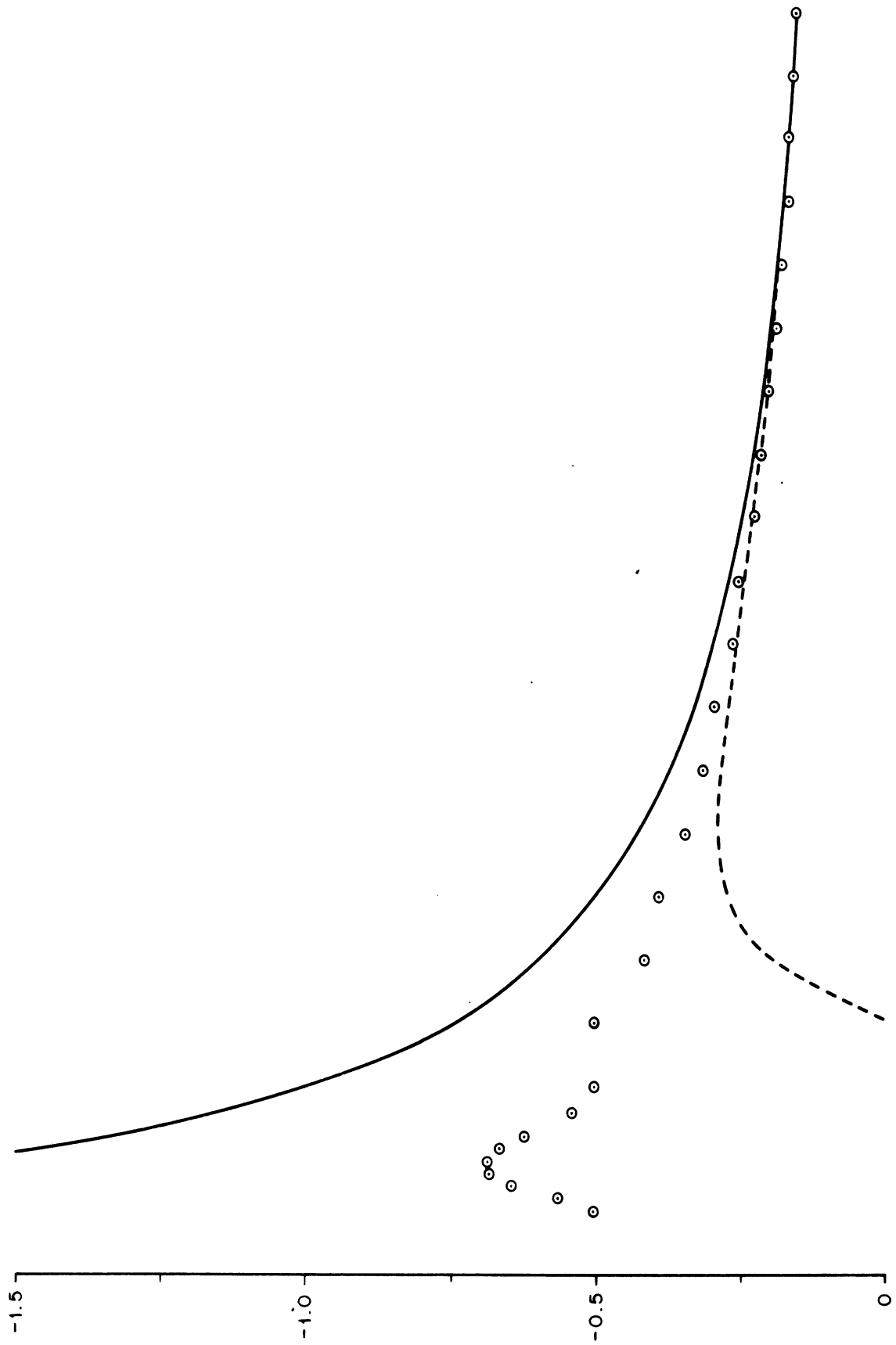

FIG. 6: COMPARISON OF THE IMAGINARY PART OF THE "ACTUAL" OPTICS CONTRIBUTION (o o o)
AND THE IMAGINARY PARTS OF THE 3-TERM (——) AND 5-TERM (- - -) OPTICS EXPRESSIONS

in the case of the soft sphere. All of the terms in (68) are essential to obtain this result. The omission of even the one involving τ^{-3} in the exponent greatly increases the amplitude of oscillation for ρ near 10, and leads to quite large and rapid variations for ρ near unity. Indeed, for $\rho < 2$ the behavior of the "actual" optics component is changed out of all recognition if this (or any other) term in (68) is neglected.

To facilitate the comparison with $G^o e^{2i\rho}$, curves representing the real and imaginary parts of both the 3- and 5-term optics expressions (see Table 7) have been included in Figs. 5 and 6. Taking first the real parts (Fig. 5) we note that the retention of the last two terms in (71) has only a negligible effect for $\rho \geqslant 7$, a fact which is otherwise obvious from Table 7. As ρ decreases, however, the values obtained from the 3-term expression fall progressively below those of the "actual" contribution, and though the trends are the same, the estimates are too small by at least a factor 2 for all $\rho < 2$, and become negative when $\rho = 1.511$. Nevertheless, the 3-term expression is superior to the 5-term one on the whole. The latter tends to overestimate the actual contribution, and does so by a rapidly increasing amount for $\rho < 3.5$.

With the imaginary parts (see Fig. 6) the differences between the 3- and 5-term expressions are somewhat more apparent for the larger ρ, but are still negligible if $\rho \geqslant 7$. The 5-term expression now underestimates the actual contribution when $\rho < 5$, and the curve falls away rapidly for $\rho < 3.5$. In contrast, the curve based on the 3-term expression has the right qualitative behavior even down to values of ρ in a neighborhood of 2. It also tends to overestimate the actual contribution and because of this the modulus of the 3-term expression is, for $\rho < 7$, more accurate than either its real or imaginary part. This is evident from Fig. 7 and constitutes what is, perhaps, the clearest demonstration of the numerical superiority of the 3-term expression for G^o. The modulus is within 10 percent of the required value for $\rho \geqslant 1.8$.

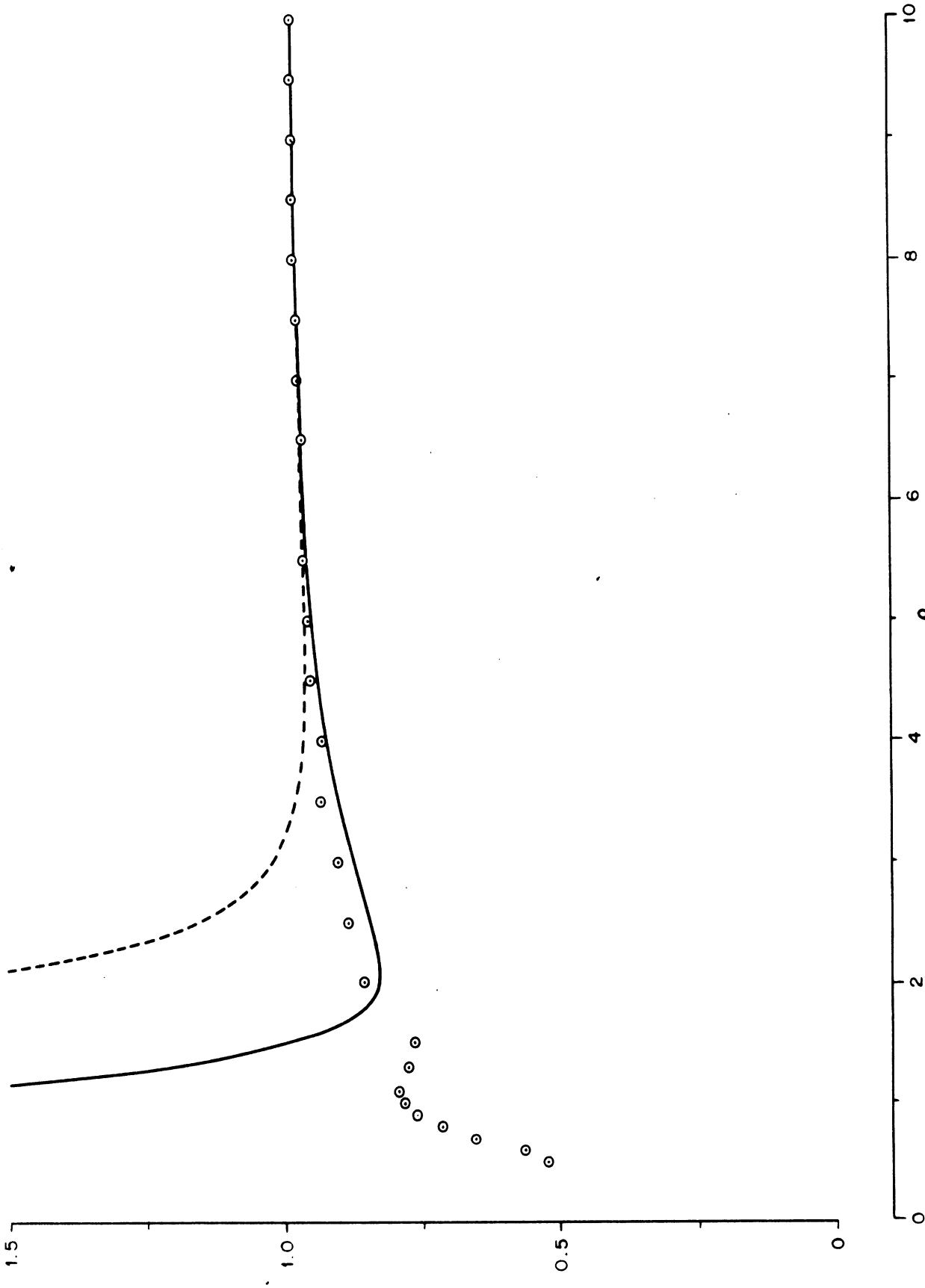

FIG. 7: MODULUS OF "ACTUAL" OPTICS CONTRIBUTION (⊙⊙⊙), COMPARED WITH 3-TERM (——) AND 5-TERM (– – –) APPROXIMATIONS

3.5 Remarks

The creeping wave contribution to the far field amplitude is considerably greater for a hard sphere than for a soft sphere. The ratio of the two exceeds 100 if $\rho \geqslant 5.2$, and it is not therefore surprising that the extent to which the oscillations of G as a function of ρ can be suppressed is somewhat less for the hard body. In addition, the higher order terms in the asymptotic expression for G^c are more important in the hard case, and have a larger effect on the resulting phase and amplitude, but by retaining the term involving τ^{-3} in the exponential factor on the right hand side of (68), which term was negligible in the corresponding expression for a soft sphere, the values obtained for the real and imaginary parts of G^c are sufficient to account for almost all of the oscillations of G. Only the slightest trace of oscillation remains for $\rho \gg 1$, and though the amplitude does build up to a maximum of 5 to 10 percent for ρ near 2, it would seem that (68) is an accurate approximation to the actual creeping wave contribution if $\rho \geqslant 7$, and an adequate approximation (sufficient for most practical purposes) for ρ down to 2.5 or below. Because of the comparatively regular behavior of $(G - G^c)e^{2i\rho}$ as a function of ρ, it is even possible that (68) is applicable for ρ as small as unity, but there is no obvious way in which this can be verified. What is more, the rapid variation of the imaginary part near $\rho = 0.9$ (see Fig. 6) is almost certainly evidence of a failure of (68). We also note that the sensibly linear variation of $\arg G^c$ with ρ, characteristic of the larger ρ, ceases to hold for $\rho < 0.9$. By applying a least squares analysis to the values of $\arg G^c$ listed in Table 6, we have

$$\arg G^c = 187.455\rho + 313.191 \text{ (degrees)} \qquad (72)$$

for $1.0 \leqslant \rho \leqslant 10.0$. The implied phase velocity of the surface wave is $0.9602\,c$, and for the above range of ρ, (72) is in error by no more than 3^o. When $\rho = 0.6$, however, the error is 14^o.

Turning now to the optics component, the 5-term expression for G^o shown in equation (69) is quite accurate for values of ρ of order 10 or greater, and con-

tinues to be in good agreement with the "actual" contribution down to $\rho = 5$, but its performance then falls off rapidly. It is inappropriate for $\rho < 3$. The 3-term expression obtained by omitting the terms in ρ^{-3} and ρ^{-4} is not much inferior for $\rho \geqslant 3$, and is definitely superior for $\rho < 3$. Nevertheless, even it ceases to have any relevance for $\rho < 2$. With the soft sphere the failure could be overcome, at least in part, by reverting to a 2-term expression, but this does not work for the hard sphere inasmuch as the modulus of the "actual" contribution is less than unity for all ρ.

Our ability to accurately predict the optics component using a single, simple uniform expansion is therefore limited to $\rho \geqslant 2$ (approx.), and this in turn leads to a corresponding restriction on the values of ρ for which the cross section can be estimated satisfactorily. To illustrate the accuracy that can be achieved, equations (68) and (69) give $|G|^2 = 0.53784$, 0.67563 and 0.82280 for $\rho = 3.0$, 2.0 and 1.5, and these are in error by 7.3, 16.4 and 26.7 percent respectively.

IV
A PERFECTLY CONDUCTING SPHERE

The third and final problem to be investigated is the scattering of a plane electromagnetic wave by a metallic sphere whose conductivity is assumed infinite. This is, perhaps, the most widely treated of all problems in diffraction theory, and as much of the analysis is quite similar to that which we have already given for the soft and hard spheres, the details will be omitted wherever possible.

4.1 The Analysis

Consider a perfectly conducting sphere of radius a whose center is at the origin of a Cartesian coordinate system (x, y, z). A plane electromagnetic wave is incident in the direction of the negative z axis, and since there is no loss of generality in taking its electric vector to be in the x direction, we have

$$\underline{E}^i = \hat{x} e^{-ikz} \quad , \qquad \underline{H}^i = -\hat{y} Y e^{-ikz} \tag{73}$$

where Y is the intrinsic admittance of free space.

In terms of the spherical polar coordinates (R, θ, ϕ) previously defined, the incident and scattered fields can be expressed as sums of spherical vector wave functions, leading to the standard Mie series form of solution (Stratton, 1941). The far field components are then obtained by replacing the radial functions by the first terms of their asymptotic expansions for large kR, and for the particular case of back scattering

$$\underline{E}^s = \hat{x} S \frac{e^{ikR}}{kR} \quad , \qquad \underline{H}^s = \hat{y} Y S \frac{e^{ikR}}{kR} \tag{74}$$

where the (scalar) far field amplitude S is given by

$$S = -i \sum_{n=1}^{\infty} (-1)^n (n+\tfrac{1}{2}) \left\{ \frac{\left[\rho j_n(\rho)\right]'}{\left[\rho h_n^{(1)}(\rho)\right]'} - \frac{j_n(\rho)}{h_n^{(1)}(\rho)} \right\} . \tag{75}$$

In all directions other than back ($\theta = 0$) and forward ($\theta = \pi$) scattering, the sphere has a depolarizing effect and the resulting far field amplitude is a vector quantity.

For sufficiently small ρ, S has the power series expansion

$$S = \frac{3}{2}\rho^3 \left\{ 1 - \frac{5}{54}\rho^2 + \frac{i}{3}\rho^3 + \frac{17}{900}\rho^4 + \frac{2i}{5}\rho^5 + O(\rho^6) \right\} \tag{76}$$

(see Goodrich et al, 1961, where the coefficients of the next four higher powers of ρ are also shown). As with the series for the soft and hard sphere, the right hand side of (76) is convergent for $\rho < 1$. It is comparable to the hard body solution (49) in the powers of ρ that occur, but is quite different from the series for the soft body.

The above series is obviously inappropriate to the larger ρ. There is, however, an alternative representation of S which is well suited to values of $\rho \gg 1$, and this can be obtained by application of a Watson transformation to (75). Though the procedure is similar in most respects to that given in Section 2.2, there is one major difference: whereas for the soft and hard spheres it was necessary to apply the transform to the series representing the total (incident plus scattered) field with the radial dependence included, the fact that the far field amplitude (75) is already the difference of two series enables us to transform S directly.

Using the expression (7) for the spherical Bessel function as a sum of Hankel functions, equation (75) becomes

$$S = -\frac{i}{2} \sum_{n=1}^{\infty} (-1)^n (n+\tfrac{1}{2}) \left\{ \frac{\left[\rho h_n^{(2)}(\rho)\right]'}{\left[\rho h_n^{(1)}(\rho)\right]'} - \frac{h_n^{(2)}(\rho)}{h_n^{(1)}(\rho)} \right\} ,$$

which can be written as

$$S = -\frac{1}{4}\int_{C'}\left\{\frac{\left[\rho h^{(2)}_{\nu-1/2}(\rho)\right]'}{\left[\rho h^{(1)}_{\nu-1/2}(\rho)\right]'} - \frac{h^{(2)}_{\nu-1/2}(\rho)}{h^{(1)}_{\nu-1/2}(\rho)}\right\}\sec\nu\pi\ \nu d\nu \tag{77}$$

where C' is a path enclosing in a clockwise sense the poles of $\sec\nu\pi$ for $\nu > 1/2$. As such, the contour differs from that in Section 2.2 in its exclusion of the pole at $\nu = 1/2$. Providing due account is taken of the appropriate residue, the path can be pulled over the pole, and since

$$h^{(1)}_{o}(\rho) = -\frac{i}{\rho}e^{i\rho},$$

we have

$$S = \frac{i}{2}e^{-2i\rho} - \frac{1}{4}\int_{C}\left\{\frac{\left[\rho h^{(2)}_{\nu-1/2}(\rho)\right]'}{\left[\rho h^{(1)}_{\nu-1/2}(\rho)\right]'} - \frac{h^{(2)}_{\nu-1/2}(\rho)}{h^{(1)}_{\nu-1/2}(\rho)}\right\}\sec\nu\pi\ \nu d\nu, \tag{78}$$

where C is as defined in Section 2.2.

The original analysis is now applicable. For the lower portion of the path we use the identity

$$\sec\nu\pi = e^{-2i\nu\pi}\sec\nu\pi + 2ie^{-i\nu\pi}\tan\nu\pi \tag{79}$$

(see equation 9). If this is inserted into (78), the integral corresponding to the first term of (79) can have its path reflected in the origin of the ν plane and combined with the integral over the upper part of C. The resulting contour can then be closed in the upper half plane, and the integral evaluated as a sum of residues from the zeros $\nu = \nu_n$ of $\left[\rho h^{(1)}_{\nu-1/2}(\rho)\right]'$ and the zeros $\nu = \nu_m$ of $h^{(1)}_{\nu-1/2}(\rho)$. This is the creeping wave contribution S^c to the far field amplitude. The remaining integral, obtained from the second term on the right hand side of (79), constitutes the optics field S^o, and hence

$$S = S^c + S^o$$

with

$$S^c = -\frac{i\pi}{2}\sum_n \left[\frac{\frac{\partial}{\partial\rho}\left\{\rho^{1/2}H_\nu^{(2)}(\rho)\right\}}{\frac{\partial}{\partial\nu}\frac{\partial}{\partial\rho}\left\{\rho^{1/2}H_\nu^{(1)}(\rho)\right\}}\ \nu\sec\nu\pi\right]_{\nu=\nu_n}$$

$$+\frac{i\pi}{2}\sum_m \left[\frac{H_\nu^{(2)}(\rho)}{\frac{\partial}{\partial\nu}H_\nu^{(1)}(\rho)}\ \nu\sec\nu\pi\right]_{\nu=\nu_m} \tag{80}$$

and

$$S^o = \frac{i}{2}e^{-2i\rho} + \frac{i}{2}\int_{\infty - i\epsilon}^{o}\left\{\frac{\frac{\partial}{\partial\rho}\left(\rho^{1/2}H_\nu^{(2)}(\rho)\right)}{\frac{\partial}{\partial\rho}\left(\rho^{1/2}H_\nu^{(1)}(\rho)\right)} - \frac{H_\nu^{(2)}(\rho)}{H_\nu^{(1)}(\rho)}\right\}e^{-i\nu\pi}\tan\nu\pi\ \nu d\nu. \tag{81}$$

For convenience and ease of comparison with the corresponding results for soft and hard spheres, the spherical Hankel functions have again been replaced by their cylindrical equivalents.

Expressions analogous to those of equations (80) and (81), but for a quantity

$$S_1(0) = iS\ , \tag{82}$$

have been found by Senior and Goodrich (1964). The formula for S^o given in equation (81) is identical (apart from the use of cylindrical functions) to that for $-iS_1^o(0)$ contained in equation (24) of this Reference, but it should be noted that the expressions derived by Senior and Goodrich for $S_1^c(\theta)$ in the immediate vicinity of $\theta = 0$ are in error by a minus sign. The correct results can be obtained by replacing $S_1^c(\theta)$ by $-S_1^c(\theta)$ in their equations (21) and (48), and $S_1^c(0)$ by $-S_1^c(0)$ in (23 and (32). Equation (23) is, for example, then equivalent to (80) above.

4.2 Evaluation of the Creeping Wave and Optics Contributions

Most of the analysis involved in the derivation of asymptotic formulae for S^c and S^o is readily available in the literature and/or is so similar to that which has gone before that only the barest details will suffice.

Starting with the creeping wave component, the second sum on the right hand side of (80) differs only by a factor 2 from the soft sphere contribution (12), and we can therefore take over directly the results of Section 2.2. The first series is also comparable to the hard sphere contribution (50), but the change from $\rho^{-1/2}$ to $\rho^{1/2}$ in the differentiated functions does produce some differences in analysis which are reflected in modifications to the higher order terms in the expansions. Since

$$\frac{\partial}{\partial\rho}\left\{\rho^{1/2}J_\nu(\rho)\right\} = \rho^{1/2}\left\{\frac{\partial}{\partial\rho}J_\nu(\rho) + \frac{1}{2\rho}J_\nu(\rho)\right\},$$

we have, from (16) and (52),

$$\frac{\partial}{\partial\rho}\left\{\rho^{1/2}J_\nu(\rho)\right\} = -\frac{\rho^{1/2}}{\tau^2}\left[\mathrm{Ai}'(x) - \frac{1}{60\tau^2}\left\{(x^3+9)\mathrm{Ai}(x) - 4x\mathrm{Ai}'(x)\right\}\right.$$

$$\left. + \frac{1}{2520\tau^4}\left\{\frac{3}{4}x^4\mathrm{Ai}(x) + \left(\frac{7}{20}x^5 - \frac{17}{2}x^2\right)\mathrm{Ai}'(x)\right\} + O(\tau^{-6})\right]$$

(Scott, 1949), which can be written as

$$\frac{\partial}{\partial\rho}\left\{\rho^{1/2}J_\nu(\rho)\right\} = -\frac{\rho^{1/2}}{\tau^2}\left\{1 + \frac{x}{15\tau^2} - \frac{1}{\tau^4 x}\left(\frac{37}{6300}x^3 + \frac{9}{800}\right) + O(\tau^{-6})\right\}$$

$$\cdot\,\mathrm{Ai}'\left\{x - \frac{x}{60\tau^2}(x^3+9) + \frac{1}{\tau^4 x^3}\left(\frac{2}{1575}x^6 + \frac{3}{400}x^3 - \frac{9}{800}\right) + O(\tau^{-6})\right\}.$$

Hence,

$$\frac{\partial}{\partial\rho}\left\{\rho^{1/2}H_\nu^{(1)}(\rho)\right\} = 2\omega^2\,\frac{\rho^{1/2}}{\tau^2}\left\{1+\frac{x}{15\tau^2}-\frac{1}{\tau^4 x}\left(\frac{37}{6300}x^3+\frac{9}{800}\right)+O(\tau^{-6})\right\}\mathrm{Ai}'(y) \tag{83}$$

where

$$\omega^2 y = x-\frac{1}{60\tau^2 x}(x^3+9)+\frac{1}{\tau^4 x^3}\left(\frac{2}{1575}x^6+\frac{3}{400}x^3-\frac{9}{800}\right)+O(\tau^{-6}) \quad , \tag{84}$$

and if this is now inverted to give x as a function of y, an expression for the zeros $\nu=\nu_n$ is obtained in the form

$$\nu_n = \rho+e^{i\frac{\pi}{3}}\tau\beta_n-\frac{e^{-i\frac{\pi}{3}}}{60\tau\beta_n}(\beta_n^3-9)+\frac{1}{1400\tau^3\beta_n^3}(\beta_n^6-7\beta_n^3+\frac{63}{4})+O(\tau^{-5}) \tag{85}$$

where the β_n are, as before, the zeros of the Airy integral derivative Ai'(-y). The first three terms on the right hand side of (85) have previously been found by Scott (1949), Franz (1954) and others, and the first two terms are the same as for the zeros in the hard body solution (see equation 57).

The asymptotic evaluation of the factor

$$\left[\frac{\frac{\partial}{\partial\rho}\left\{\rho^{1/2}H_\nu^{(2)}(\rho)\right\}}{\frac{\partial}{\partial\nu}\frac{\partial}{\partial\rho}\left\{\rho^{1/2}H_\nu^{(1)}(\rho)\right\}}\right]_{\nu=\nu_n}$$

follows closely the procedure given in Section 3.2, the only essential difference being the change in the expression for y as a function of x. Differentiating (84)

$$\omega^2\frac{\partial y}{\partial x} = 1-\frac{1}{60\tau^2}\left(2x-\frac{9}{x^2}\right)+\frac{1}{\tau^4}\left(\frac{2}{525}x^2+\frac{37}{800x^4}\right)+O(\tau^{-6}) \quad ,$$

giving

$$\frac{1}{\partial y/\partial x} = \omega^2 \left\{ 1 + \frac{\omega^2}{60\tau^2 y^2}(2y^3 - 9) - \frac{\omega}{5600\tau^4 y^4}(12y^6 - 189) + O(\tau^{-6}) \right\},$$

from which we have

$$\left[\frac{\frac{\partial}{\partial \rho}\left\{\rho^{1/2} H_\nu^{(2)}(\rho)\right\}}{\frac{\partial}{\partial \nu}\frac{\partial}{\partial \rho}\left\{\rho^{1/2} H_\nu^{(1)}(\rho)\right\}} \right]_{\nu=\nu_n} = -\frac{\tau}{2\pi} e^{-i\frac{\pi}{6}} \left\{ 1 + \frac{e^{i\frac{\pi}{3}}}{60\tau^2\beta_n^2}(2\beta_n^3 + 9) + \frac{e^{-i\frac{\pi}{3}}}{5600\tau^4\beta_n^4}(12\beta_n^6 - 189) + O(\tau^{-6}) \right\} \frac{1}{\beta_n \left\{ Ai(-\beta_n) \right\}^2} .$$

The expression for the amplitude factor of the creeping waves is therefore

$$\left[\frac{\nu\frac{\partial}{\partial \rho}\left\{\rho^{1/2} H_\nu^{(2)}(\rho)\right\}}{\frac{\partial}{\partial \nu}\frac{\partial}{\partial \rho}\left\{\rho^{1/2} H_\nu^{(1)}(\rho)\right\}} \right]_{\nu=\nu_n} = -\frac{\tau^4}{\pi} e^{-i\frac{\pi}{6}} \left\{ 1 + \frac{e^{i\frac{\pi}{3}}}{60\tau^2\beta_n^2}(32\beta_n^3 + 9) - \frac{e^{-i\frac{\pi}{3}}}{5600\tau^4\beta_n^4}(128\beta_n^6 + 189) + O(\tau^{-6}) \right\} \frac{1}{\beta_n \left\{ Ai(-\beta_n) \right\}^2} \qquad (86)$$

and this is identical to the result obtained by Senior and Goodrich (1964).

Each of the zeros ν_n corresponds to a creeping wave mode and if we also expand $\sec \nu\pi$ in a series of exponentials, convergent for $\mathrm{Im}.\nu > 0$, substitution from equations (23), (85) and (86) into (80) leads to a representation of the creeping wave component S^c in the form

$$S^c = \tau^4 e^{i\frac{\pi}{3}} \sum_n \left\{ 1 + \frac{e^{i\frac{\pi}{3}}}{60\tau^2\beta_n^2}(32\beta_n^3+9) - \frac{e^{-i\frac{\pi}{3}}}{5600\tau^4\beta_n^4}(128\beta_n^6+189) \right.$$

$$\left. + O(\tau^{-6}) \right\} \cdot \frac{1}{\beta_n \{Ai(-\beta_n)\}^2} \sum_{\ell=0}^{\infty} (-1)^\ell \exp\left[i(2\ell+1)\pi \left\{ \rho + e^{i\frac{\pi}{3}} \tau\beta_n \right.\right.$$

$$\left. - \frac{e^{-i\frac{\pi}{3}}}{60\tau\beta_n}(\beta_n^3 - 9) + \frac{1}{1400\tau^3\beta_n^3}\left(\beta_n^6 - 7\beta_n^3 + \frac{63}{4}\right) + O(\tau^{-5}) \right\} \Big] - \tau^4 e^{i\frac{\pi}{3}} \sum_m \left\{ 1 \right.$$

$$\left. + e^{i\frac{\pi}{3}} \frac{8\alpha_m}{15\tau^2} - e^{-i\frac{\pi}{3}} \frac{4\alpha_m^2}{175\tau^4} + O(\tau^{-6}) \right\} \cdot \frac{1}{\{Ai'(-\alpha_m)\}^2}$$

$$\cdot \sum_{\ell=0}^{\infty} (-1)^\ell \exp\left[i(2\ell+1)\pi \left\{ \rho + e^{i\frac{\pi}{3}} \tau\alpha_n - e^{-i\frac{\pi}{3}} \frac{\alpha_n^2}{60\tau} + \frac{\alpha_n^3 - 10}{1400\tau^3} + O(\tau^{-5}) \right\} \right] \tag{87}$$

where the second set of terms has been taken directly from equation (24). This is a more detailed version of the expression derived by Senior and Goodrich (1964), and the extent to which it can be simplified without substantial loss of accuracy is explored in the next section.

The optics contribution to the far field amplitude is given by equation (81), and the asymptotic evaluation for large ρ is again based on the Debye formula (26) for the Hankel function. In practice, either of two approaches can be used. In the first of these the integral is split up into two parts, with one involving the differentiated functions and the other the undifferentiated ones. The latter integral is identical to that which has already been evaluated in connection with the soft sphere. For the former we note that

$$\frac{\partial}{\partial\rho}\left\{\rho^{1/2}H_\nu^{(1)}(\rho)\right\} = \rho^{-1/2}H_\nu^{(1)}(\rho)+\rho\frac{\partial}{\partial\rho}\left\{\rho^{-1/2}H_\nu^{(1)}(\rho)\right\}$$

and hence, from (26) and (61),

$$\frac{\partial}{\partial\rho}\left\{\rho^{1/2}H_\nu^{(1)}(\rho)\right\} = \sqrt{\frac{2\sin\beta}{\pi}}\; e^{i\rho(\sin\beta-\beta\cos\beta)+i\frac{\pi}{4}} \cdot \sum_{m=0}^{\infty}\frac{(m-\frac{1}{2})!}{(-\frac{1}{2})!}\left(\frac{-2i}{\rho\sin\beta}\right)^m\left(B_m+\frac{A_{m-1}}{2m-1}\right) \qquad (88)$$

providing the coefficient A_{-1} is regarded as zero. An expression for the ratio of the differentiated functions then follows from equation (62) on replacing B_m by $B_m+\frac{A_{m-1}}{2m-1}$, and this enables us to make use of at least some of the expansions developed for the hard sphere. Nevertheless, the time-consuming task of multiplying and collecting together long strings of terms still remains. The alternative approach is to combine the expansions for the two Hankel function ratios before multiplying by the exponential terms in (81), thereby enabling us to profit from some cancellation of terms common to the two ratios. By and large, however, there is little to choose between the methods, and since the required expression for S^o is available in the literature, we shall content ourselves with a mere statement of results.

From the expansions which Logan (1960) has derived for the bistatic far field components of the scattered electric vector, it can be shown that in the particular case of back scattering ($\theta = 0$)

$$S^o = -\frac{\rho}{2}e^{-2i\rho}\left\{1-\frac{i}{2\rho}+\frac{1}{2\rho^4}+O(\rho^{-5})\right\}. \qquad (89)$$

Logan is believed to the the only one who has carried out the expansion to this order and the absence of terms $O(\rho^{-2})$ and $O(\rho^{-3})$ within the brackets is of particular

interest. The fact that there is no term in ρ^{-2} is confirmed by the work of Senior and Goodrich (1964) and is in agreement with the results of a near-field analysis (Weston, 1961).

4.3 Numerical Considerations

As in the case of soft and hard spheres, the above expressions for S^c and S^o are only asymptotic for large ρ, and there is consequently no justification for expecting them to provide accurate numerical answers for ρ as small as 3 or even unity. The sphere problem, however, is fundamental to electromagnetic scattering and many of the techniques for cross section prediction are based on its solution. For lack of any other method it is often necessary to use these techniques when the radii of curvature of the body are not, in fact, large compared with the wavelength, and it is therefore desirable to have some feel for the accuracy of (87) and (89) not only for $\rho \gg 1$ but when it is near unity as well.

The phase of the optics component S^o identifies it as the expected return from the front face of the sphere, and the whole expression can be interpreted as the specular contribution. The leading term is that predicted by geometrical optics, and the first two terms can be obtained by the physical optics method. Since there are no terms in ρ^{-2} or ρ^{-3} within the bracketed part of (89), it is obvious that the physical optics solution is extremely accurate for large ρ, and for all $\rho > 2.24$ the second real term (in ρ^{-4}) corrects the first by less than 10 percent. The absence of any terms in ρ^{-2} and ρ^{-3}, and the relatively small magnitude of the coefficient of ρ^{-4}, are in marked distinction to the corresponding expressions for soft and hard spheres.

The other component S^c is attributable to creeping waves, and the phenomenological description of these is the same as in the scalar problems. In contrast to these cases, however, there are now two types of waves present, and from a consideration of the magnitudes of their contributions, it is appropriate to call the

first set of waves "major" and the second set "minor". The minor waves are represented by the second pair of sums in (87) and are identical to those supported by a soft sphere. In an approximate sense we can regard the corresponding surface field disturbances as being responsible for transporting the normal component of the magnetic vector around the sphere. The major waves are represented by the first pair of sums and can be associated with the normal component of the surface electric* field. To a first order they are identical to the waves on a hard sphere, but there are differences in the higher order terms that are important for the smaller ρ.

Although the expression for S^c is a highly complicated one as it stands, a drastically simplified version is sufficient for most numerical work. The attenuation of all waves is large enough for us to ignore the contributions from waves which have completed one or more circuits of the sphere, and we can therefore replace each summation over ℓ by its first term ($\ell=0$) alone. As indicated in the discussion of the soft sphere, we can omit all minor waves except the dominant one ($m=1$), and the same is also true of the major waves. A numerical comparison of the contributions from the first and second major waves ($n=1$ and 2 respectively) and the first and second minor waves has been given by Senior and Goodrich (1964) and from the table that they present it is apparent that the minor waves can, in fact, be omitted in their entirety. For $\rho=5$, for example, the contribution of the dominant minor wave is less than 0.35 percent of that from the dominant major wave, and the ratio decreases rapidly with increasing ρ.

Even with these simplifications we have not reached the limit of permissible reductions in the expression for S^c. In the amplitude factor for the dominant major wave, the term $O(\tau^{-4})$ produces amplitude and phase corrections less than 1 percent and 1^o respectively when $\rho=5$, and in the exponential the term in τ^{-3} gives

* In recognition of this fact, Senior and Goodrich (1964) introduced the terms E- and H- waves to denote the major and minor ones respectively.

only a 2.3° phase shift for ρ as small as unity. The preceding term in the exponential is, however, more important, but with the above modifications to equation (87) the expression for the creeping wave component becomes

$$S^c = \tau^4 e^{i\frac{\pi}{3}} \left\{ 1 + \frac{e^{i\frac{\pi}{3}}}{60\tau^2\beta_1^2}(32\beta_1^3 + 9) + O(\tau^{-4}) \right\} \cdot \frac{1}{\beta_1 \left\{ Ai(-\beta_1) \right\}^2}$$

$$\cdot \exp\left\{ i\pi\rho - e^{-i\frac{\pi}{6}} \tau\pi\beta_1 - \frac{e^{i\frac{\pi}{6}}}{60\tau\beta_1}(\beta_1^3 - 9) + O(\tau^{-3}) \right\} \qquad (90)$$

where β_1 and $Ai(-\beta_1)$ are given in Section 3.4. This should be an accurate approximation to (87) for ρ greater than (about) unity.

To facilitate the subsequent numerical investigation, it is convenient to introduce a function G defined in terms of the far field amplitude S by equation (39). G is, in effect, a voltage gain and is such that the back scattering cross section, normalized to its high frequency limit πa^2, is $|G|^2$. With G^c and G^o defined in a similar manner, the normalized creeping wave and optics components are

$$G^c = \tau e^{i\frac{\pi}{3}} \left\{ 1 + \frac{e^{i\frac{\pi}{3}}}{60\tau^2\beta_1^2}(32\beta_1^3 + 9) + O(\tau^{-4}) \right\} \cdot \frac{1}{\beta_1 \left\{ Ai(-\beta_1) \right\}^2}$$

$$\cdot \exp\left\{ i\pi\rho - e^{-i\frac{\pi}{6}} \tau\pi\beta_1 - \frac{e^{i\frac{\pi}{6}}}{60\tau\beta_1}(\beta_1^3 - 9) + O(\tau^{-3}) \right\} \qquad (91)$$

and

$$G^o = -e^{-2i\rho} \left\{ 1 - \frac{i}{2\rho} + \frac{1}{2\rho^4} + O(\rho^{-5}) \right\} . \qquad (92)$$

The Mie series representation of G is

$$G = -\frac{2i}{\rho}\sum_{n=1}^{\infty}(-1)^n(n+\frac{1}{2})\left\{\frac{\left[\rho j_n(\rho)\right]'}{\left[\rho h_n^{(1)}(\rho)\right]'} - \frac{j_n(\rho)}{h_n^{(1)}(\rho)}\right\} \tag{93}$$

and this (or some series quite closely related to it) has formed the basis for several independent determinations of the back scattering behavior of spheres. One of the earliest of the more comprehensive computations was made by the Scientific Computing Service Ltd. in England using the expression for S shown in equation (75), and Hey et al (1956) have tabulated the resulting values of S for $\rho = 0(0.01)10$. Perhaps the most comprehensive of all, however, is the computation of

$$G^* e^{-2i\rho}$$

(the asterisk denotes the complex conjugate) carried out by the Cornell Aeronautical Laboratory with a maximum of 70 terms in the expression for G, and Bechtel (1962) has tabulated the real and imaginary parts, argument, modulus and modulus squared (i.e. the normalized cross section) of this quantity for $\rho = 0(0.02)50$. It is this data that we shall use to assess the numerical accuracy of the asymptotic formulae for G^c and G^o.

In Fig. 8 the familiar curve of the normalized back scattering cross section as a function of ρ is plotted for $0 \leqslant \rho \leqslant 10$. For small ρ we have, from equations (39) and (76),

$$|G|^2 \sim 9\rho^4,$$

leading to an initial rise which is over three times as rapid as for the hard sphere (see Fig. 3). The cross section rises to a maximum of 3.655 for $\rho = 1.03$, and thereafter oscillates with a decreasing amplitude about a mean level which, as ρ increases, approaches unity from above.

One of the features of Fig. 8 that is most apparent is the extreme regularity of the oscillations for almost all values of ρ, and though the depth of oscillation

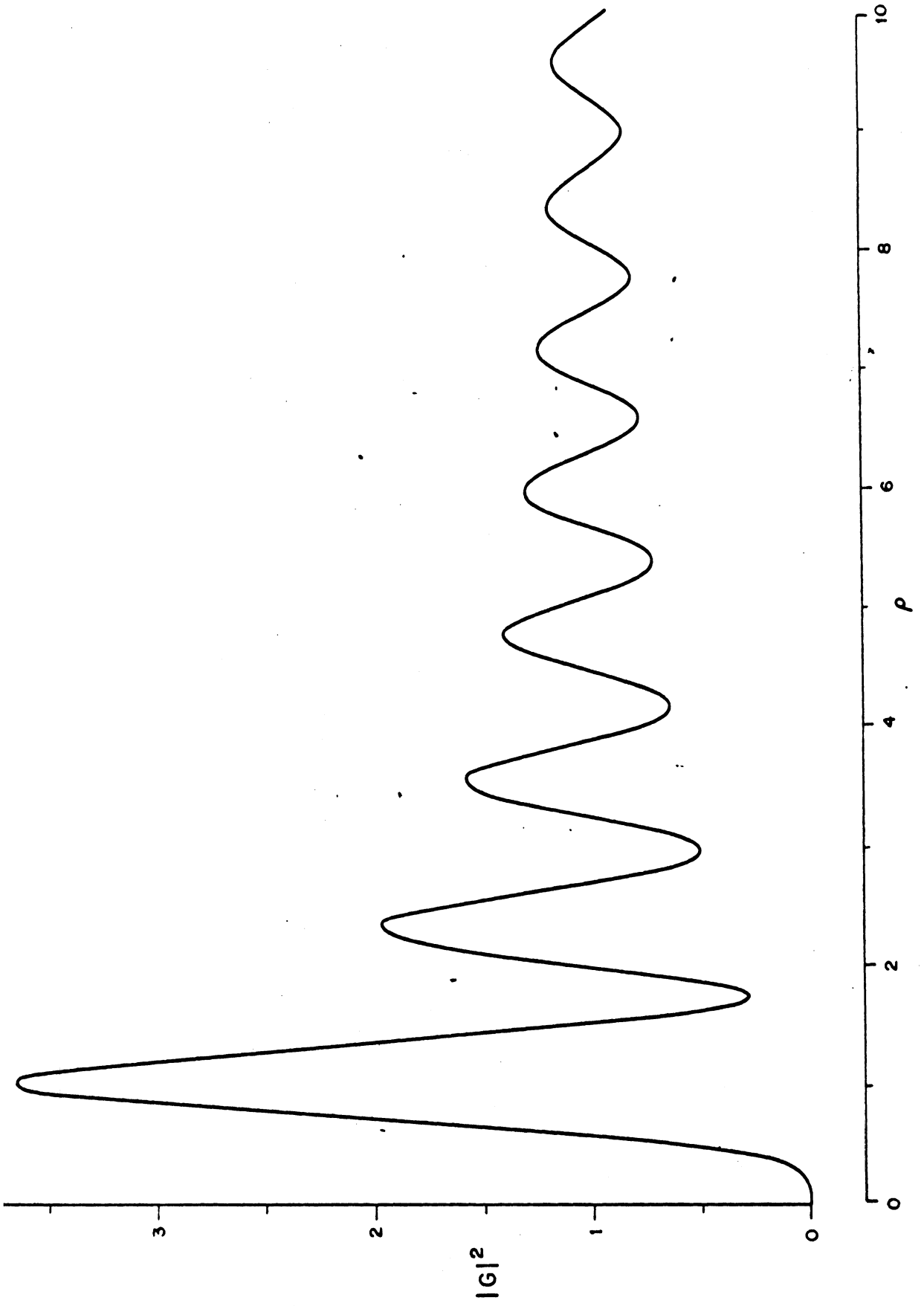

FIG. 8: NORMALIZED BACK SCATTERING CROSS SECTION OF A PERFECTLY CONDUCTING SPHERE

does, of course, decrease with increasing ρ, the separation between adjacent maxima and minima is remarkably unchanged. The locations of the turning points can be estimated by graphical interpolation of the data tabulated by Bechtel (1962), and these are listed in Table 9. If we ignore the first maximum, the separations are almost* constant, averaging 0.602(7) with a standard deviation of only 0.0076 over the 13 readings. This reinforces our belief that there are but two significant contributors to the cross section and strongly suggests that over a range extending from $\rho = 10$ down to the first minimum (or below) the physical mechanism responsible for the scattering remains the same. At the larger values of ρ, however, the back scattering is composed of a specular return and a creeping wave contribution, with the interference between them producing the oscillations. It is without question that this picture is applicable for ρ near 10, and the regularity of the behavior for ρ down to (about) 1.8 may now indicate that the same phenomenological description holds for the smaller ρ also. Were this so, the average phase velocity of the creeping wave disturbance for the range $1.8 < \rho < 10$ would be 0.9779c.

The maximum and minimum values of $|G|^2$ are also given in Table 9, and by taking the adjacent turning points in pairs, the values of the two contributing components, G_1 and G_2, can be determined on the assumption that they are constant from one turning point to the next. It is seen that G_1 decreases from 1.22 when $\rho = 1.74$ to unity when $\rho = 9.58$, with most of the decrease taking place for the smaller ρ. There is some oscillation, but its amplitude decays quite rapidly, and is less than 2 percent of the mean level for ρ greater than (about) 2. G_2 also decreases, and does so in a somewhat more uniform manner. It is less than 8 percent of G_1 for $\rho = 9.58$. In Fig. 9 the values of G_1 and G_2 are denoted by circles placed at the mid-points of the appropriate ρ-intervals.

* The spacing is even more uniform if the cross section σ/λ^2 is plotted as a function of ρ, since it avoids the "stretching" produced by the other normalization.

Table 9: Deductions from Data for $|G|^2$ (Bechtel, 1962)

Max/min	ρ	Separation in ρ	$\lvert G\rvert^2$	G_1	G_2
M	1.028		3.655		
m	1.744	0.716	0.285	1.223	0.689
M	2.334	0.590	1.969	0.969	0.435
m	2.957	0.623	0.506	1.057	0.346
M	3.554	0.597	1.589	0.986	0.275
m	4.164	0.610	0.635	1.029	0.232
M	4.762	0.598	1.410	0.992	0.196
m	5.368	0.606	0.717	1.017	0.171
M	5.966	0.598	1.307	0.995	0.148
m	6.572	0.606	0.773	1.011	0.132
M	7.171	0.599	1.240	0.996	0.117
m	7.775	0.604	0.813	1.007	0.106
M	8.376	0.601	1.194	0.997	0.095
m	8.980	0.604	0.844	1.006	0.087
M	9.579	0.599	1.160	0.998	0.079

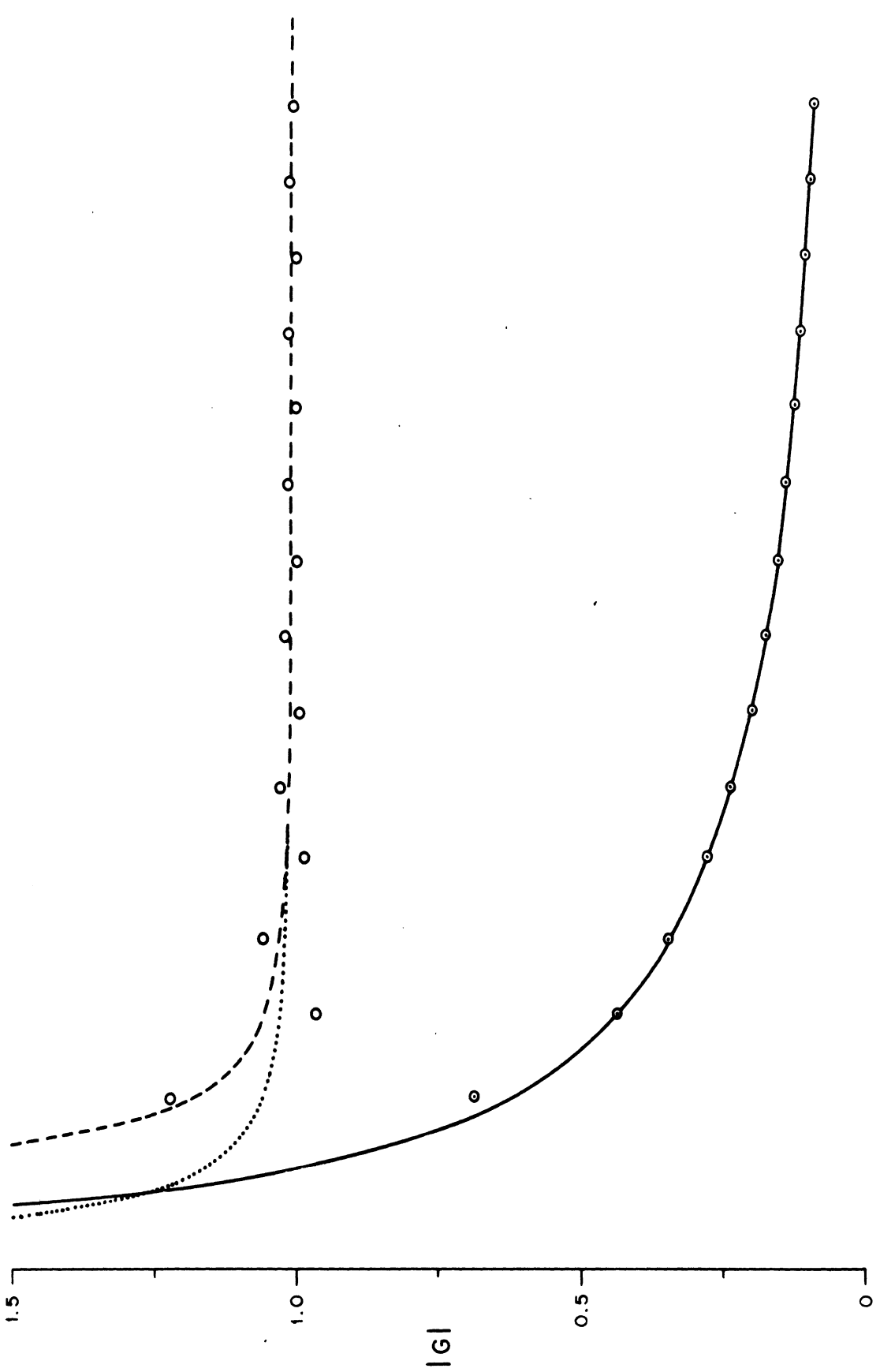

FIG. 9: COMPARISON OF DEDUCED VALUES OF G_2 (⊙⊙⊙) AND G_1 (○○○) WITH THEORETICAL EXPRESSIONS FOR $|G^c|$ (——) AND $|G^o|$ USING 3 TERMS (– – –) AND 2 TERMS (· · · ·) IN EQUATION (94)

Using equation (91) the amplitude and phase of the theoretical creeping wave component G^c have been computed for a series of values of ρ in the range $0.5 \leqslant \rho \leqslant 10.0$. The results are given in Table 10 and the amplitude is shown as a solid line in Fig. 9. The agreement with the points representing G_2 is excellent, and even for $\rho = 1.386$ (the smallest value for which G_2 can be found) the discrepancy is less than 7 percent. For the optics component it is again convenient to treat $G^o e^{2i\rho}$ which, from equation (92), has the asymptotic expansion

$$G^o e^{2i\rho} = -\left\{1 - \frac{i}{2\rho} + \frac{1}{2\rho^4} + O(\rho^{-5})\right\} . \qquad (94)$$

The real and imaginary parts of this expression have been determined for the same selected ρ, and are listed in Table 11 under the heading "3-term optics". The modulus is plotted in Fig. 9 as a broken line, and agrees well with the open circles representing G_1. As ρ decreases, the modulus follows the mean of the gradually increasing oscillations possessed by G_1, and though it departs somewhat from this mean for ρ less than (about) 2.5, it is almost identical to G_1 at the smallest value of ρ, $\rho = 1.386$, for which G_1 is known.

The above comparisons are, at most, a test on the moduli of the creeping wave and optics components, and because of the assumptions inherent in the derivation of G_1 and G_2, and the resulting uncertainties associated with their values, a more stringent type of test is desirable. For the reasons given earlier, the most critical of all procedures is to compare the real and imaginary parts of the theoretical optics component $G^o e^{2i\rho}$ with those of the "actual" component $(G - G^c)e^{2i\rho}$, where G is obtained from the exact Mie series (93). Using the values of G provided by Bechtel (1962), with those changes necessitated by his different definition and time convention, and the data for G^c computed from equation (91) and listed in Table 10, the real and imaginary parts of $(G - G^c)e^{2i\rho}$ have been determined for selected values of ρ. These are shown in Table 11, and are plotted in Fig. 10. The extent to which the oscillations have been suppressed is highly gratifying. For ρ

Table 10: Theoretical Creeping Wave Component

ρ	$\left\|G^c\right\|$	arg G^c (degrees)
0.5	1.57835	265.128
0.6	1.34287	283.796
0.7	1.17107	302.537
0.8	1.03970	322.146
0.9	$9.35709 \cdot 10^{-1}$	340.136
1.0	$8.51149 \cdot 10^{-1}$	358.963
1.1	$7.80905 \cdot 10^{-1}$	377.802
1.3	$6.70616 \cdot 10^{-1}$	415.490
1.5	$5.87663 \cdot 10^{-1}$	453.178
1.7	$5.22767 \cdot 10^{-1}$	490.837
1.9	$4.70479 \cdot 10^{-1}$	528.481
2.0	$4.47937 \cdot 10^{-1}$	547.295
2.5	$3.60246 \cdot 10^{-1}$	641.232
3.0	$2.99686 \cdot 10^{-1}$	734.981
3.5	$2.55202 \cdot 10^{-1}$	828.548
4.0	$2.21091 \cdot 10^{-1}$	921.945
4.5	$1.94092 \cdot 10^{-1}$	1015.195
5.0	$1.72196 \cdot 10^{-1}$	1108.302
5.5	$1.54092 \cdot 10^{-1}$	1201.296
6.0	$1.38887 \cdot 10^{-1}$	1294.161
6.5	$1.25950 \cdot 10^{-1}$	1386.923
7.0	$1.14821 \cdot 10^{-1}$	1479.584
7.5	$1.04436 \cdot 10^{-1}$	1572.191
8.0	$9.66983 \cdot 10^{-2}$	1664.667
8.5	$8.92401 \cdot 10^{-2}$	1757.091
9.0	$8.26233 \cdot 10^{-2}$	1849.445
9.5	$7.67202 \cdot 10^{-2}$	1941.730
10.0	$7.14274 \cdot 10^{-2}$	2033.961

Table 11. Comparison of Optics Components

ρ	$(G-G^c)e^{2i\rho}$		3-term optics	
	Real	Imag.	Real	Imag.
0.5	-0.89060	1.59476	-9.00000	1.00000
0.6	-1.05473	1.00152	-4.85802	0.83333
0.7	-1.06412	0.87844	-3.08247	0.71429
0.8	-1.03637	0.71561	-2.22070	0.62500
0.9	-1.05693	0.61885	-1.76208	0.55556
1.0	-1.06175	0.51293	-1.50000	0.50000
1.1	-1.03367	0.42142	-1.34151	0.45455
1.3	-0.95395	0.36137	-1.17506	0.38462
1.5	-0.96194	0.36082	-1.09877	0.33333
1.7	-0.98882	0.32669	-1.05987	0.29412
1.9	-1.00835	0.29213	-1.03837	0.26316
2.0	-1.01817	0.27002	-1.03125	0.25000
2.5	-0.99229	0.19445	-1.01280	0.20000
3.0	-1.00034	0.17900	-1.00617	0.16667
3.5	-1.00295	0.13841	-1.00333	0.14286
4.0	-0.99560	0.12888	-1.00195	0.12500
4.5	-1.00415	0.11136	-1.00122	0.11111
5.0	-0.99707	0.09890	-1.00080	0.10000
5.5	-1.00165	0.09330	-1.00055	0.09091
6.0	-0.99989	0.08123	-1.00039	0.08333
6.5	-0.99936	0.07874	-1.00028	0.07692
7.0	-1.00141	0.07056	-1.00021	0.07143
7.5	-0.99876	0.06617	-1.00016	0.06667
8.0	-1.00117	0.06304	-1.00012	0.06250
8.5	-0.99945	0.05806	-1.00010	0.05882
9.0	-1.00017	0.05649	-1.00008	0.05556
9.5	-1.00035	0.05195	-1.00006	0.05263
10.0	-0.99948	0.05044	-1.00005	0.05000

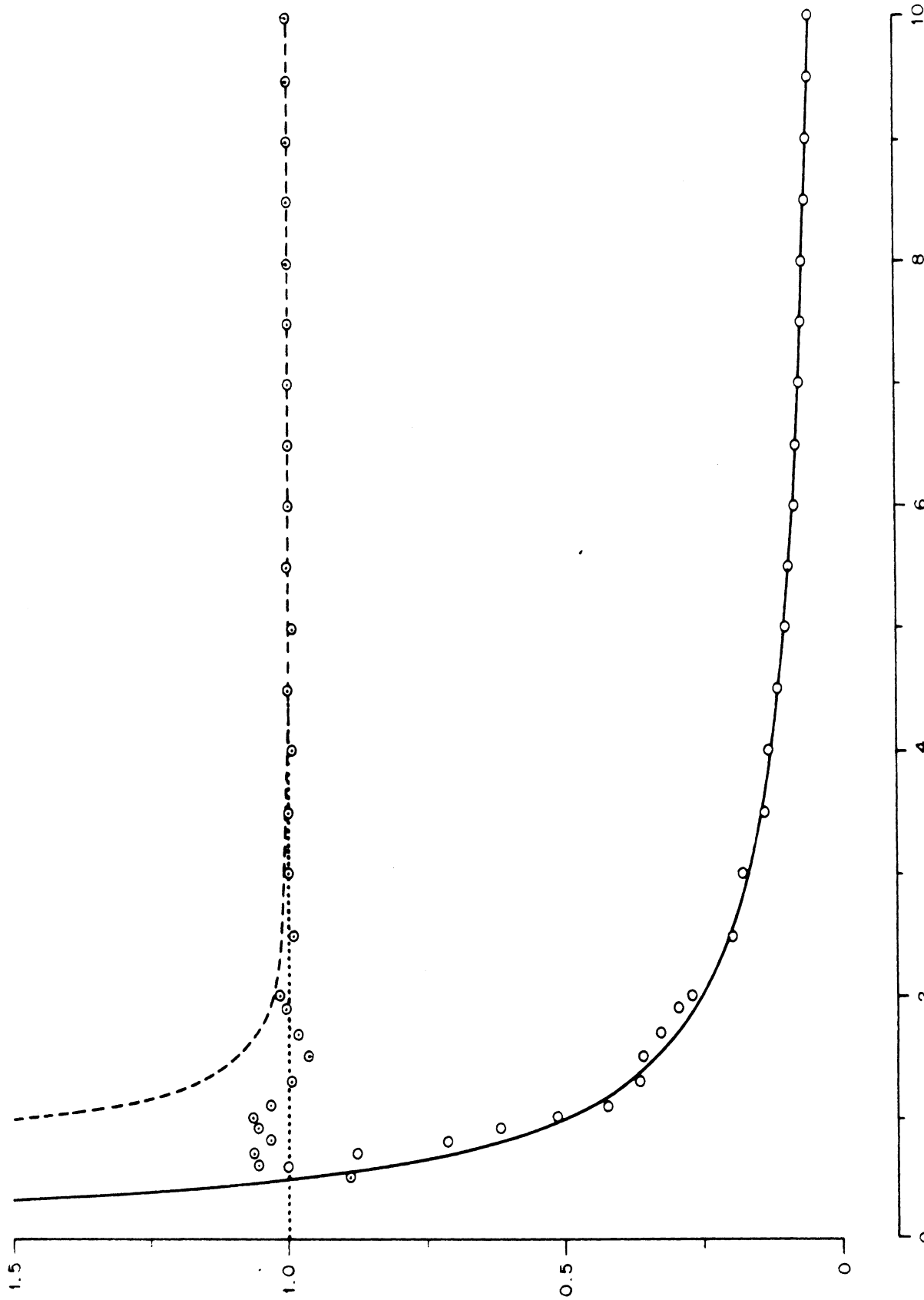

FIG. 10: COMPARISON OF THE NEGATIVE REAL (⊙⊙⊙) AND IMAGINARY (o o o) PARTS OF THE "ACTUAL" OPTICS CONTRIBUTION WITH THE 3-TERM (——, ——) AND 2-TERM (· · · · ——) OPTICS EXPRESSIONS

near 10 the real part is oscillating with an amplitude of less than 0.1 percent, and it is not until ρ has decreased to about 5 that the oscillation (now of amplitude 3 percent) has become visible in Fig. 10. As ρ decreases still further, the amplitude builds up to a maximum of around 8 percent (for $\rho \sim 1$), and for $\rho < 0.7$ the negative real part itself decreases from its peak value of 1.06(approx.). The imaginary part is also devoid of any significant oscillation until ρ has fallen to below 3, and even then the variations are quite small. The only interval in which a systematic departure from the uniform trend is obvious is $1 < \rho < 2$, and for $\rho < 1$ any variations are swamped by the rapid increase in the imaginary part, which takes it up to a value of 1.59 for $\rho = 0.5$.

Superimposed on Fig. 10 are the curves representing the imaginary and negative real parts of the 3-term optics expression, taken from Table 11. The imaginary part is in almost perfect agreement down to (about) $\rho = 4$, and a glance at Table 11 shows that the discrepancy does not exceed 1 percent unless $\rho < 4.5$. Thereafter the theoretical curve follows the mean of the small oscillations possessed by the "actual" component, and is in error by as much as 10 percent for ρ in the vicinity of 1.5. When ρ is less than unity, the curve has the right trend, but lags behind the required values, leading to a progressively increasing percentage error as ρ gets smaller. If anything, the real part of the 3-term expression is in even better agreement with the "actual" component for the larger ρ, and when ρ is near 10 the error is of order 0.05 percent. As ρ decreases, however, there is a tendency for the asymptotic formula to overestimate the component. This is quite noticeable for $\rho < 3.5$ and gets worse as ρ gets smaller. For ρ less than (about) 2, the theoretical expression is inadequate due to the rapid (and undesired) increase in its negative real part.

Since the values of the negative real part of the "actual" optics component are still oscillating around unity for ρ as small as 0.7, it is obvious that an expression for $G^o e^{2i\rho}$ in which the term in ρ^{-4} is ignored will be numerically more

effective than the 3-term expression. The real part is then -1 independently of ρ, and its negative is shown as the dotted line in Fig. 10. The modulus of the 2-term expression is also represented by the dotted curve in Fig. 9, and though this does not fit the values of G_1 as well as does the 3-term one, it should be noted that for small ρ the values of both G_1 and G_2 are somewhat suspect because of the assumption of components which remain constant between turning points. A comparison of the real and imaginary parts of $G^o e^{2i\rho}$ with those of $(G-G^c)e^{2i\rho}$ is a much more critical test, and Fig. 10 clearly shows the numerical superiority of the 2-term expression for $G^o e^{2i\rho}$ when ρ is less than 4. To judge from Table 11, the omission of the term in ρ^{-4} also improves the agreement for the larger values of ρ.

To illustrate the accuracy with which the far field amplitude can be calculated using the asymptotic formulae for G^c and G^o, the modulus and argument of

$$G = G^c + G^o$$

have been computed for specimen values of ρ using equations (91) and (92) with the term in ρ^{-4} omitted from the bracketed expression on the right hand side of (92). The results are given in Table 12, along with the corresponding exact values deduced from Bechtel's tabulation. From the error columns (a negative sign indicates that the estimate is too small), it would appear that the modulus is not in error by more than 4 percent unless ρ is less than unity, but as ρ decreases further the asymptotic formulae underestimate the true modulus by an ever increasing amount. More surprising, perhaps, is the accuracy with which the argument is predicted. In most instances the errors are comparable to those involved in the numerical evaluation of the expression for G^c, and it is only for $\rho < 0.7$ that there is any sign of a large and progressive increase.

4.4 Remarks

Although the creeping wave contribution to the far field amplitude in scattering by a metallic sphere is comparable to that in the hard acoustic case for values

Table 12: Comparison of Far Field Amplitudes

ρ	Asymptotic		Exact		Error	
	Modulus	Arg (degrees)	Modulus	Arg (degrees)	Mod (%)	Arg (^{o})
0.5	0.50232	306.985	0.72772	3.026	-30.97	-56.041
0.6	0.73791	354.547	1.02230	5.535	-27.82	-10.988
0.7	1.16918	5.848	1.33066	9.091	-12.14	- 3.243
0.8	1.51428	13.104	1.61122	13.533	- 6.02	- 0.429
0.9	1.73128	17.815	1.81492	18.329	- 4.61	- 0.514
1.0	1.85337	21.718	1.90724	22.718	- 2.83	- 1.000
1.1	1.86986	24.636	1.88354	26.026	- 0.73	- 1.390
1.3	1.61398	28.031	1.56662	27.968	3.02	0.063
1.5	1.07810	21.092	1.03712	20.624	3.95	0.468
1.7	0.56844	345.285	0.55815	341.941	1.84	3.344
1.9	0.74546	280.277	0.77042	281.821	- 3.68	- 1.544
2.0	0.97729	271.180	1.00406	270.962	- 2.67	0.218
2.5	1.31933	252.111	1.31150	252.344	0.60	- 0.233
5.0	1.08400	329.738	1.08113	329.803	0.27	- 0.065
10.0	0.96449	114.793	0.96397	114.767	0.05	0.026

of ρ near unity, and is somewhat larger for ρ of order 10, the asymptotic formula for G^c is extremely effective in suppressing the oscillations in the back scattering cross section for $\rho > 5$, and is more than adequate even down to $\rho = 0.7$. Based on the behavior of the real and imaginary parts of $(G - G^c)e^{2i\rho}$ as functions of ρ, it is therefore concluded that the expression for G^c given in equation (91) is an accurate approximation to the true creeping wave component for values of ρ as small as unity or less. It should be noted, however, that the omission of any term in (91) may significantly decrease this accuracy, and the retention of the term in τ^{-1} in the exponent is particularly important. We shall discuss this further in the next section. We also note that the variation in arg G^c as a function of ρ is remarkably uniform in view of the many terms contributing towards it. Based on the values of arg G^c for $\rho = 1.0(0.5)10.0$ listed in Table 10, a least squares fit to a straight line behavior gives

$$\begin{aligned} \arg G^c &= (186.033\rho + 176.327) \quad \text{degrees} \\ &= \pi\,(1.03352\rho + 0.97959) \quad \text{radians.} \end{aligned}$$

The maximum discrepancies occur at the end points of the range and are less than 3^o.

Since there are no terms in ρ^{-2} or ρ^{-3} in the expression for $G^o e^{2i\rho}$, the 3-term expression is tantamount to a 5-term one as regards the highest power of ρ occurring. This is very accurate numerically for ρ near 10, but as ρ decreases it has a tendency to overestimate the (negative) real part of the "actual" component. For ρ less than (about) 2, it is inadequate. The 2-term expression does not suffer from this defect. It is in good agreement with the actual values even down to $\rho = 1$ and is, in fact, somewhat better for larger values of ρ as well. The resulting formula for the theoretical optics component is then

$$G^o = -e^{-2i\rho}\left\{1 - \frac{i}{2\rho} + O(\rho^{-4})\right\} \tag{95}$$

(cf the corresponding equation 46 for the hard acoustic sphere) and, in combination with (91), enables the far field amplitude to be computed with an accuracy of better than 4 percent in modulus and 4^{o} in argument for all $\rho \geqslant 1$.

V
DISCUSSION

In all of the sphere problems considered, the Mie series representations of the far field amplitude have been recast into forms suitable for asymptotic evaluation for ρ large compared with unity. The resulting expressions split naturally into components whose phases identify them with a specular contribution from the front face of the sphere and a creeping wave contribution due to a disturbance which has traveled around the back of the sphere, and each of these is normally regarded as a high frequency type of scattering. This is certainly true of a specular return, and our philosophy of creeping waves is also based on a study of bodies whose radii of curvature are much larger than the wavelength. There is consequently no reason to expect that these concepts will continue to have application when the sphere radius is less than, say, one wavelength. Even if the conceptual picture were to remain unchanged at the smaller values of ρ, one could hardly expect the formulae to continue to provide accurate estimates of the scattering. Nevertheless, they appear to do so. In the electromagnetic problem the errors are still insignificant when $\rho = 1$, and for $0.7 < \rho < 1.0$ the high frequency approximation is superior to the Rayleigh formula for cross section prediction purposes.

A comparison of high and low frequency data for scattering by a metallic sphere is actually quite illuminating. The Rayleigh formula is based on the dipole terms in the low frequency expansion and, as such, is valid only for $\rho \ll 1$. In spite of this it is often used to compute the scattering from objects whose characteristic dimension, a, is near $\lambda/2\pi$ on the assumption that the resulting errors will be less than if a high frequency expression were employed. From equation (39) and (76) the Rayleigh approximation is

$$G = 3\rho^2, \tag{96}$$

and the phase is therefore in error to the extent that the argument of the actual far field amplitude departs from zero. As evident from the middle columns in Table 12,

the phase discrepancy increases from 3^{o} for $\rho = 0.5$ to 18^{o} for $\rho = 0.9$, and exceeds the phase error associated with the high frequency approximation (91) for all $\rho \geqslant 0.65$. Turning now to the modulus, equation (96) gives $|G| = 0.75$ for $\rho = 0.5$, increasing to 1.47 when $\rho = 0.7$ and 2.43 when $\rho = 0.9$. The corresponding percentage errors are 3.06, 10.47 and 33.89 respectively, and exceed those of (91) for all $\rho \geqslant 0.71$. We should therefore use the asymptotic expansion for G in preference to the Rayleigh formula whenever ρ is greater than (about) 0.7, and whereas the former tends to underestimate $|G|$ throughout the interval $0.7 \leqslant \rho \leqslant 10.0$, the latter overestimates it by an amount which increases with ρ.

It is, of course, obvious that the high frequency picture will ultimately fail as ρ becomes small compared with unity, but the agreement that we obtained in Section 4.3 would indicate that the portions of the surface field responsible for the specular and creeping wave returns continue to scatter in a substantially independent manner for values of ρ as small as, perhaps, 0.7. This is despite the fact that for $\rho = \pi/2$ the first Fresnel zone, which is often regarded as the minimum area necessary for the generation of a specular contribution, has expanded to fill the whole of the illuminated region. Any further reduction in ρ then decreases the zone size accordingly, and the slight oscillation in the imaginary part of the "actual" optics component near $\rho = 1.5$, leading to a partial failure in the estimate for G^{o}, could be attributable to this. Numerically at least, the failure is only temporary, and it is not until ρ has dropped to about 0.5 that the progressive errors of the high frequency approximation have increased to such a point that its estimates of the scattering are no longer valuable. As evidenced by the accuracy of the Rayleigh formula, the electrical size of the sphere is now small enough for the scattering to be volume-dominated, and no theory based on contributions from individual portions of the surface could then succeed.

As with any of the so-called canonical problems in scattering theory, one of the main reasons for investigating the solution in extreme detail is to understand the

nature of the scattering and, hopefully, to separate out those features which may have application to other and more general shapes. The above analysis of sphere scattering should be viewed in this context, and many of our approximate techniques for cross section estimation have been derived in this manner.

Creeping waves are a case in point. They provide one of the two significant contributions to the back scattering from a sphere, and the discussion that we have given strongly suggests that they are not a purely high frequency phenomenon. It is to be expected that they will be equally important with any smooth convex body, but can we use the understanding gained from the sphere to compute the creeping wave effect when the radii of curvature of the surface are not constant? Unfortunately this has not yet proved possible. The one technique available at the moment is valid only for radii large compared with the wavelength and its predictions are no longer accurate when ka is of order unity.

In the course of developing the geometrical theory of diffraction, Keller (1958) was led to a generalization of the work of Fock in which, for any convex body of large radius, a creeping wave is assumed to follow a geodesic on the surface with characteristics which are functions only of the local curvature in the direction of travel. Locally, therefore, the wave behaves as though on a circular cylinder of the appropriate radius, with an attenuation which is an integrated function of the distance ℓ and is proportional to

$$\int_0^{\ell} \frac{ds}{\left\{R(s)\right\}^{2/3}}$$

where R(s) is the radius of curvature at the point s along the path. In the particular case of a soft sphere of radius a, the net contribution to the normalized far field amplitude in the back scattering direction differs from (41) in the omission of those terms which are not common to the cylinder. It is, in fact,

$$\tilde{G}_s^c = -\frac{2\tau e^{i\frac{\pi}{3}}}{\left\{Ai'(-\alpha_1)\right\}^2} \exp\left\{i\pi\rho - e^{-i\frac{\pi}{6}}\tau\pi\alpha_1\right\} \tag{97}$$

where the tilde is used to denote the Keller approximation, and the suffix "s" indicates that the sphere is soft. Similarly, for a hard sphere

$$\tilde{G}_h^c = -\frac{2\tau e^{i\frac{\pi}{3}}}{\beta_1\left\{Ai(-\beta_1)\right\}^2} \exp\left\{i\pi\rho - e^{-i\frac{\pi}{6}}\tau\pi\beta_1\right\}, \tag{98}$$

and if (97) and (98) are compared with (41) and (68) respectively, it is obvious that they must be accurate when ρ is large. For the smaller ρ, however, the omission of the higher order terms leads to significant discrepancies between the "actual" creeping wave contributions and those predicted by (97) and (98), and the discrepancies cannot be removed (or reduced) by retaining more terms in (97) and (98) inasmuch as these differ from the required terms for a sphere.

The scattering of an electromagnetic wave by a convex metallic shape is treated by regarding the creeping waves as essentially scalar disturbances whose properties can be ascertained from the solutions for scattering by the corresponding soft and hard bodies. According to this theory, any electromagnetic "ray" striking the surface at grazing incidence excites two creeping waves with strengths proportional to the normal components of the incident electric and magnetic vectors. These travel independently along the geodesic as though they were hard and soft body waves respectively, and the vector character of the scattering is then recovered from the magnitudes of the two components at the point of launch. The resulting expression for the creeping wave contribution to the back scattering amplitude for a sphere is

$$\tilde{G}_v^c = \frac{1}{2}\left(\tilde{G}_s^c - \tilde{G}_h^c\right) \tag{99}$$

where $\tilde{G}_s^c$ and $\tilde{G}_h^c$ are defined as above.

The existence of such a relation between the vector and scalar solutions, at least to the first order in $1/\rho$, is evident from the Mie series representations. In the vector problem the complete far field amplitude (93) can be written alternatively as

$$G_v = \frac{i}{\rho} e^{-2i\rho} - \frac{2i}{\rho} \sum_{n=0}^{\infty} (-1)^n (n+\tfrac{1}{2}) \left\{ \frac{\left[\rho j_n(\rho)\right]'}{\left[\rho h_n^{(1)}(\rho)\right]'} - \frac{j_n(\rho)}{h_n^{(1)}(\rho)} \right\}$$

and the sum over the second term in braces is, simply half the soft body solution. Hence

$$G_v = \frac{i}{\rho} e^{-2i\rho} + \frac{1}{2} G_s - \frac{2i}{\rho} \sum_{n=0}^{\infty} (-1)^n (n+\tfrac{1}{2}) \frac{\left[\rho j_n(\rho)\right]'}{\left[\rho h_n^{(1)}(\rho)\right]'} \tag{100}$$

and the last sum is obviously similar to the hard body solution. Formally at least

$$\frac{\left[\rho j_n(\rho)\right]'}{\left[\rho h_n^{(1)}(\rho)\right]'} = \frac{j_n'(\rho)}{h_n^{(1)'}(\rho)} \frac{\left\{1 + \frac{1}{\rho} \frac{j_n(\rho)}{j_n'(\rho)}\right\}}{\left\{1 + \frac{1}{\rho} \frac{h_n^{(1)}(\rho)}{h_n^{(1)'}(\rho)}\right\}}$$

$$\sim \frac{j_n'(\rho)}{h_n^{(1)'}(\rho)} + \frac{i}{\rho^3} \frac{1}{\left\{h_n^{(1)'}(\rho)\right\}^2} ,$$

giving

$$G_v \simeq \frac{1}{2}(G_s - G_h) \tag{101}$$

where, to the first order in $1/\rho$, we have neglected the leading term on the right hand side of (100). Since this holds for the complete far field amplitude G, it provides an approximation to the optics component as well as to the creeping wave contribution. Thus, from equations (42) and (69),

$$\frac{1}{2}(G_s^o - G_h^o) = -e^{-2i\rho}\left\{1 - \frac{i}{2\rho} - \frac{1}{\rho^2} + \frac{5i}{2\rho^3} + \frac{17}{2\rho^4} + O(\rho^{-5})\right\} \tag{102}$$

which agrees with the expression for G_v^o (see equation 92) through terms of order $1/\rho$ in the brackets. We also note that the "physical optics" approximations to G_s^o and G_h^o, though accurate only to the first order, lead to an expression for G_v^o accurate to the first two orders when fed into (101).

The above representation of G_v in terms of scalar solutions is only asymptotic for large ρ, but it is obvious from equation (100) that a precise representation can be found. Instead of a rigid sphere, let us consider a body whose rigidity increases with increasing ρ, and which does not become completely rigid until ρ has become infinite. If the appropriate condition at its surface is

$$\left(\frac{\partial}{\partial\rho} + \frac{1}{\rho}\right) U = 0 \quad , \tag{103}$$

the normalized far field amplitude in the back scattering direction under this mixed boundary condition is

$$G_m = \frac{2i}{\rho}\sum_{n=0}^{\infty}(-1)^n(2n+1)\frac{[\rho j_n(\rho)]'}{[\rho h_n^{(1)}(\rho)]} \quad , \tag{104}$$

and thus

$$G_v = \frac{i}{\rho}e^{-2i\rho} + \frac{1}{2}(G_s - G_m) \quad . \tag{105}$$

It is doubtful, however, if this has application to bodies more general than the sphere, and any confidence in its physical implications is somewhat reduced by the fact that it holds only in the back scattering direction. Away from $\theta = 0$, G_v is related to G_s and G_m through an infinite and complicated series of vector differential operations as functions of θ.

To see the type of accuracy that can be achieved with the geometrical theory of diffraction, let us consider the approximation (99) to the creeping wave contribution to the back scattering from a metallic sphere. For numerical purposes, $\tilde{G}_s^c$ is negligible compared with $\tilde{G}_h^c$ and hence

$$\tilde{G}_v^c \sim -\frac{1}{2}\tilde{G}_h^c$$

where $\tilde{G}_h^c$ is as shown in equation (98). The modulus and argument of $\tilde{G}_v^c$ have been computed for selected values of ρ in the range $0.5 \leqslant \rho \leqslant 10.0$, and the results are given in Table 13 along with a comparison with the more accurate data for the vector creeping wave taken from Table 10. It will be observed that the argument of the Keller approximation is in error by more than 30^o for $\rho \leqslant 3.0$, and the modulus by a factor 2 or more for $\rho < 2.3$. Even more striking are the discrepancies, particularly in the modulus, when ρ is of order 10. These are almost entirely due to neglecting the term $O(\tau^{-1})$ in the exponent of (91), and reinforce the comments made about this in Section 3.3. For the optics component, the Keller approximation is identical to that in (94) and is therefore quite accurate. It is, in fact, more accurate than for the hard sphere, and this is even more true* with the creeping wave component.

Although this comparison is not meant to detract from Keller's theory which, at the moment, provides our only means for determining the creeping wave contri-

*The considerable discrepancies between G_h^c and $\tilde{G}_h^c$ are evident on multiplying the first column in Table 13 by a factor 2 (to get $|\tilde{G}_h^c|$) and comparing the resulting values with the more accurate data in Table 6.

Table 13: Comparison of Creeping Wave Components

ρ	$\lvert\tilde{G}_v^c\rvert$	Arg $\tilde{G}_v^c$ (degrees)	$\lvert\tilde{G}_v^c\rvert/\lvert G_v^c\rvert$	Arg G_v^c - Arg $\tilde{G}_v^c$
0.5	$3.75939 \cdot 10^{-1}$	207.762	0.2382	57.366
0.6	$3.58092 \cdot 10^{-1}$	229.381		54.415
0.7	$3.41838 \cdot 10^{-1}$	250.618	0.2919	51.919
0.8	$3.26992 \cdot 10^{-1}$	271.559		50.587
0.9	$3.13381 \cdot 10^{-1}$	292.254	0.3349	47.882
1.0	$3.00852 \cdot 10^{-1}$	312.775	0.3535	46.188
1.1	$2.89273 \cdot 10^{-1}$	333.125	0.3704	44.677
1.3	$2.68542 \cdot 10^{-1}$	373.427	0.4004	42.063
1.5	$2.50486 \cdot 10^{-1}$	413.307	0.4262	39.871
2.0	$2.13971 \cdot 10^{-1}$	511.691	0.4777	35.604
2.5	$1.86083 \cdot 10^{-1}$	608.771	0.5165	32.461
3.0	$1.64001 \cdot 10^{-1}$	704.960	0.5472	30.021
3.5	$1.46052 \cdot 10^{-1}$	800.494	0.5723	28.054
4.0	$1.31162 \cdot 10^{-1}$	895.524	0.5932	26.421
4.5	$1.18612 \cdot 10^{-1}$	990.149	0.6111	25.046
5.0	$1.07894 \cdot 10^{-1}$	1084.444	0.6266	23.858
5.5	$9.86409 \cdot 10^{-2}$	1178.461	0.6401	22.835
6.0	$9.05777 \cdot 10^{-2}$	1272.242	0.6522	21.919
6.5	$8.34955 \cdot 10^{-2}$	1365.817	0.6629	21.106
7.0	$7.72317 \cdot 10^{-2}$	1459.214	0.6726	20.370
7.5	$7.16578 \cdot 10^{-2}$	1552.453	0.6861	19.738
8.0	$6.66709 \cdot 10^{-2}$	1645.551	0.6895	19.116
8.5	$6.21876 \cdot 10^{-2}$	1738.522	0.6969	18.569
9.0	$5.81395 \cdot 10^{-2}$	1831.374	0.7037	18.066
9.5	$5.44698 \cdot 10^{-2}$	1924.132	0.7100	17.598
10.0	$5.11312 \cdot 10^{-2}$	2016.790	0.7158	17.171

bution for a general smooth convex body, it does show the necessity for an improved treatment if the computations are to be accurate when the radii of curvature are not large compared with the wavelength. What is required is some way of including the effect of the curvature transverse to the plane of the geodesic, which will therefore allow us to dispense with the simulation by a cylinder. An investigation having this as its objective is now being carried out.

VI
ACKNOWLEDGMENTS

The author is indebted to Mr. L. P. Zukowski for checking the algebra associated with the evaluation of the optics components for the soft and hard spheres; to Messrs Prakash Sikri and J. A. Ducmanis for programming the Mie series evaluations for these spheres; and to Mr. H. E. Hunter for carrying out all of the required hand computations.

VII
REFERENCES

Bechtel, M.E. (1962) "Scattering Coefficients for the Backscattering of Electromagnetic Waves from Perfectly Conducting Spheres," Cornell Aeronautical Laboratory Report No. AP/RIS-1.

Franz, W. (1954) "On the Green's Functions of the Cylinder and Sphere," Z. fur Naturforschung 9, pp. 705-716.

Goodrich, R.F., B.A. Harrison, R.E. Kleinman and T.B.A. Senior (1961) "Diffraction and Scattering by Regular Bodies - I: The Sphere," The University of Michigan Radiation Laboratory Report No. 3648-1-T.

Hey, J.S., G.S. Stewart, J.T. Pinson and P.E.V. Prince (1956) "The Scattering of Electromagnetic Waves by Conducting Spheres and Discs," Proc. Phys. Soc. B 69, pp. 1038-1049.

Keller, J.B. (1958) "A Geometrical Theory of Diffraction," appearing in "Calculus of Variations and its Applications," Proc. Symp. Appl. Math., Vol. 8 (McGraw-Hill Book Co., Inc., New York).

Keller, J.B., R.M. Lewis and B.D. Seckler (1956) "Asymptotic Solutions of Some Diffraction Problems," Commun. Pure Appl. Math. 9, pp. 207-265.

Logan, N.A. (1959) "General Research in Diffraction Theory, Vol. 1," Lockheed Missiles and Space Division Technical Report No. LMSD-288087.

Logan, N.A. (1960) "Scattering Properties of Large Spheres," Proc. IRE 48, p. 1782.

Miller, J.C.P. (1946) The Airy Integral (Cambridge University Press).

Scott, J.M.C. (1949) "An Asymptotic Series for the Radar Scattering Cross Section of a Spherical Target," Atomic Energy Research Establishment (Harwell, England) Technical Memorandum T/M 30.

Senior, T.B.A. (1960) "Scalar Diffraction by a Prolate Spheroid at Low Frequencies," Can. J. Phys. 38, pp. 1632-1641.

Senior, T.B.A. (1961) "The Convergence of Low Frequency Expansions in Scalar Scattering by Spheroids," The University of Michigan Radiation Laboratory Report No. 3648-4-T.

Senior, T.B.A. (1965a) "The Back Scattering Cross Section of a Perfectly Conducting Sphere," The University of Michigan Radiation Laboratory Memorandum No. 7030-505-M.

Senior, T.B.A. (1965b) "Control of the Acoustic Scattering Characteristics of a Rigid Sphere by Surface Loading," J. Acous. Soc. Amer. 37, pp. 464-475.

Senior, T.B.A. and R.F. Goodrich (1964) "Scattering by a Sphere," Proc. IEE (London) 111, pp. 907-916.

Stratton, J.A. (1941) Electromagnetic Theory (McGraw-Hill Book Co., Inc., New York).

Watson, G.N. (1948) A Treatise on the Theory of Bessel Functions (Cambridge University Press).

Weston, V.H. (1961) "Near-Zone Back Scattering from Large Spheres," Appl. Sci. Res. B 9, pp. 107-116.

UNCLASSIFIED

Security Classification

DOCUMENT CONTROL DATA - R&D

(Security classification of title, body of abstract and indexing annotation must be entered when the overall report is classified)

1 ORIGINATING ACTIVITY (Corporate author) The University of Michigan Department of Electrical Engineering Radiation Laboratory	2a REPORT SECURITY CLASSIFICATION UNCLASSIFIED 2b GROUP

3 REPORT TITLE

Analytical and Numerical Studies of the Back Scattering Behavior of Spheres.

4 DESCRIPTIVE NOTES *(Type of report and inclusive dates)*

Technical Report

5 AUTHOR(S) *(Last name, first name, initial)*

Senior, T. B A.

6 REPORT DATE	7a TOTAL NO. OF PAGES	7b NO. OF REFS
June 1965	105	18

8a CONTRACT OR GRANT NO.	9a ORIGINATOR'S REPORT NUMBER(S)
AF 04(694)-683	7030-1-T
b. PROJECT NO.	
c.	9b OTHER REPORT NO(S) *(Any other numbers that may be assigned this report)*
d	

10 AVAILABILITY/LIMITATION NOTICES

Qualified requestors may obtain copies of this report from Defense Documentation Center, Cameron Station, Alexandria, Virginia 22314

11 SUPPLEMENTARY NOTES	12 SPONSORING MILITARY ACTIVITY
	USAF Ballistic Systems Division Norton AFB, California 92409

13 ABSTRACT

When a smooth convex body is illuminated by a plane wave, an important feature of the electromagnetic scattering is the effect of the creeping waves which are launched in the vicinity of the shadow boundary and contribute to the back scattered field after having traversed the rear. Although usually regarded as a high frequency phenomena appropriate only when the radii of curvature are large in comparison with the wavelength ($ka \gg 1$), studies of data for the back scattering of a plane electromagnetic wave by a perfectly conducting sphere suggest that the concept is still valid for ka as small as unity. A relatively simple expression for the creeping wave component is found to be accurate for all $ka \geqslant 1$.

DD FORM 1 JAN 64 1473

UNCLASSIFIED

Security Classification

14 KEY WORDS	LINK A		LINK B		LINK C	
	ROLE	WT	ROLE	WT	ROLE	WT
diffraction and scattering numerical analysis spheres						

INSTRUCTIONS

1. ORIGINATING ACTIVITY: Enter the name and address of the contractor, subcontractor, grantee, Department of Defense activity or other organization *(corporate author)* issuing the report.

2*a*. REPORT SECURITY CLASSIFICATION: Enter the overall security classification of the report. Indicate whether "Restricted Data" is included. Marking is to be in accordance with appropriate security regulations.

2*b*. GROUP: Automatic downgrading is specified in DoD Directive 5200.10 and Armed Forces Industrial Manual. Enter the group number. Also, when applicable, show that optional markings have been used for Group 3 and Group 4 as authorized.

3. REPORT TITLE: Enter the complete report title in all capital letters. Titles in all cases should be unclassified. If a meaningful title cannot be selected without classification, show title classification in all capitals in parenthesis immediately following the title.

4. DESCRIPTIVE NOTES: If appropriate, enter the type of report, e.g., interim, progress, summary, annual, or final. Give the inclusive dates when a specific reporting period is covered.

5. AUTHOR(S): Enter the name(s) of author(s) as shown on or in the report. Enter last name, first name, middle initial. If military, show rank and branch of service. The name of the principal author is an absolute minimum requirement.

6. REPORT DATE: Enter the date of the report as day, month, year; or month, year. If more than one date appears on the report, use date of publication.

7*a*. TOTAL NUMBER OF PAGES: The total page count should follow normal pagination procedures, i.e., enter the number of pages containing information.

7*b*. NUMBER OF REFERENCES: Enter the total number of references cited in the report.

8*a*. CONTRACT OR GRANT NUMBER: If appropriate, enter the applicable number of the contract or grant under which the report was written.

8*b*, 8*c*, & 8*d*. PROJECT NUMBER: Enter the appropriate military department identification, such as project number, subproject number, system numbers, task number, etc.

9*a*. ORIGINATOR'S REPORT NUMBER(S): Enter the official report number by which the document will be identified and controlled by the originating activity. This number must be unique to this report.

9*b*. OTHER REPORT NUMBER(S): If the report has been assigned any other report numbers *(either by the originator or by the sponsor)*, also enter this number(s).

10. AVAILABILITY/LIMITATION NOTICES: Enter any limitations on further dissemination of the report, other than those imposed by security classification, using standard statements such as:

(1) "Qualified requesters may obtain copies of this report from DDC."

(2) "Foreign announcement and dissemination of this report by DDC is not authorized."

(3) "U. S. Government agencies may obtain copies of this report directly from DDC. Other qualified DDC users shall request through

_____."

(4) "U. S. military agencies may obtain copies of this report directly from DDC. Other qualified users shall request through

_____."

(5) "All distribution of this report is controlled. Qualified DDC users shall request through

_____."

If the report has been furnished to the Office of Technical Services, Department of Commerce, for sale to the public, indicate this fact and enter the price, if known.

11. SUPPLEMENTARY NOTES: Use for additional explanatory notes.

12. SPONSORING MILITARY ACTIVITY: Enter the name of the departmental project office or laboratory sponsoring *(paying for)* the research and development. Include address.

13. ABSTRACT: Enter an abstract giving a brief and factual summary of the document indicative of the report, even though it may also appear elsewhere in the body of the technical report. If additional space is required, a continuation sheet shall be attached.

It is highly desirable that the abstract of classified reports be unclassified. Each paragraph of the abstract shall end with an indication of the military security classification of the information in the paragraph, represented as *(TS)*, *(S)*, *(C)*, or *(U)*.

There is no limitation on the length of the abstract. However, the suggested length is from 150 to 225 words.

14. KEY WORDS: Key words are technically meaningful terms or short phrases that characterize a report and may be used as index entries for cataloging the report. Key words must be selected so that no security classification is required. Identifiers, such as equipment model designation, trade name, military project code name, geographic location, may be used as key words but will be followed by an indication of technical context. The assignment of links, rules, and weights is optional.